View metadata, citation and similar papers at core.ac.uk
brought to you by CORE
provided by Multimedia ONline ARchiv CHemnitz

External Reactive Power Compensation of Permanent Magnet Synchronous Generator

zur Erlangung des akademischen Grades eines "Dr.-Ing."

an der Technischen Universität Chemnitz
Fakultät Elektrotechnik und Informationstechnik

vorgelegt

von Dipl.-Ing. Amr Singer

geboren am 21.9.1974
Kairo Ägypten

Chemnitz, den 24.11.2009

Gutacher :

Prof Dr. Ing. W. Hofmann

Prof Dr. Ing. W. Schufft

Preface

This work has been done at the department of Electrical Machine and Drives at Technical University of Chemnitz, Germany. This research work has been funded by the German Environment Foundation. I would like to express my gratitude to the German Environment Foundation for their support.

I would like to thank Prof. Dr. Hofmann for his guidance, support, and encouragement. I would also thank him for his valuable remarks. I would like to thank Prof. Dr. Schufft for his valuable remarks.

I would also like to thank my colleagues in the department of Electrical Machine and Drives for the friendly atmosphere. I would to express my gratitude to the electrical workshop at the Technical University of Chemnitz for their help in executing the experiment.

Last, but not least, I am grateful for the endurance, encouragement and support from my father, my mother and my wife who made it possible to finish this thesis.

Content

Abbreviations and Symbols

A	Area of wind turbine
C	Capacitance, Acceleration moment coefficient, Damping torque coefficient of the blade
D	Displacement power
E	Energy Losses
f	Switching frequency of the inverter
I	Current
J	Moment of inertia
K	coefficient of the turbine
L	Inductance
m	Modulation index, torque
M	Mutual inductance
P	Active Power
Q	Reactive power
R	Resistance, Controller
S	Apparent power , Lapace variable
T	Time

u_{μ}	Commutation angle of the diode
U	Voltage
v	Velocity
X	Reactance
z_p	Pole pair
Z	Impedance
δ	Power angle of the generator
θ	Angle of the wind turbine rotor
λ	Tip speed ratio
ρ	Air density
φ	Power factor angle
ψ	Flux linkage
ω	Angular velocity

Suffix and prefix

1	Primary winding of the transformer
2	Secondary winding of the transformer
5	Fifth harmonic filter
A	Acceleration
AF	Active filter
C	Compensation
CEO	Threshold of IGBT

D	Damping winding
d	Direct axis
d`	Direct axis short circuit transient
d``	Direct axis short circuit subtransient
do	Average voltage
do`	Direct axis open circuit transient
do``	Direct axis open circuit subtransient
E	excitation
el	Electrical
F	LC filter
Fe	Iron losses
Ff	Fundamental component
G	Generator
h	Magnetising inductance
K	Short circuit
L	Load
LC	Filter losses
Lcu	Copper losses
LfW/D	Forward losses in diode
LfW/T	Forward losses in IGBT
Loff/D	Switching off losses in diode
Loff+ on/T	Switching on and off losses in IGBT
LT	Copper losses in transformer
l	Left component

RG	Rotor blades
r	Right component
q	Quadrature axis
S	Stator of the generator
SK	Harmonic component
T	Transformer
tip	Tip of the turbine
X	Hypothetical resistance of diode
W	Mechanical wind

1

Introduction

The use of wind energy is not a new idea. Mankind has been using it since antiquity. For centuries windmills with watermills were the only source of motive power for many applications, some of which are even still being used today such as sailing, pumps for irrigation or drainage, or grinding grain. With the industrial revolution, the importance of windmills as primary industrial energy source was replaced by steam and internal combustion engines.

The first wind turbine to generate electricity was built by American scientist and businessman Charles Brush in 1888. It was 17 meters tall with 144 cedar rotor blades, and it had a capacity of 12 kilowatts. Later, in the year 1891, Danish inventor Poul La Cour discovered that faster rotating wind turbines with fewer rotor blades generate more electricity than slow moving turbines with many rotor blades. Using this knowledge, he developed the first wind electrical generating wind turbines to incorporate modern aerodynamic design principles. The 25-kilowatt machines used four bladed rotors in order to increase the efficiency. By the end of World War I, the use of these machines spread throughout Denmark. During 1930s thousands of small wind turbines were built in rural areas across the United States. One to three kilowatts in capacity, the turbines at first were providing lighting for farms but later their use was extended to power appliances and farm machinery. With the electrification of the industrialized world, the role of wind power decreased.

Fossil fuels showed to be more competitive in providing electrical power on large scales.

The revival of the wider interest in wind power started after the oil crisis of 1973. As public concerns about environmental issues such as air pollution and climate change grew, governments all around the industrial world took a greater interest in using renewable energy as a way to decrease greenhouse gases and other emissions. Since the research in wind power utilization did not stop due to competition of fossil fuels, solid foundation of theories and practical experience brought modern technology and materials into use. Wind turbine installations increased in Germany, Sweden, Canada, Great Britain and the United States encouraged by government sponsored programs.

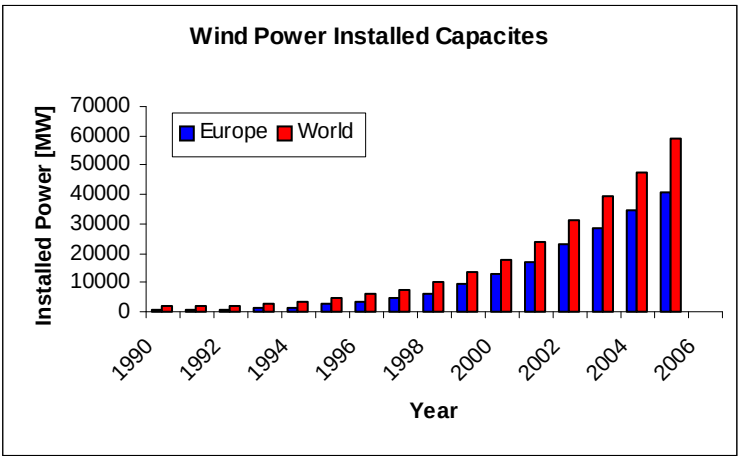

Fig. 1- 1 Wind power capacities in world in Europe from 1990 to 2006 according to European Energy Association

Today, wind power is the world's fastest growing energy technology. Although it currently produces less than 1% of world-wide electricity use, it accounts for 23% of electricity use in Denmark, 4.3% in Germany and approximately 8% in Spain. Figure 1-1 shows growth of installed capacities in world and Europe for the last 15 years. The wind power targets set by the industry and by the European Commission during the last decade have all

been exceeded. The European Wind Energy Association has set new targets for the EU-15 to have installed 75,000 MW. These capacities, which are going to be 10.6% of total European installed generation capacity, or 28% of total new generation capacity, generating 5.5% of European electricity, 167 TWh per year, will provide power equivalent to the needs of 34 million European households or 86 million people.

The revolution of wind industry in Germany in the future is limited by the supply of suitable landscape for wind parks and also ecological consequences. In addition to a natural shortage of inland locations are the concern of the nature and landscape protection. One solution to this problem is to increase the percentage consumption of electricity from wind energy rather than conventional energy sources. The offshore installation of wind turbines is a huge source of energy [16]. However this brings a number of serious technical problems, such as:

- Transportation and installation of the system components.
- Network Connection.
- Maintenance and Diagnostics.
- Compliance of nature conservation.

Because of the greater energy yield, it is necessary to use MW offshore wind power plant wind turbines. Difficult access locations and high maintenance costs require an extremely reliable operation. This could lead to encourage other generator types particularly high gearless permanent magnet synchronous generators because of their almost maintenance free and the improvement in the efficiency despite their higher investment costs. Even the choice of power electronic part and its cost and reliability should be considered. As it plays an important role in which voltage level and network types in offshore applications will primarily exist. Currently, in particular, the dc voltage connection via submarine cable to a network coupling station on the coast is greatly favored [26]. In this case, the decision between the diode rectifiers or IGBT converters should be decided. Due to the lower power

losses and higher reliability additional to due lack of control single, make the usage of a diode rectifier with permanent magnet synchronous generator is preferred. A disadvantage is that operating speed range is limited. This results that by a constant dc voltage excitation or fixed excitation by the permanent magnet only a very small speed range with reasonable torque output to operate. Possible alternatives would be a variable supply voltage compensation or passive means, such as capacitors. Another possibility is the use of active compensators, which is controllable voltage that can be a portion of the rating of the complete system. In this case the generator with limited output power feeding the diode rectifier can operate up to the rated power.

1.1 State of art technology

The current status in the field of powerful wind power plant is a competitive situation between high pole gearless synchronous machine and double feed asynchronous slip ring machine marked with gearbox [21],[72]. Both versions are variable speed by using a stator side or rotor side frequency inverter designed so that a frequency adjustment is possible. For onshore wind power plant competition there is currently a balanced assessment. The advantages for the double fed asynchronous slip ring machine shown in fig. 1-2 [80],[100]:

- Full coverage of the speed setting range by over or under synchronous speed.
- The regulation of active and reactive power flow with the help of the rotor inverter on the rotor and stator side.
- Entirely decoupled load independent adjustability of capacitive and inductive reactive power on the stator side.
- The extremely high stability through a fast control of voltage grid.

- The use of less expensive machines low pole geometries (4 or 6-pole with higher utilization).

- The reduced rating rotor side inverter, which is about 20-30% of rated power.

The doubly fed asynchronous generator (DFIG) is widely used. Repower Systems Company manufactures 5MW power plant with 126 m rotor diameter while Vestas Company manufactures asynchronous generator of rated of 3MW power plant.

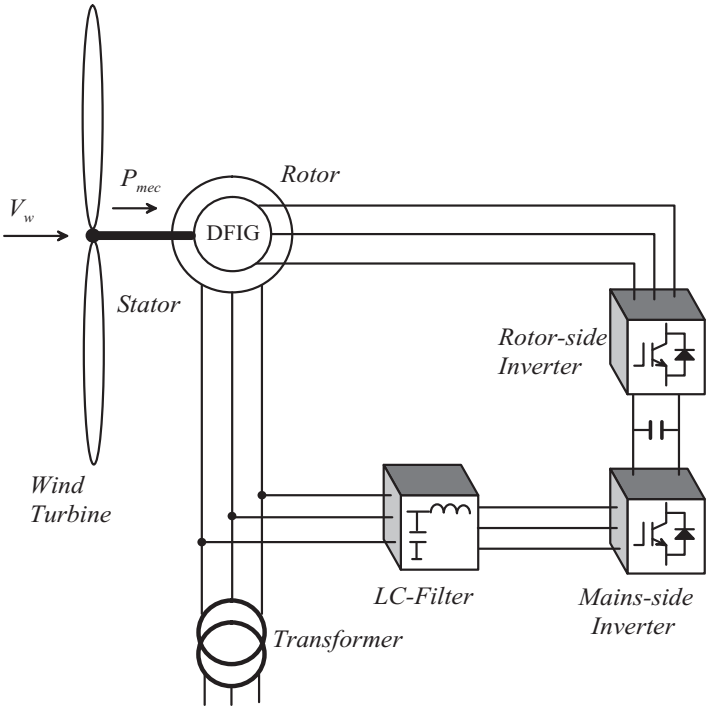

Fig. 1- 2 Doubly fed asynchronous slip ring machine

The disadvantages of doubly fed asynchronous machine:

- The use of slip ring machine.
- The need for a mechanism to speed adjustment.

The advantages of the high pole synchronous machine shown in fig 1-3:

- The saving of expensive volume.
- The avoidance of gear damage.
- A reduction drives vibrations.
- The overall efficiency is very good.

Large plants of 2 MW as Enercon E-82 stand for the electrically excited variant. Permanent generators are currently up to 2000 kW used by Lagerwey Company and up to 800kW by the company Genesys.

The disadvantages of this principle are:

- Complicated high pole machines run with poor utilization compared low pole machines.
- Larger outside diameter with increasing performance (5 MW), to considerable difficulties in overland transportation, even at the coastal production.
- The frequency inverter is rated to the full rated power of generator, which leads to higher dimensions and a weight increase and the use of coolants are required.

For electrical excitation [57],[62]:

- Dc current is fed to the rotor windings through brushes that are used for excitation. The brushes are affected by environmental conditions.

- Brushless excitation increases the cost.

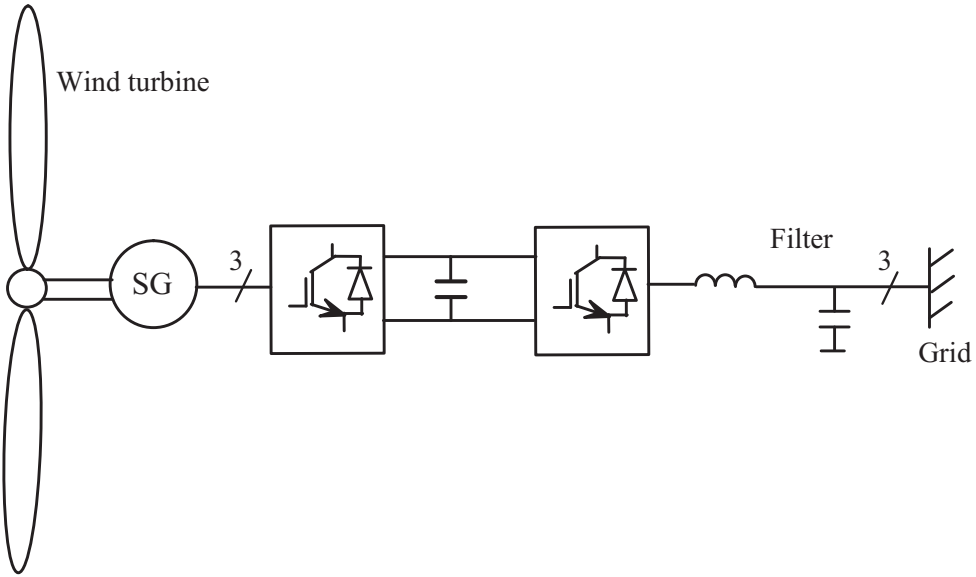

Fig. 1- 3 High pole synchronous machine

For permanent magnet excitation:

- Eliminates the excitation losses but the cost of permanent magnets, the machine is considerably more expensive.

- Control of the terminal voltage is no longer possible because of the permanent magnet.

- Cheaper magnets types such as NdFeB magnets are not capable to withstand corrosion. Special coating of galvanise such as Sn, Zn, Ni compounds (multi-layer coating), or Parylene coatings (plastic layer) is required to perform this task. Both methods increase the cost of the magnet.

- For the accident case for the power outage, a circuit device is required to disconnect the winding due to the presence of the internal induced voltage.

- A constant speed operation with a direct network connection brings greater interpretation difficulties, which are discussed in details [17], and also the deviation from the rated speed of the overall system. As result the pitch angle is necessary [11].

For off-shore applications

Medium voltage transformer is used to connect the offshore wind power plant near the coast to the network. For offshore locations is currently a dc transmission via submarine cables favoured in order to avoid the creation of capacitive reactive power. This also helps to decouple the wind turbine from three phase network [23]. Even in onshore wind parks can be connected to a dc bus bar. Then dc bus bar is connected to network connection through an inverter and transformer. This configuration increases the overall efficiency compared to a large number of single coupling transformers. The connection of offshore wind park can be realised in three different configurations [34]:

- dc-string

- dc-star

- dc park

Either the transformer or a dc / dc converter voltage is used on the dc side. This depends on the voltage level. The permanent magnet synchronous gearless machine with uncontrolled rectifiers connect to dc network is the most reliable solution in offshore operation However, the rapid adjustment of the maximum power point no longer directly on the inverter made, but it has done though the pitch angle adjustment. This is a slow, inaccurate and lead to an additional burden on the rotor blades. Also additional oscillations will be present. Since practically there is no possibility to stabilise the machine, except by inserting a suitable damper winding. A disadvantage of permanent

magnet synchronous machine is the load depend voltage. A comparison high pole synchronous generator in connection with various configurations is discussed in [22]. When comparing permanently synchronous generators with diodes or IGBT converters, the latter configuration increases the efficiency in the partial load operation. However, the reliability effect for the diode rectification and makes this solution attractive for offshore applications. From the power system, especially the three phase transmission technology methods to compensate for reactive and distortion performance are known [20],[56],[60]. Active filter in series, parallel filters or combined series and parallel compensation filter are presented in [13],[96]. The series compensator is used to control the amplitude of the voltage and the phase. Parallel compensator is used to compensate the harmonic current [65]. These methods provide an attractive solution to constant magnet of the permanent magnet synchronous generator which will implemented in this research work.

1.2 Objectives of this research

In order to verify the theoretical analysis and simulation results a 25kVA synchronous generator, which is driven by a dc machine, is used as prototype of the complete wind power plant. The synchronous generator is feeding a dc network. The following terms were considered:

- Improving the performance of the permanent magnet synchronous machine connected to a dc grid through a diode rectifier regarding power factor and efficiency.

- Examining different types of active filters.

- Clarification of the power plant properties regulated during normal operation.

- Recommendations on the implementation of the permanent magnet synchronous machine with diode rectifier and active compensation filter based on normal operation

- Choose of the suitable control algorithm.

- Increase the output power of the synchronous generator.

- Stabilising the output voltage the synchronous generator.

1.3 Thesis outline

The following chapters in this thesis present the theoretical base, the simulation and the experimental result obtained. The problems that face the implementation of the permanent magnet synchronous generator are discussed in chapter two. The first problem is the dependency of the terminal voltage on the size of the magnet and impedance of the generator. Furthermore the generator is not capable of delivering the rated power at rated excitation. Mathematical derivation of the required reactive compensation for the fundamental frequency is considered at the beginning. Then numerical analysis is used to take the harmonics into consideration. Finally comparison between the active filter and hybrid is presented.

Chapter three focuses on modeling different components of the system, starting from the synchronous generator, the rectifier, dc network and the compensation voltage. The compensation voltage is realised by the inverter output voltage, which is filtered by LC filter and fed through the coupling transformer. A description and simulation of the space vector modulation is presented. The control strategy is also described and the derivation of controller is presented. Simulation results with and without compensation are evaluated. Finally the simulation results with passive and without passive filter are compared.

Chapter four focuses on modeling of the wind turbine and coupling between the wind turbine and synchronous generator. Chapter five presents the dimensioning and the construction of the experiment is described. The aim of chapter is to verify the proposed theory of the static synchronous series compensation applied to the permanent magnet synchronous generator in the pervious chapters. Chapter five provides also a discussion of the obtained results. Finally the efficiency of the system is calculated. Chapter six presents the conclusion and the results.

2

Reactive Power Compensation

This chapter focuses on the application of permanent magnet synchronous generator in wind power plant connected to dc grid. The terminal voltage of the generator depends on the internal induced voltage and synchronous impedance of the generator. The output power of the generator is limited by the fixed magnet. Different reactive power compensation configurations are discussed in order to solve these problems. The required reactive power compensation is deduced for the fundamental frequency at the beginning. Afterwards numerical analysis is presented to take the harmonics into consideration. Finally the implementation of the active filter and hybrid filter to the permanent magnet synchronous generator is compared.

2.1 Problem description

Actual tendency in the area of the wind power for high power plants in MW range has been realised. There are the variable speed operation, the direct drive coupling and the pitch control of rotor blades. Furthermore a continual increment of power stations in the megawatt class can be observed because of the installation costs. Besides the usage of induction machine in partial speed range, the high pole permanent magnet synchronous generator has many

future prospects [7],[63],[84]. Especially when operating offshore wind plant the maintenance issue becomes the overruling factor, since maintenance or replacement of major components as generator or gearbox is extremely difficult. Furthermore the well known advantages of permanent magnet synchronous generator are the high power to weight ratio and higher efficiency. Since this research work is concerned with the permanent magnet synchronous generator, the operating curve of synchronous generator feeding a dc grid should be obtained. A 25KVA electrical excited salient pole synchronous generator connected to dc machine through a rectifier bridge is tested in the lab by changing the excitation and the rotation speed as shown in fig 2-1.The generator was driven by dc controlled motor. The speed range from 1000 to 2000 rpm was chosen in order to resemble the operation of wind turbine taking into consideration the gearbox. The measurements indicated that the maximum output power of the synchronous generator increases with increase the rotation speed and the increment of the excitation voltage U_E as shown in fig. 2-2. In order to research the rated output power of the generator over excitation is necessary.

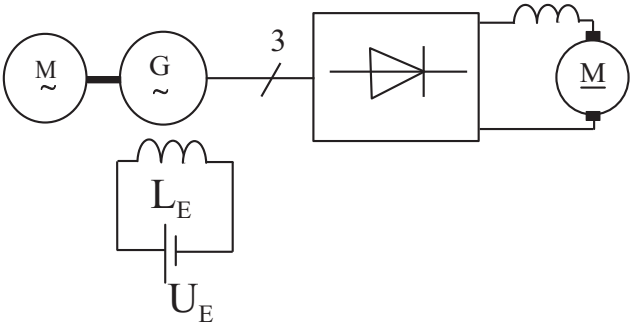

Fig. 2- 1 Layout of the experiment in the Lab

The measurement of synchronous generator at the rated rotation speed of 1500 rpm that the terminal voltage decreases with increment of the stator current due to the voltage drop on generator synchronous reactance and the generator resistance as shown in fig 2-3.

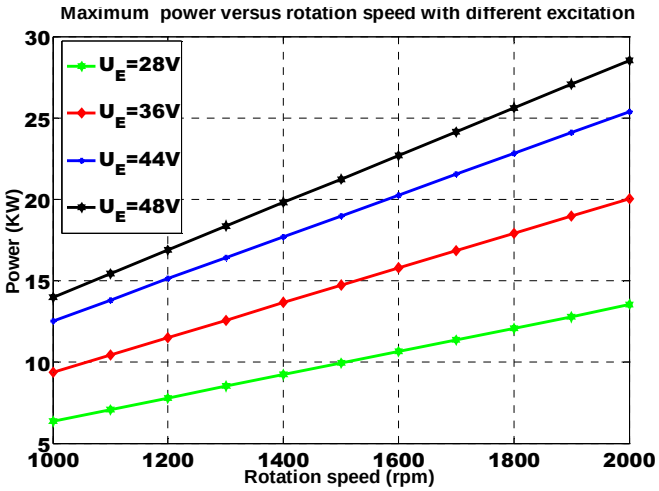

Fig. 2- 2 Measured output power versus rotation speed at different excitation levels

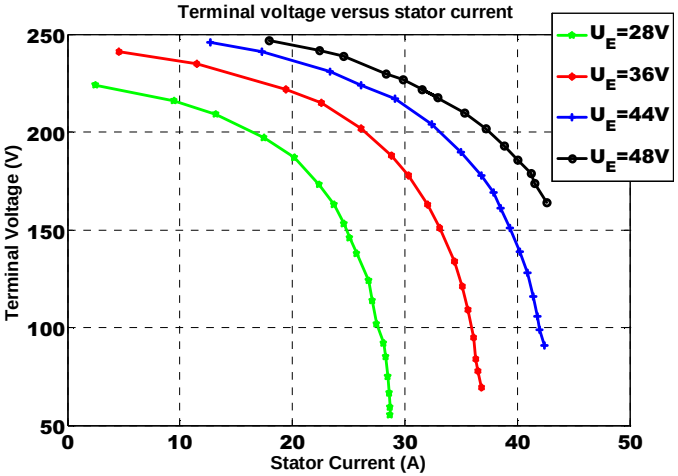

Fig. 2- 3 Measured terminal voltage versus stator current at different excitation levels

In order to analyse the previous measurement, it is necessary to build an equivalent circuit that describes the complete system. At first we will focus on the fundamental frequency and then afterwards we will consider the other harmonics. Here is the equivalent of the fundamental frequency, which is shown in fig 2-4.

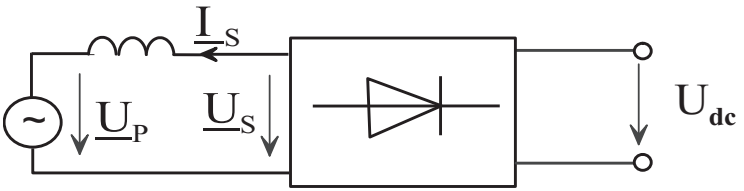

Fig. 2- 4 Equivalent circuit of the generator connected to dc grid

Regarding the equivalent circuit, we can write the following equation [67],[84]:

$$\underline{U}_S = \underline{U}_P + jX_S \underline{I}_S \qquad \textbf{(2-1)}$$

Where $\underline{U}_S=U_S e^{j\varphi}$ is the terminal voltage, $\underline{U}_P=U_P e^{j(\varphi+\delta)}$ is the internal induced voltage, $\varphi=\pi+\varphi_B$ is the angle between the terminal voltage and the current.

For simplicity the saliency of the generator and the resistance of the generator are neglected. X_S is the synchronous reactance of the generator. The terminal voltage U_S is function of the generator current I_S, the synchronous reactance and internal induced voltage. If we substitute in equation 2-1 with the terminal voltage and internal induced voltage, we obtain the following equation:

$$\underline{I}_S = -j\frac{U_S}{X_S}e^{j(\pi+\varphi_B)} + j\frac{U_P}{X_S}e^{j(\pi+\delta+\varphi_B)} \qquad \textbf{(2-2)}$$

If we rewrite the eq.2-2 of the current into the real and imaginary axis, where $I_K=U_p/X_S$ the steady state short circuit.

$$\frac{I_S}{I_K} = -\frac{U_S}{U_P}\sin\varphi_B + \sin(\varphi_B + \delta) \qquad \textbf{(2-3)}$$

$$0 = \frac{U_S}{U_P}\cos\varphi_B - \cos(\varphi_B + \delta) \qquad \textbf{(2-4)}$$

If we square the pervious equations 2-3 & 2-4 and add them together we can get rid of the power angle δ and we get the following equation:

$$(\frac{I_S}{I_K})^2 + (\frac{U_S}{U_P})^2 + 2\frac{U_S I_S}{U_P I_K}\sin\varphi_B = 1 \qquad \textbf{(2-5)}$$

Equation 2-5 presents a family of curves for constant internal induced voltage, which were obtained from the measurements. The phase diagram of the fundamental frequency in fig 2-5 shows that when the current increases from I_{s1} to I_{s2} the voltage drop on the generator reactance increases. As a result the terminal voltage of generator will also decrease from U_{S1} to U_{S2} for constant internal induced voltage U_p as shown in the phase diagram. This explains the measurements of the terminal voltage versus the generator current.

The increment in the generator current is accompanied with the increase in the output power till certain operating point, which depends on the excitation. If the excitation voltage increases, output power will increase also. Beyond this operating point increase in the generator current, the output power will decline as shown in fig 2-6.

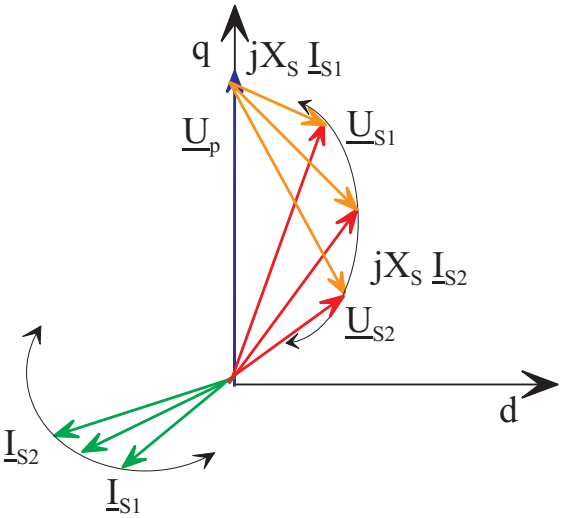

Fig. 2- 5 Phasor diagram of the generator to connected dc grid in operating points 1& 2

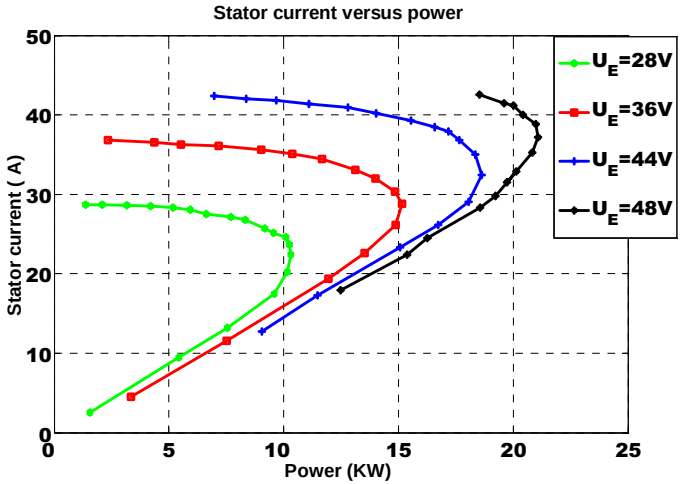

Fig. 2- 6 Measured stator current versus output power at different excitation levels

The reason for the decline in the output power is clear. If we look at the power factor versus power curve, we will recognise that the power factor declines slowly till the same operating point, which the further increase in the generator current will result in increasing the output power of the generator. Afterward the power factor will drop sharply with increase in the generator current and decline in the generator output power as shown in fig 2-6 and fig 2-7. This is due to the decrease of terminal voltage of the generator and the increase of the voltage drop on the synchronous reactance.

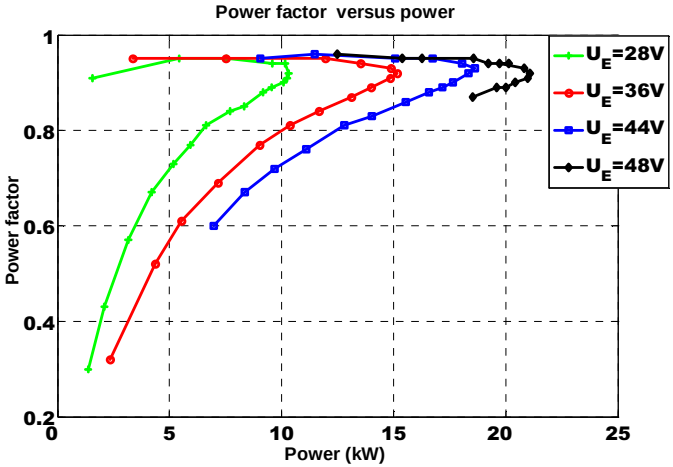

Fig. 2- 7 Measured power factor over output power at different excitation levels

The previous analysis reveals that our problem to provide variable source of reactive power to generator. As result the output power of the generator will increase and terminal voltage will become constant regardless of the variation of the loading. Since the generator is similar to the transmission lines, we will use the compensation methods applied to the transmission lines to the generator. The internal induced voltage presents the sending voltage, while the terminal voltage of the generator is similar to the receiving end voltage. The synchronous reactance is similar to the impedance of the transmission lines.

2.2 Reactive power compensation in transmission lines

Reactive power compensation corresponds to voltage control through controlling the reactive power in the transmission line, which in turn controls the voltage magnitude. The reactive power Q is needed by the electrical motor in order to produce the magnetic flux. This Reactive power is a steady state property and defined as the imaginary part of the complex value of the apparent power S

$$\underline{S} = \underline{U}_2 \underline{I}_S^* = P + jQ \qquad \textbf{(2-6)}$$

Consider that we neglect the resistance of the transmission line and consider only the reactance of the transmission line, which is connected to stiff bus as shown in fig. 2.8. The transfer of the active and reactive are coupled and given by the following equations [71]:

$$P = U_2 I_S \cos\varphi \qquad \textbf{(2-7)}$$

$$Q = U_2 I_S \sin\varphi \qquad \textbf{(2-8)}$$

Where U_1 is the sending end voltage, U_2 is the receiving end voltage; φ is the angle between the terminal voltage and current. This reactive current contributes to the effective value of the transmission line current. Thus the reactive current will increase the required current to deliver the active power to the load. This has also an influence on the efficiency of the transmission line since the transmission has also a resistance. The losses are directly proportional to the square of the current. The large amount of reactive power transfer causes significant voltage drop [82].

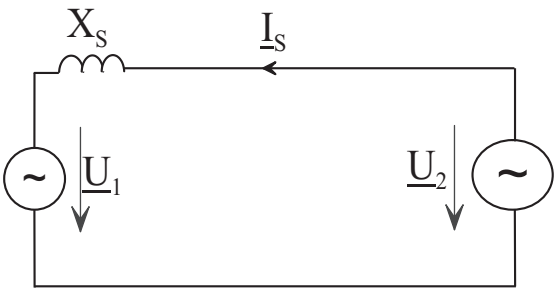

Fig. 2- 8 Equivalent circuit of the transmission line

Since our research is concerned with the permanent magnet synchronous generator, we have a fixed magnetic flux. This limits the output power of the generator and the terminal voltage will drop by loading. External reactive power compensation can provide the required reactive power to the load. External compensation also enables flat voltage profile despite of the increase of the delivered active power.

We will begin going by discussing different compensation methods applied to transmission line:

- Shunt capacitor
- Series capacitor
- Passive filter
- Shunt active filter
- Series active filter
- Hybrid filter
- United power quality conditioner

Shunt capacitors provide the simplest method of reactive power compensation and are used in many industrial plants and transmission lines. They are usually installed at the incoming of the plant in parallel with the load. Since the capacitive current leads the capacitive voltage by 90°, which corresponds, to reactive power generation. However the shunt capacitor must vary according to the variation of loading. The shunt capacitors have many advantages [75], [78]:

- Reduces the voltage drop in the transmission lines
- Reduces the losses in the transmission lines
- Reduces the size of the incoming transformers
- Reduction of the size of the cables

The Shunt capacitor improves power factor. The following equation presents delivered reactive power

$$Q_C = U_2^2 \omega C \qquad \textbf{(2-9)}$$

The following equation presents the required capacitance of shunt capacitor which is required to improve the power factor cos φ_{old} to cos φ_{new}:

$$C = \frac{P}{\omega U_2^2}(\tan\varphi_{old} - \tan\varphi_{new}) \qquad \textbf{(2-10)}$$

The phasor diagram of the improvement of the power factor resulting from the installation of the capacitor bank is illustrated in fig 2-10. It is obvious that the active power is constant. There is a decrease in the needed reactive power from the grid due to the presence of the capacitor bank, which deliver a portion of the required reactive power. As result the apparent power is reduced from S_{old} to S_{new} .

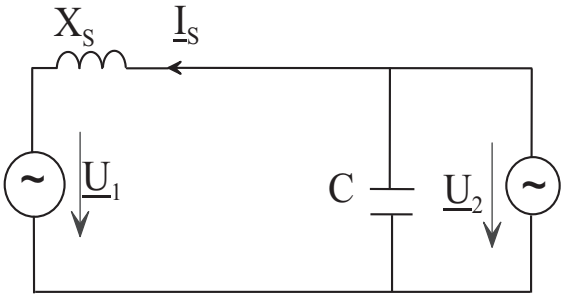

Fig. 2- 9 Shunt capacitor compensation

Thyristor controlled shunt capacitor provides more advanced solution. Such an alternative enables fast control of reactive compensation instead of using contactors for switching the capacitor.

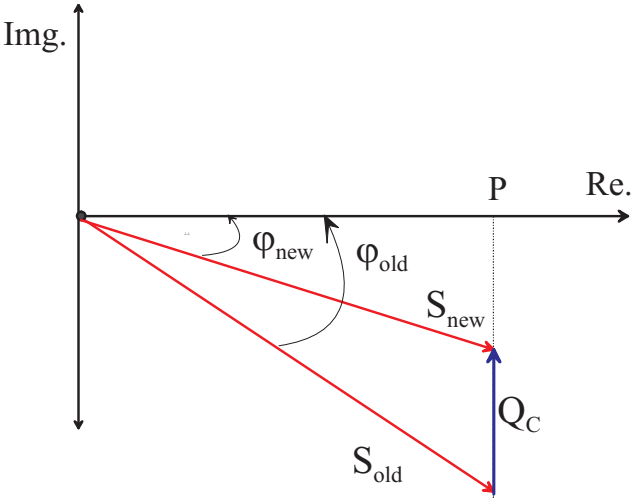

Fig. 2- 10 Phasor diagram of shunt compensation

Series capacitances with the transmission line act as reactive power compensation [89],[96]. The equivalent circuit is shown in fig 2-11. Series capacitor presents impedance opposite to the inductance of the transmission line. Thereby the overall voltage drop is reduced by the installations of the series capacitances.

The transmitted power can be increased through the transmission line by the connection of series capacitance because the overall impedance of the transmission line will be reduced. The power equation is given by eq. 2-11. Where δ is the power angle, X_C is the series capacitance.

$$P = -\frac{U_1 U_2 \sin\delta}{X_S - X_C} \qquad \textbf{(2-11)}$$

The generation of the usage non-sinusoidal current in the transmission line results from the presence the rectifiers and non-linear loads, which have non-linear characteristics. This fast change in the required reactive power of these loads for example the arc furnaces and the production of harmonics by the diodes, thysistor and other power electronic device has serious effects on the power system. Their effects include flicker and interference in industrial application in the transmission and distribution [2],[19],[87].

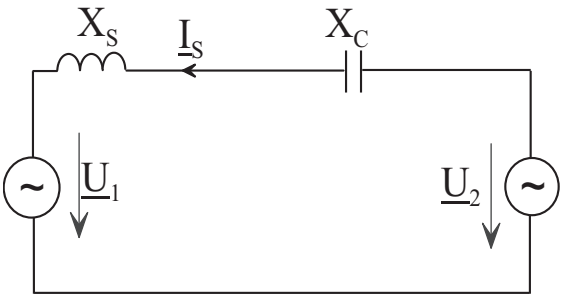

Fig. 2- 11 Series capacitor compensation

According to the Fourier analysis, every periodic waveform can be regarded as a summation of several sinusoidal waveforms with different frequencies,

i.e. the fundamental and multiple of the fundamental frequency. When we apply Fourier analysis to the non-sinusoidal current, we find out that it contains the fundamental frequency and harmonics of order 6k±1 where k is any positive integer. Current harmonics result distortion in the terminal voltage of the transmission line and increase the losses, which cause thermal stress. In non-sinusoidal system the reactive power is divided into the fundamental reactive power Q_1 and displacement power D, where I_1 is the fundamental current, where φ_1 is the angle between the fundamental voltage and current, where the apparent S is defined in the following equation and is illustrated in fig.2-12.

$$Q_1 = UI_1 \sin \varphi_1 \qquad \textbf{(2-12)}$$

$$D = U\sqrt{(I_2^2 + I_3^3 + ... + I_n^2} \qquad \textbf{(2-13)}$$

$$S^2 = P^2 + Q_1^2 + D^2 \qquad \textbf{(2-14)}$$

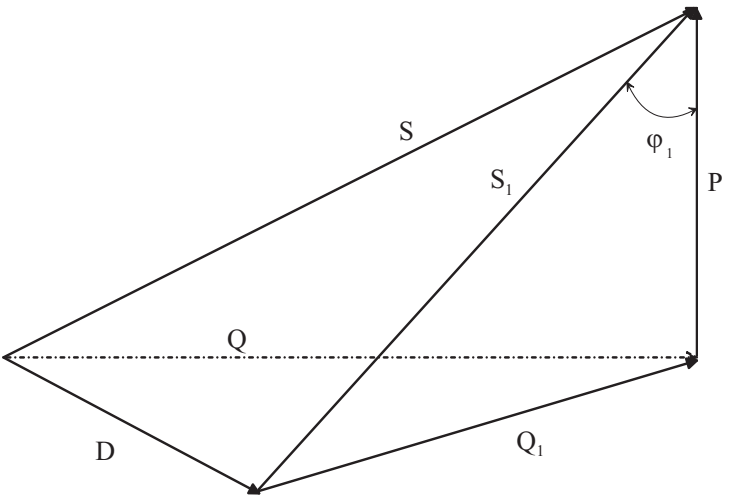

Fig. 2- 12 Power diagram for non-sinusoidal current

In order to get rid of the harmonics current, Shunt harmonic filter should be used as shown fig. 2-13. To achieve the best results, the harmonic filter should be located nearby the source of harmonic currents. Shunt passive filters reduced the harmonic by providing low impedance paths for the harmonic currents. The passive filter consists of LC filter tuned for specific harmonic. The shunt filter has the following problems [45]:

- The performance of passive filter depends on the system impedance at harmonic frequencies.
- The source impedance is not accurately known and change with system configuration.
- At certain frequency resonance occurs between the source and the shunt filter. This is called harmonic amplification.

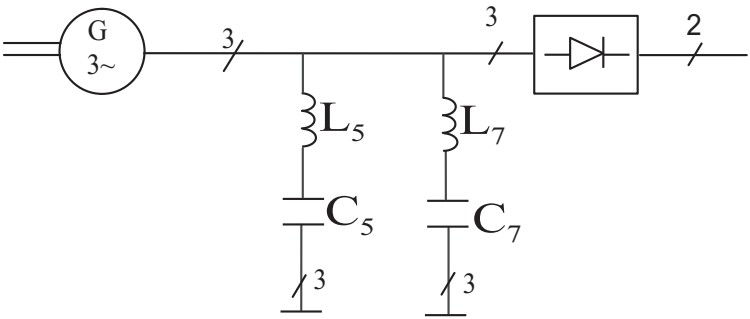

Fig. 2- 13 Passive filter for harmonic compensation

Shunt active filter consists of a controllable voltage or current source. They are similar to the PWM inverters used for ac motor drives. The voltage source converter (VSC) based shunt AF is the most common type used nowadays. The PWM converter should have a high switching rate in order to reproduce accurately the compensating currents [1],[30].

Normally the switching frequency is more than ten times the maximum frequency of the highest load current, which should be compensated. The shunt AF compensates the current harmonics by injecting equal but opposite harmonic compensating current. In this case the shunt active filter operates as a current source injecting harmonic components generated by the rectifier but phase shifted by 180°. The equivalent circuit of shunt active filter is shown in fig. 2-14. Also shunt active filter has own disadvantages [38], [49]:

- It is difficult to construct a large rated current source with a rapid current response.
- High initial cost and running costs.

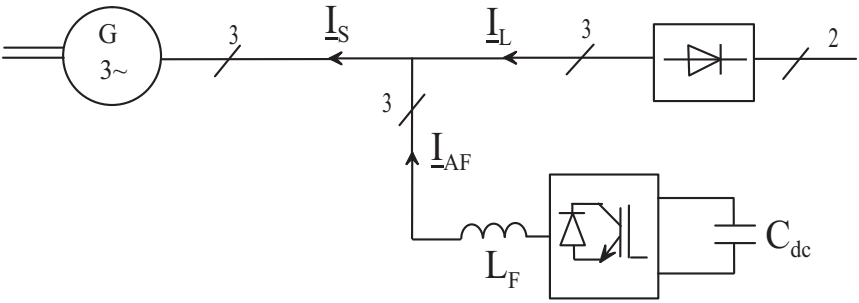

Fig. 2- 14 Shunt active filter for harmonic compensation

Series Active filter for voltage compensation can be generally considered as dual circuit of shunt active filter. Series Active filters are connected in series with the transmission line through a coupling transformer. VSC are suitable as the controlled source for series AF, the principal configuration of series AF are similar to shunt filter. The operation principle of AF series is the isolation of the harmonics between the load and the source.

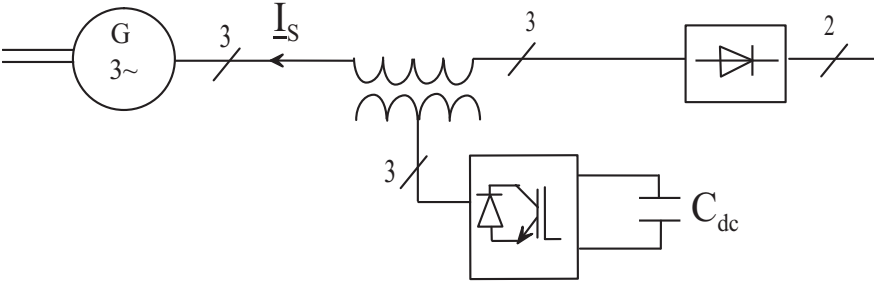

Fig. 2- 15 Series active filter

This goal is achieved by injecting the harmonic voltage through the coupling transformers. The equivalent source impedance can be considered infinite for the harmonics. It is considered ideally zero impedance for the fundamental frequency. Harmonic isolation is achieved by means of the infinite impedance for the current harmonics in series with the source [4], [5],[12].

Hybrid filter consists of a combination of shunt/series and shunt passive filters. The main goal of the hybrid filters is to decrease the cost and improve the efficiency. The passive filters reduce the harmonic content of the load whereas active filter isolates the rest of the harmonic content, which is not filtered by the passive filters. Furthermore the rating of the active filter can be decreased compared to active filter alone and thus reduce the cost [44],[103].

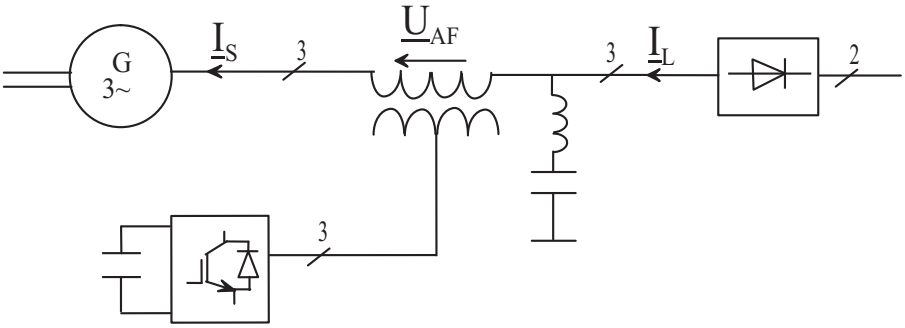

Fig. 2- 16 Hybrid filter for harmonic compensation

The optimal solution to harmonic reduction regarding performance is the combination of a shunt active filter as well as a series active filter with a common dc link [37]. This combination is called as unified power quality conditioner (UPQC). The function of UPQC is performed by both the series active filter and shunt active filter. The series active filter performs harmonic isolation while the shunt active filter performs harmonic current filtering and dc link voltage regulation by covering the losses of VSC and passive components.

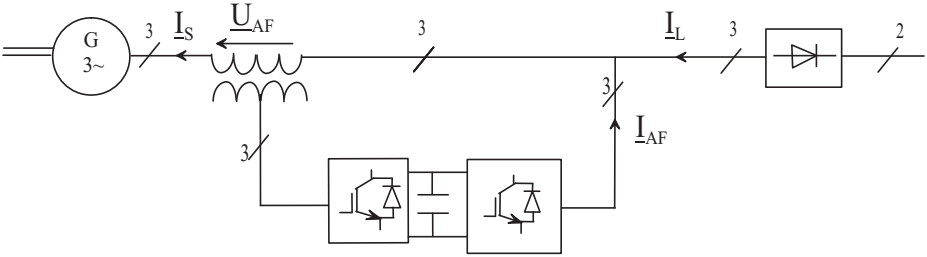

Fig. 2- 17 United power quality conditioner

The UPQC are applicable in power distribution systems close to loads that generate harmonic currents, which may affect other harmonic sensitive loads, connected to the same bus terminals. Table 2-1 specifies the tasks assigned to each active filter in UPQC approach [18],[25],[81].

Series active filter	**Shunt active filter**
To compensate supply voltage harmonics	To compensate load current harmonics
To block harmonic currents flowing to source	To compensate reactive power of the load
To improve stability	To regulate the capacitor voltage of the dc link

Table 2-1 Function series and shunt active in UPQC

2.3 Active power compensation

Our discussion was limited to the transmission line, now we will extend our discussion to synchronous generator. The output power equation of the synchronous generator, which is presented in eq. 2-15, showed that we have only three parameters to control since the magnet flux is constant. Static synchronous series compensator can change the impedance of the generator. Voltage regulator changes the terminal voltage while phase regulator changes the power angle. Static synchronous compensator (STATCOM) generates reactive power.

$$P = -3\frac{U_P U_S \sin\delta}{X_S} \qquad \textbf{(2-15)}$$

2.3.1 STATCOM

The STATCOM is mainly used in transmission lines in order to stabilise the voltage of the power system to maintain adequate voltage magnitude. When the load is increased, the actual power transmitted to the load will increase. If the power system is not able to provide the required reactive power, this will cause voltage instability. The STATCOM is usually installed in the middle of the transmission line. The STATCOM may also be located such that it divides the line into three equal parts in the case of very long transmission line. As result we will have constant voltage profile.

The main function of STATCOM is to generate the required reactive power. Its function is similar to that of an ideal synchronous machine whose reactive power is varied by excitation control [8],[13],[14]. The equivalent circuit of shunt compensation is shown in fig.2-18. The compensator current I_C is quadrature with the terminal voltage of the generator. It leads the terminal voltage with 90 degree as shown in the phasor diagram fig.2-19. Rectifier current is the summation of generator current I_S and the compensation current I_C as in eq. 2-18.

The internal induced voltage and terminal voltage are following:

$$\underline{U}_P = jU_P \qquad \underline{U}_S = \frac{U_S}{U_P}\underline{U}_P e^{-j\delta}$$

The voltage can be written as following with current resolved in d axis and q axis:

$$\underline{U}_S = \underline{U}_P + jX_{Sd}\underline{I}_{Sd} + jX_{Sq}\underline{I}_{Sq} \qquad \textbf{(2-16)}$$

The generator current is expressed in the following equation.

$$\underline{I}_S = \frac{U_S \cos\delta - U_P}{X_{Sd}} - j\frac{U_S \sin\delta}{X_{Sq}} \quad \textbf{(2-17)}$$

$$\underline{I}_N = \underline{I}_C + \underline{I}_S \quad \textbf{(2-18)}$$

STATCOM does not increase the electrical power as shown in eq. 2-19 but stabilises the terminal voltage of the generator as shown in eq. 2-20.

$$P = -\frac{3U_P U_S \sin\delta - 1.5U_S^2 \sin 2\delta}{X_{Sd}} - \frac{1.5U_S^2 \sin 2\delta}{X_{Sq}} \quad \textbf{(2-19)}$$

$$\underline{U}_S = jX\,\underline{I}_C \quad \textbf{(2-20)}$$

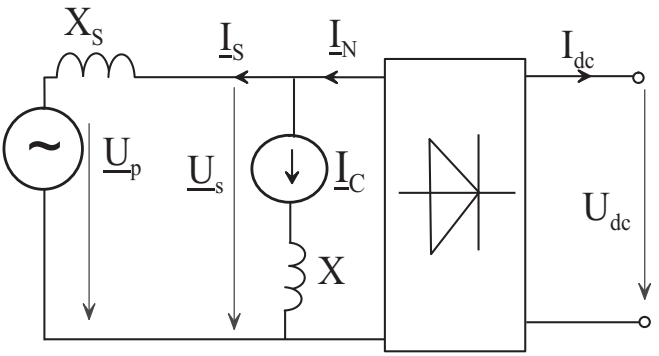

Fig. 2- 18 STATCOM applied to PSG

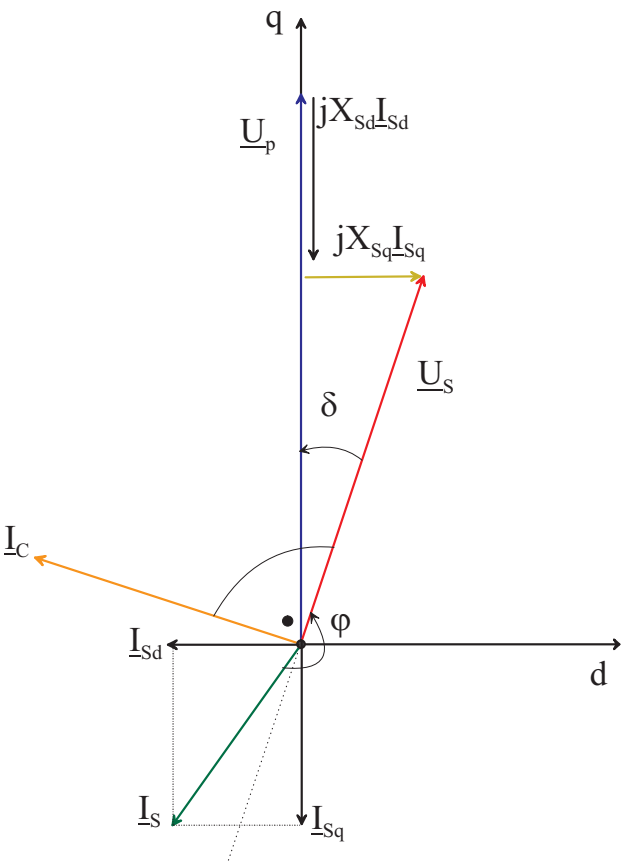

Fig. 2- 19 Phasor diagram of STATCOM applied to PSG

2.3.2 Phase regulator

The phase regulator is mainly used in transmission line in order to control the transmission angle to maintain balanced power flow in multiple paths or to control it in order to increase the transient and dynamic stabilities of the system. The main function of the phase regulator is the addition of an

appropriate quadrature component to the prevailing terminal voltage in order to increase its angle to the desired value [41],[73],[94]. The phasor diagram of the phase regulator compensation is shown fig. 2-20. U_C lags the terminal voltage by 90 degree. The current is calculated with eq. 2-21. The relationship between the power P and phase regulator U_C with considering the salient pole synchronous generator impedance is given by eq. 2-23.

$$\underline{U}_P = jU_P \qquad \underline{U}_S = \frac{U_S}{U_P}\underline{U}_P e^{-j\delta_o}$$

The voltage can be expressed as follows:

$$\underline{U}_S = \underline{U}_P + jX_{Sd}\underline{I}_{Sd} + jX_{Sq}\underline{I}_{Sq} - \underline{U}_C \qquad \textbf{(2-21)}$$

The generator current is the summation of the direct and quadrature current

$$\underline{I}_S = \frac{U_S\cos\delta_o - U_P - U_C\sin\delta_o}{X_{Sd}} - j\frac{U_S\sin\delta_o + U_C\cos\delta_o}{X_{Sq}} \qquad \textbf{(2-22)}$$

The output power is expressed in the following equation

$$P = -\frac{3U_PU_S\sin\delta_o - 3U_SU_C\sin^2\delta_o - 1.5U_S^2\sin 2\delta_o}{X_{Sd}} - \frac{1.5U_S^2\sin 2\delta_o + 3U_SU_C\cos^2\delta_o}{X_{Sq}} \qquad \textbf{(2-23)}$$

The phase regulator increases the output power of the generator, which is desired.

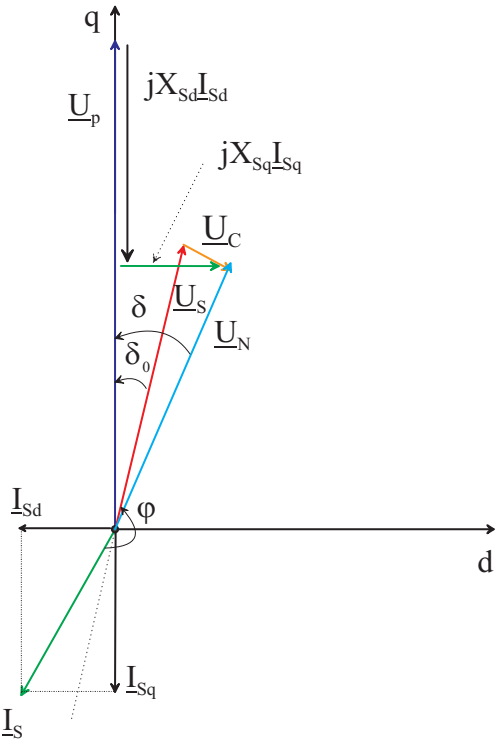

Fig. 2- 20 Phasor diagram of phase regulator applied to PSG

2.3.3 Voltage regulator

The main function of voltage regulator is the addition of an appropriate voltage in phase to the prevailing terminal voltage in order to increase its magnitude to the desired value [15],[28],[43]. The phasor diagram in fig. 2-21 shows the compensation voltage in phase with the terminal voltage. The

current is calculated by eq. 2-25. The relationship the power P and voltage regulator U_C with the considering saliency the pole generator impedance is given by eq.2-26.

The internal induced voltage and terminal voltage are following:

$$\underline{U}_P = jU_P \qquad \underline{U}_S = \frac{U_S}{U_P}\underline{U}_P e^{-j\delta}$$

The voltage can be expressed as follows:

$$\underline{U}_S = \underline{U}_P + jX_{Sd}\underline{I}_{Sd} + jX_{Sq}\underline{I}_{Sq} - \underline{U}_C \qquad \textbf{(2-24)}$$

The generator current is the summation of the direct and quadrature current

$$\underline{I}_S = \frac{U_S\cos\delta - U_P + U_C\cos\delta}{X_{Sd}} - j\frac{U_S\sin\delta + U_C\sin\delta}{X_{Sq}} \qquad \textbf{(2-25)}$$

The output power is expressed in the following equation

$$P = -\frac{3U_PU_S\sin\delta - 1.5U_SU_C\sin^2\delta - 1.5U_S^2\sin 2\delta}{X_{Sd}} - \frac{1.5U_S^2\sin 2\delta + 3U_SU_C\sin 2\delta}{X_{Sq}} \qquad \textbf{(2-26)}$$

The voltage regulator increases the electrical output power of the permanent magnet synchronous generator.

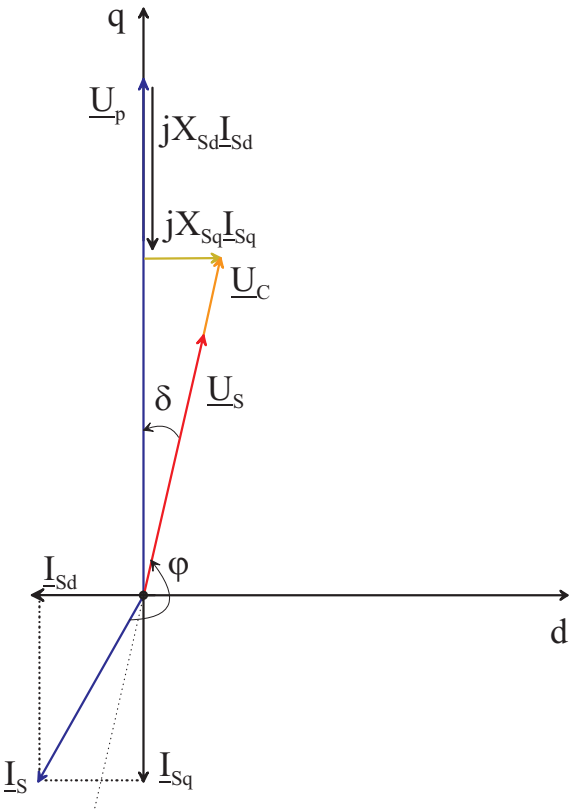

Fig. 2- 21 Phasor diagram of voltage regulator applied to PSG

2.3.4 Static synchronous series compensation

Static synchronous series compensation is mainly used in transmission lines in order to increase the transmitted power in the power system. It is immune to classical network resonance and provides controllable compensation voltage over identical capacitive and inductive range. The compensation voltage is independent from the magnitude of the line current. The main function of

SSSC is changing the impedance of the transmission line as if we are adding a capacitance or inductance by applying a compensation U_c which increases and decreases the voltage across the impedance respectively and thereby the current and power will increase or decrease respectively [42],[46],[97]. Fig. 2-22 shows the equivalent circuit of the SSSC. In order to apply SSSC, the angle φ between current and terminal voltage is about 180 degrees and because of the rectifier bridge, must be obtained. Then U_C lags the current angle by 90 degrees to act as a capacitor as shown in the phasor diagram in fig. 2-23. The relationship between output power P and compensation voltage U_C with considering salient pole synchronous generator impedance is given by eq.2-29. X_{Sd} is direct axis reactance, X_{Sq} is quadrature axis reactance.

The voltage can be written as follows:

$$\underline{U}_S = \underline{U}_P + jX_{Sd}\underline{I}_{Sd} + jX_{Sq}\underline{I}_{Sq} + \underline{U}_C \qquad \textbf{(2-27)}$$

The generator current is the summation of the direct and quadrature current

$$\underline{I}_S = \frac{U_S \cos\delta - U_P + U_C \sin(\delta+\varphi)}{X_{Sd}} - j\frac{U_S \sin\delta - U_C \cos(\delta+\varphi)}{X_{Sq}} \qquad \textbf{(2-28)}$$

The output power is expressed in the following equation

$$P = -\frac{3U_P U_S \sin\delta - 3U_S U_C \sin\delta \sin(\delta+\varphi) - 1.5U_S^2 \sin 2\delta}{X_{Sd}} - \frac{1.5U_S^2 \sin 2\delta - 3U_S U_C \cos\delta \cos(\delta+\varphi)}{X_{Sq}} \qquad \textbf{(2-29)}$$

The SSSC increases the electrical output power of the generator.

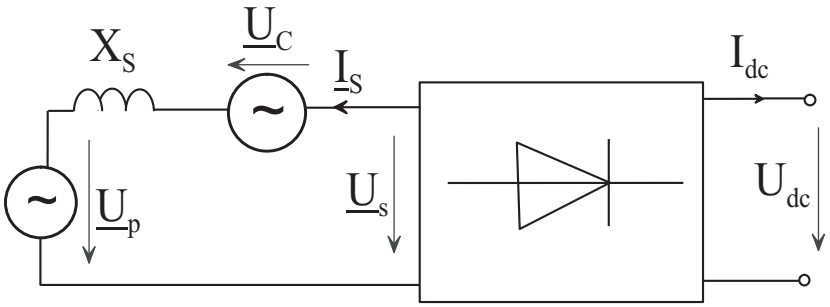

Fig. 2- 22 Series compensation equivalent circuit

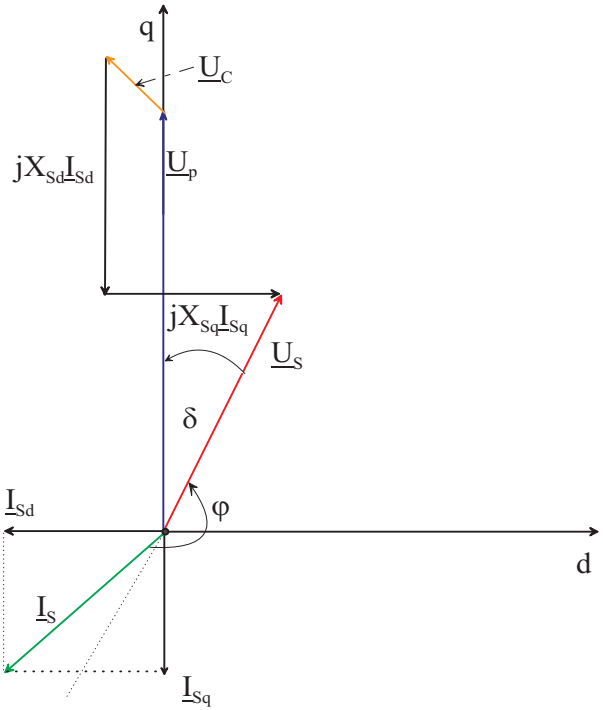

Fig. 2- 23 Phasor diagram of Series compensation applied to PSG

2.3.5 Analysis of different compensation methods

2.3.5.1 Required reactive power for different compensation

After we have obtained the equation for different compensation methods and we have concluded that STATCOM does not increase the output power of generator, the remaining compensation methods will be applied to PSG with reactance X_{Sd} and X_{Sq} are both 0.8 p.u. The output active power which results from different compensations with various excitation is over excited U_p/U_S=1.2, under excited U_p/U_S=0.8, and normal excited U_p=U_S are calculated.

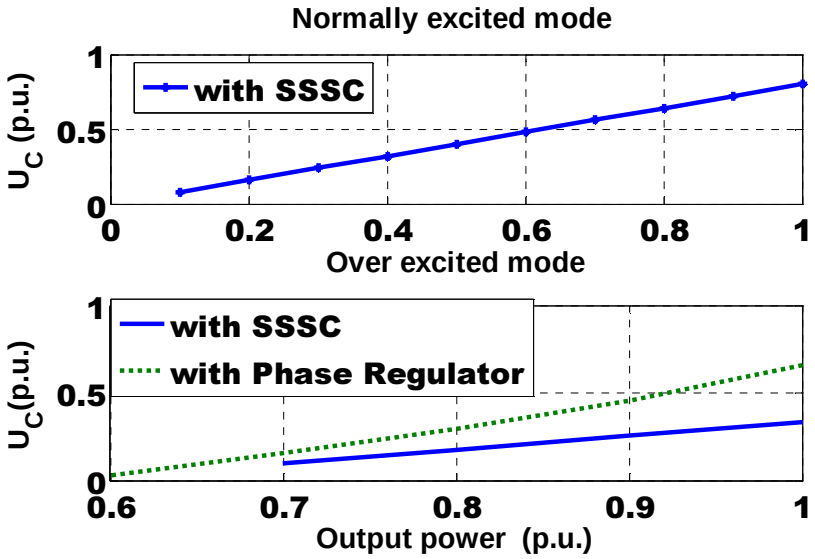

Fig. 2- 24 Required compensation voltage versus output power in normal and over excited mode

From the calculation at under excited the generator will not be able to provide the rated terminal U_S=1 p.u with the different compensation methods. The voltage regulator does not provide reactive power so the increase in active power will be accompanied with increase of required reactive power from the generator. As result we must increase the internal induced voltage U_p. Phase regulator provides reactive power but U_p must be greater than U_S. SSSC provides reactive power and it is the only method that can operate in the normal excited mode U_p=U_S.

Fig.2-24 shows the required compensation voltage versus power for different compensation methods for normal and over excited modes. Phase regulation requires about 40% more compensation voltage than SSSC at overexcited in order to obtain the same power. At normal excitation SSSC can also increase electric power up to the rated power. The required reactive power is more in the case of the phase regulation than SSSC. The required reactive power for both compensation methods in the over excited mode is shown in fig. 2-25.Phase regulation requires more reactive power than SSSC.

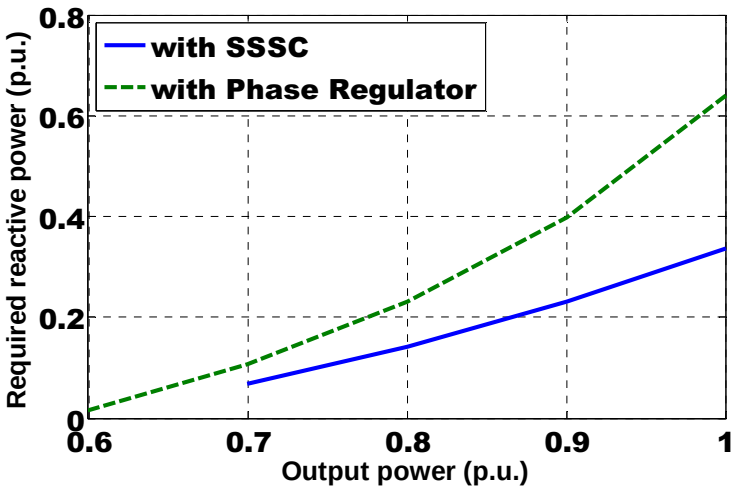

Fig. 2- 25 Required reactive power versus output power in over excited mode

2.3.5.2 Efficiency of inverter

In order to calculate the efficiency of each type of compensation, the losses in the inverter and in generator must be calculated. The losses as shown in eq. 2-30 represent conduction losses, switching off and on losses in the IGBT and switching off losses in the diode while the switching on losses in diode are neglected.

U_{CEO} is the threshold collector emitter voltage when the collector current is zero in the IGBT, r_{CE} is the on state resistance of IGBT, U_{FO} is the threshold of the diode, r_F is the on state resistance of the diode. cos φ is the power factor, m is the modulation index.

$$P_{Ltotal} = 6\left(P_{LfW/T} + P_{Lon/T} + P_{Loff/T} + P_{Loff/D} + P_{LfW/D}\right) \quad \textbf{(2-30)}$$

$$P_{LfW/T} = \frac{1}{2}\left(\frac{U_{CEO}}{\pi}\hat{i}_1 + \frac{r_{CE}}{4}\hat{i}_1^2\right) + m\cos\varphi\left(\frac{U_{CEO}}{8}\hat{i}_1 + \frac{r_{CE}}{3\pi}\hat{i}_1^2\right) \quad \textbf{(2-31)}$$

$$P_{LfW/D} = \frac{1}{2}\left(\frac{U_{FO}}{\pi}\hat{i}_1 + \frac{r_F}{4}\hat{i}_1^2\right) - m\cos\varphi\left(\frac{U_{Fo}}{8}\hat{i}_1 + \frac{r_F}{3\pi}\hat{i}_1^2\right) \quad \textbf{(2-32)}$$

f_s corresponds to the switching frequency, E_{on} and E_{off} are the turn on and turn off functions in the collector current energy of semiconductor and $\hat{i}_1$ is the fundamental amplitude of the inverter output current. These parameters E_{on}, E_{off}, U_{CEO}, r_{CE} and r_F are obtained from company data book [93].

$$P_{Loff+on/T} = \frac{1}{\pi} f_s (E_{off/T}(\hat{i}_1) + E_{on/T}(\hat{i}_1)) \quad \textbf{(2-33)}$$

$$P_{Loff/D} = \frac{1}{\pi} f_s E_{off/D}(\hat{i}_1) \quad \textbf{(2-34)}$$

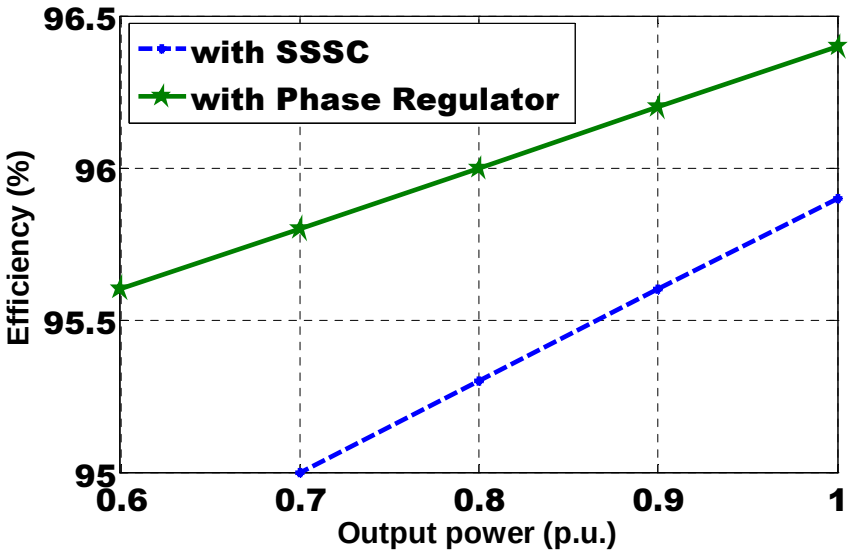

Fig. 2- 26 Efficiency of inverter with 2 kHz switching frequency in over excited mode

The inverter losses resulting from SSSC and phase regulation are calculated based on the fundamental frequency in the over excited mode. The efficiency of the different compensation methods has been calculated with considering the copper losses of the generator. The phase regulation will have better efficiency than SSSC about 0.6 % as shown in fig 2-26.

From the pervious calculation we can include that the required reactive compensation with SSSC is smaller than phase regulator. As result the rating of the inverter and the coupling transformers can be smaller than with phase regulation. The transformer apparent power is defined in eq.2-35. U_1 is the primary transformer voltage; I_1 is the primary transformer current. Figure 2-27 shows that the required rating of the coupling transformer for both phase regulation and SSSC in the over compensation mode. The rating of the transformer with phase regulation is bigger than with SSSC.

$$S_T = 3U_1 I_1 \qquad \textbf{(2-35)}$$

The other advantage is that SSSC does not need a power supply but needs only capacitor in dc link of the inverter. For these reasons SSSC method is used for this research work. Also the SSSC can be used to dampen the oscillation of the synchronous generator [64].

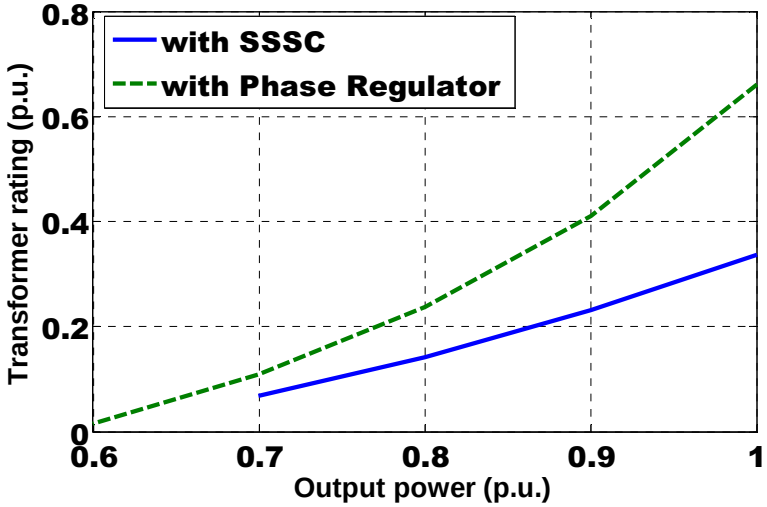

Fig. 2- 27 Transformer rating for different compensation methods

2.3.5.3 Determination of the required permanent magnet and the effect on the efficiency and the cost

In order to reach the most economical solution, we must calculate the required compensation voltage and the required mass of the permanent magnet. Here the calculation is made for surface mount permanent magnet generator. The required compensation voltage depends on ratio between the internal induced voltage U_P and the terminal voltage U_S. As the ratio U_P /U_S increases the required compensation voltage will decrease as shown in 2-24. This ratio of U_P/U_S will determine the amount of the required mass of permanent magnet for the generator [99],[101], [102]. On the other hand the cost of the generator will increase due to the cost of permanent magnet material. The required weight for a 360KVsurface mount permanent magnet synchronous generator is shown in fig 2-28. This generator has 130 poles.

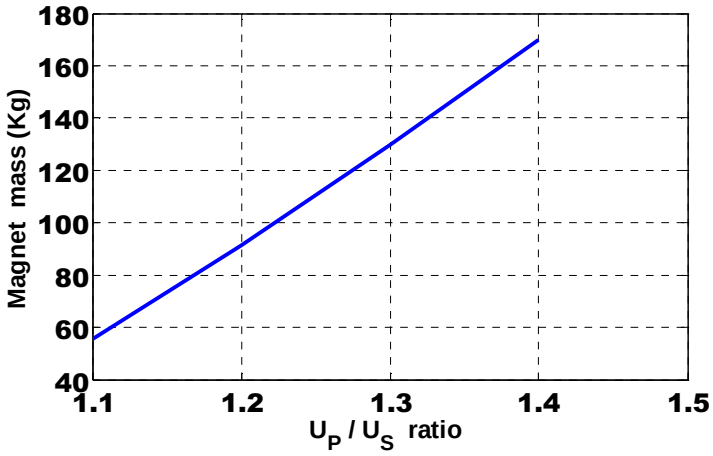

Fig. 2- 28 Required permanent magnet versus U_P/U_S ratio

The efficiency of the system including the generator, the inverter and the coupling transformers were calculated. Three different cases were calculated.

These different cases have the same output power. The first case is without SSSC at all. In this case permanent magnet is capable of providing the required reactive power, where U_P/U_S ratio is 1.4. The second case U_P/U_S ratio is 1.3 and SSSC compensation voltage is 0.21 p.u. is used. The third case U_P/U_S ratio is 1.2 and SSSC compensation voltage is 0.38 p.u. is used. The following curve shows the required compensation voltage, the required mass of the magnet permanent and the efficiency of the system. The turn ratio of the transformer is 1.5. The efficiency of the system without SSSC has the highest efficiency. This is due to the absence of the inverter and transformer losses. In the second case the system has better efficiency than the third case. This is due the smaller compensation voltage in the second case compared to the third case. This leads to smaller inverter and coupling transformer.

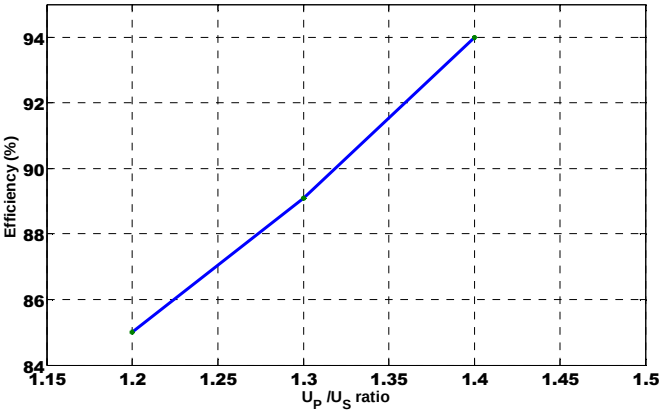

Fig. 2- 29 Efficiency of the systems with transformer turn ratio 1.5

Now the turn ratio of the transformer will be increased to 2. The efficiency of the system will increase. This is due to the decrease in the losses in the inverter. The following curve shows that the required compensation voltage, the required mass of the magnet permanent and the efficiency of the system with transformer.

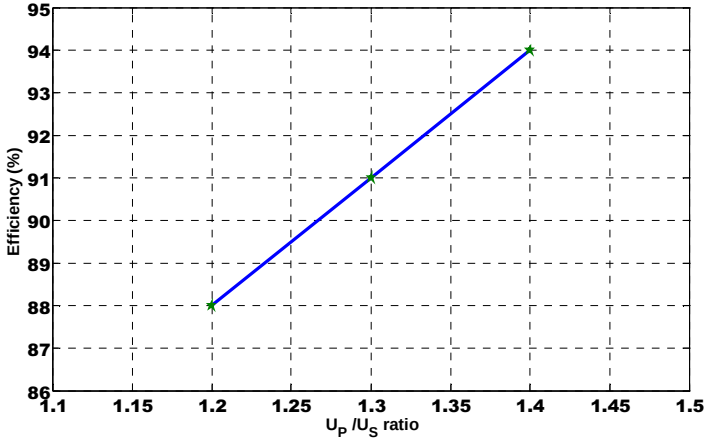

Fig. 2- 30 Efficiency of the systems with transformer turn ratio 2

Cost function including the different components of the system has to be developed. Based on this cost function an optimum solution has to be found. There must be a compromise between the cost of permanent magnet generator, the coupling transformer and the needed inverter. The generator cost function in eq. 2-36 [99],[101].

$$Cost_G = C_{Cu} m_{Cu} + C_{Fe} m_{Fe} + C_m m_m + Cost_{St} \qquad \textbf{(2-36)}$$

Here C_{Cu} is the cost of copper, which is 4Euro/Kg , m_{Cu} the mass of copper, C_{Fe} is the cost of iron which is 4Euro/Kg, m_{Fe} the mass of iron, C_m is the cost of NdFEB magnet, which is 100 Euro/Kg, m_m the mass of NdFEB magnet, $Cost_{St}$ is the cost of structure. The cost of the structure is estimated at 20870 Euro. The cost of the transformer is 62Euro / KVA according to HTT Company. The cost of inverter is 30 Euro/KW plus a fixed cost of 250 Euro according to SEMIKRON Company. The cost of the three different alternatives for 360KVA surface mounted PSG is calculated and is given in table 2-2.

U_P/U_S ratio	Compensation voltage U_C	Cost
1.4	0.0 p.u.	48177Euro
1.3	0.21 p.u	54926 Euro
1.2	0.38 p.u.	63350 Euro

Table 2-2 Cost of the system with different U_P/U_S ratios

The external compensation increases the cost of the system in general due to the cost of additional components of the system.

2.4 Hybrid Compensation

In our previous analysis we were concerned only with the fundamental frequency. Since the generator is feeding dc network through a rectifier, which has a non-linear characteristics, the generator current will be non-sinusoidal current. According to Fourier analysis, every periodic waveform can be regarded as the summation of several sinusoidal waveforms with different frequencies, i.e. the fundamental and multiple of the fundamental frequency.
In order to dimension the required compensation voltage in the presence and absence of the passive filter, the generator current must be first analysed.

To facilitate analysis, the following assumptions are made:

1) Valves are treated as ideal switches.

2) The dc current is not interrupted and free from ripple component.

3) The direct axis and quadrature axis impedance are assumed to be equal.

At the beginning the dc current I_{dc} is calculated based on the equivalent circuit, which is shown in fig 2-31. The dc current I_{dc} is expressed in eq 2-37. Where the U_{do} is th average dc voltage for the internal induced voltage and the compensation voltage at no load, R_x is the hypothetical resistance and U_{dc} is dc network voltage [79].

$$I_{dc} = \frac{U_{do} - U_{dc}}{R_X} \qquad \textbf{(2-37)}$$

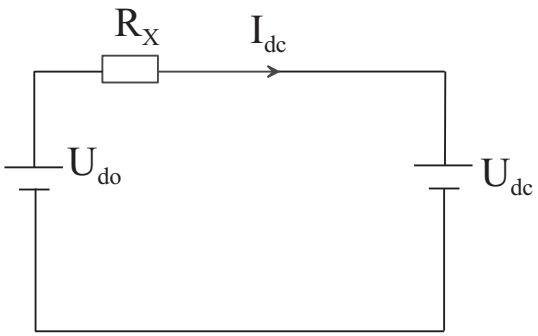

Fig. 2- 31 Dc equivalent circuit for current calculation

The load current I_L produced by the soothed dc current I_{dc} in the first half cycle [83]. The load current I_L is shown in the equivalent circuit in fig.2-32. The Fourier expansion of I_L is expressed in eq. 2-38.

$$I_L = \sum_{k=1,5,7...}^{\infty} (A_{Lk} \cos k\theta + B_{Lk} \sin k\theta) \qquad \textbf{(2-38)}$$

$$A_{Lk} = \frac{\sqrt{3} I_d (-1)^{l+1}}{\pi} [\frac{2 \sin k u_\mu}{k} + \frac{1}{1 - \cos u_\mu} \{\frac{-2 \sin k u_\mu}{k} + \frac{\sin(k+1)}{k+1}$$

$$+ \frac{\sin(k-1) u_\mu}{k-1}\}]$$

$$B_{Lk} = \frac{\sqrt{3} I_d (-1)^{l}}{\pi} [\frac{2 \cos k u_\mu}{k} + \frac{1}{1 - \cos u_\mu} \{\frac{2(1 - \cos k u_\mu)}{k} - \frac{1 - \cos(k+1)}{k+1}$$

$$- \frac{1 - \cos(k-1) u_\mu}{k-1}\}]$$

where $k = 6l \pm 1 (l = 0,1,2....)$

Where u_μ the overlap angle and calculation is based on the assumption that the inductance is infinitely large and given by

$$u_\mu = \cos^{-1}(1 - \frac{2X_S I_{dc}}{\sqrt{3}U_S}) \quad \textbf{(2-39)}$$

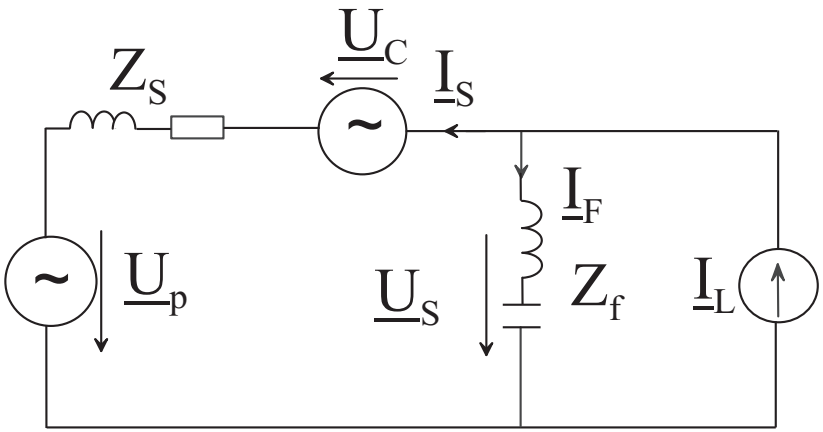

Fig. 2- 32 Equivalent circuit of SSSC and passive filter applied to PSG

Then the generator fundamental current is calculated using the equivalent circuit of the fundamental component, which is presented in fig.2-33. The equivalent of the fundamental frequency circuit consists of the generator internal induced voltage U_p with the fundamental frequency impedance of the synchronous generator and the SSSC compensation voltage. It is assumed

that the inverter does not produce any harmonics. The passive filter is in parallel with the generator and the rectifier is modelled as current source.

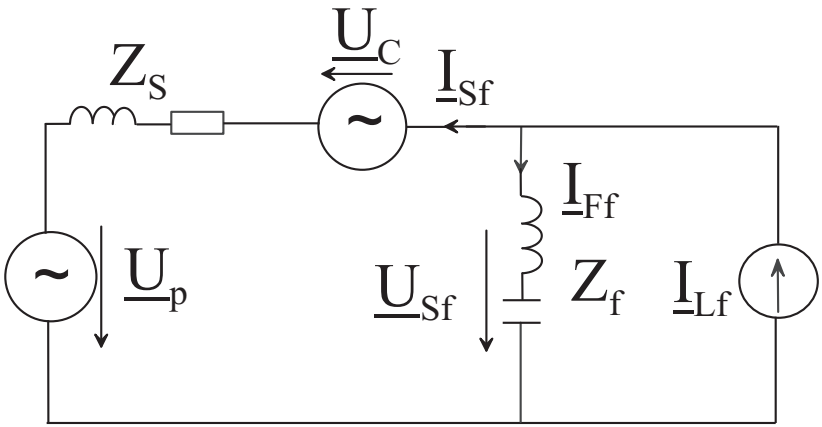

Fig. 2- 33 Equivalent circuit of SSSC and passive filter to applied to PSG of the fundamental frequency

The harmonics of the generator current are calculated using the equivalent circuit of the harmonic frequency, which is presented in fig.2-34. The equivalent circuit of the harmonic frequency consists of the impedance of the generator in parallel with the passive filter. The rectifier is modelled as a current source, where I_L is the rectifier equivalent current source. The generator harmonic current I_{Sk} and terminal harmonic voltage U_{Sk} are given by eq. 2-41 and eq. 2-42 respectively [58]. Each harmonic component of current can be calculated using equation 2-40. Since the impedance Z_F filter impedance is very small at the resonance frequency the harmonic current will flow into the filter and the terminal harmonic voltage U_{Sk} will be reduced [3],[27],[59].

$$I_{LK} = \sqrt{(A_{Lk}^2 + B_{Lk}^2)}/2 \qquad \textbf{(2-40)}$$

$$\underline{I}_{Sk} = \frac{\underline{Z}_F}{\underline{Z}_S + \underline{Z}_F} \underline{I}_{Lk} \quad \textbf{(2-41)}$$

$$\underline{U}_{Sk} = \frac{\underline{Z}_F \underline{Z}_S}{\underline{Z}_S + \underline{Z}_F} \underline{I}_{Lk} \quad \textbf{(2-42)}$$

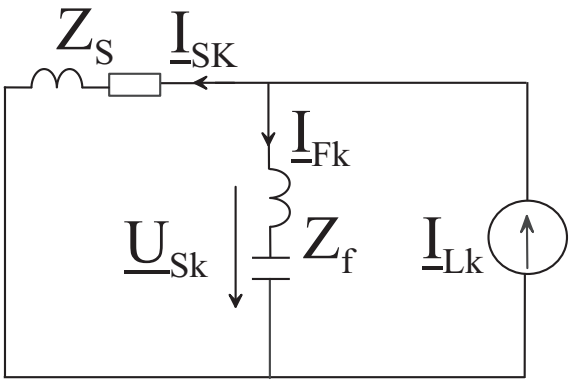

Fig. 2- 34 Equivalent circuit of SSSC and passive filter to applied to PSG of the harmonics frequency

The required compensation voltage is calculated for both cases with and without passive filter. The parameters of the electrical excited synchronous generator are used for this calculation. Table 5-1 contains the parameters of the generator. For both cases the internal induced voltage was 1.75 p.u and the machine was connected to 500V dc grid. The required compensation voltage with and without passive is presented in fig.2-35. The needed compensation voltage decreases with the installation of passive filter. This is due to the improvement in the power factor and the absence of the harmonic in the generator current and terminal voltage. The compensation voltage will be reduced by 17% by the installation of the passive filter with 0.2 p.u capacitance based on the fundamental frequency calculation. The calculation showed that passive filter with bigger capacitance, will reduce the required compensation voltage.

Passive filter is capacitive below the resonance frequency because capacitor is dominated. On the other hand the passive filter is inductive above the resonance frequency because the inductance is dominated. The passive filter with bigger capacitance will be able to provide more reactive power to the load. As result the required compensation voltage from the SSSC will be reduced.

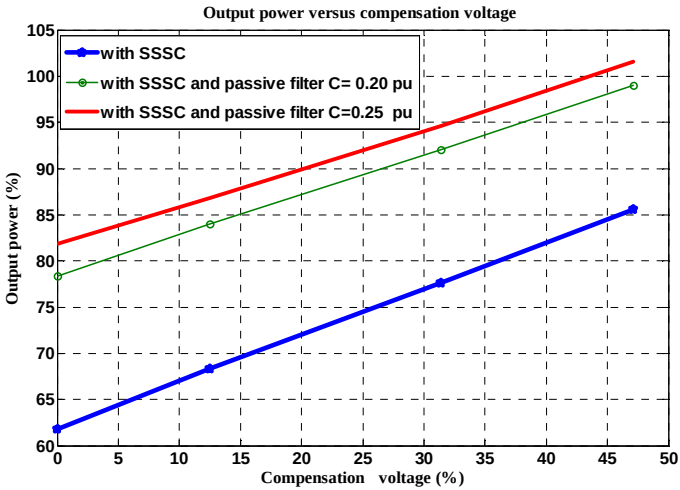

Fig. 2- 35 Calculation of the required compensation voltage

3

Simulation of Compensation Applied to Synchronous Generator

Different components of the system are modelled in this chapter. The system consists of the synchronous generator, the rectifier, dc grid, the inverter and the coupling transformers. The output voltages of the inverter are filtered by LC filter and are fed through the three single coupling transformers. Models of the coupling transformer and LC filter are developed. A description and simulation of the space vector modulation is depicted here. The control strategy is also described and the parameters of controller are deduced. Simulation results with and without compensation are discussed. Finally simulation of system with and without passive filter is evaluated.

3. 1 System components

3. 1.1 Space vector and transformation

Space vector is a mathematical description of the dynamic electrical operation of three-phase electrical system in eq. 3-1.

$$\begin{bmatrix} x_A \\ x_B \\ x_C \end{bmatrix} = \hat{x} \begin{bmatrix} \sin(\omega t) \\ \sin(\omega t - \frac{2\pi}{3}) \\ \sin(\omega t - \frac{4\pi}{3}) \end{bmatrix} \qquad \textbf{(3-1)}$$

The complex space vector is calculated from the three phase of the electrical system as defined as following:

$$\underline{x} = \frac{2}{3}(x_A + \underline{a}x_B + \underline{a}^2 x_C) \qquad \text{where } \underline{a} = e^{\frac{j2\pi}{3}} \qquad \textbf{(3-2)}$$

The magnitude x and phase angle ϑ for the polar presentation $\underline{x} = xe^{j\vartheta}$ is shown in fig 3-1. The space vector has properties of the three sinusoidal symmetrical systems, which are presented in equation eq. 3-3.The cartesian components x_α, x_β and x_o of the space vector $\underline{x}$ this transformation are defined as [35]:

$$\begin{bmatrix} x_A \\ x_B \\ x_C \end{bmatrix} = \begin{bmatrix} 1 & 0 & 1 \\ -\frac{1}{2} & \frac{\sqrt{3}}{2} & 1 \\ -\frac{1}{2} & -\frac{\sqrt{3}}{2} & 1 \end{bmatrix} \begin{bmatrix} x_\alpha \\ x_\beta \\ x_0 \end{bmatrix} \qquad \textbf{(3-3)}$$

The inverse transformation is present in the following equation. These can be transformed into the cartesian components x_α, x_β and x_o.

$$\begin{bmatrix} x_\alpha \\ x_\beta \\ x_0 \end{bmatrix} = \frac{2}{3} \begin{bmatrix} 1 & -\frac{1}{2} & -\frac{1}{2} \\ 0 & \frac{\sqrt{3}}{2} & -\frac{\sqrt{3}}{2} \\ \frac{1}{2} & \frac{1}{2} & \frac{1}{2} \end{bmatrix} \begin{bmatrix} x_\mathrm{A} \\ x_\mathrm{B} \\ x_\mathrm{C} \end{bmatrix} \qquad \textbf{(3-4)}$$

With the help of the transformation in a rotating coordinates and inverse transformation, there are presented in the following equations

$$\begin{bmatrix} x_d \\ x_q \end{bmatrix} = \begin{bmatrix} \cos\vartheta & \sin\vartheta \\ -\sin\vartheta & \cos\vartheta \end{bmatrix} \begin{bmatrix} x_\alpha \\ x_\beta \end{bmatrix} \qquad \textbf{(3-5)}$$

$$\begin{bmatrix} x_\alpha \\ x_\beta \end{bmatrix} = \begin{bmatrix} \cos\vartheta & -\sin\vartheta \\ \sin\vartheta & \cos\vartheta \end{bmatrix} \begin{bmatrix} x_d \\ x_q \end{bmatrix} \qquad \textbf{(3-6)}$$

The previous type of coordinate transformation is called parks transformation. This transformation is the amplitude invariant but the power invariant transformation the amplitude changes and 2/3 is replaced with the square of this value. The transformation helps to reduce the computation time that is needed by the microprocessor.

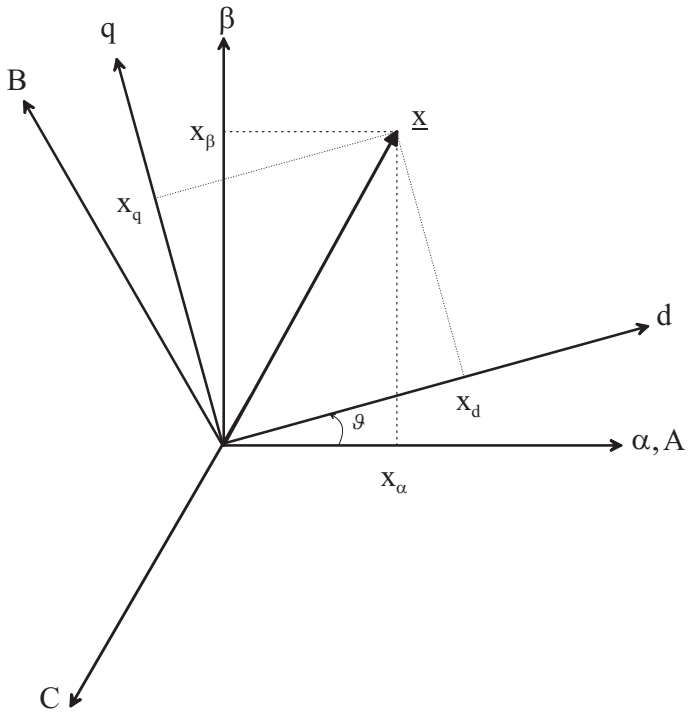

Fig. 3- 1 Diagram of different coordinates

The direct transformation from the symmetrical system to the rotating coordinate can be seen by the following matrix

$$\begin{bmatrix} x_d \\ x_q \\ x_o \end{bmatrix} = \frac{2}{3} \begin{bmatrix} \cos\vartheta & \cos(\vartheta - \frac{2\pi}{3}) & \cos(\vartheta + \frac{2\pi}{3}) \\ -\sin\vartheta & -\sin(\vartheta - \frac{2\pi}{3}) & -\sin(\vartheta + \frac{2\pi}{3}) \\ \frac{1}{2} & \frac{1}{2} & \frac{1}{2} \end{bmatrix} \begin{bmatrix} x_A \\ x_B \\ x_C \end{bmatrix} \qquad \textbf{(3-7)}$$

The inverse transformation from two phase rotating to three phase system is presented in eq. 3-8.

$$\begin{bmatrix} x_A \\ x_B \\ x_C \end{bmatrix} = \frac{2}{3} \begin{bmatrix} \cos\vartheta & -\sin\vartheta & 1 \\ \cos(\vartheta - \frac{2\pi}{3}) & -\sin(\vartheta - \frac{2\pi}{3}) & 1 \\ \cos(\vartheta + \frac{2\pi}{3}) & -\sin(\vartheta + \frac{2\pi}{3}) & 1 \end{bmatrix} \begin{bmatrix} x_d \\ x_q \\ x_0 \end{bmatrix} \quad \textbf{(3-8)}$$

3.1.2 Electrical excited synchronous generator

A synchronous generator is an ac machine whose frequency of the stator voltage under steady state conditions is proportional rotor rotation speed. The magnetic field is created by the stator current rotating at the same speed as that created by the field current or the permanent magnet on the rotor, which rotates with synchronous speed. The synchronous machine has an alternating current in the stator and dc supply in the rotor. The synchronous machine consists of two types, which are cylindrical and salient pole generator. The cylindrical rotor is used for a two and a four pole generator. The salient pole construction is better adapted to multipolar slow speed hydroelectric generators. The current and power factor of the generator are determined by the generator field excitation, impedance of the generator and the load. In normal steady state operation, the electromagnetic torque balances the mechanical torque applied to the shaft. The synchronous machine can be used in different applications as follows:

- In a generator operation, the prime mover torque acts in the direction of the rotation of the rotor, pushing the rotor mmf wave ahead of the resultant air gap flux. Also the internal induced voltage leads the terminal voltage by power angle δ. In over excited mode, the internal induced voltage is greater than the terminal voltage so the generator provides reactive power to grid while in under excited mode the

generator the internal induced voltage is smaller than the terminal voltage and takes reactive power from the grid.

- In a motor operation, the resultant air gap is flux ahead of the rotor mmf wave. Also the internal induced voltage lags the terminal voltage by power angle δ. In over excited mode, the internal induced voltage is greater than the terminal voltage so the motor provides reactive power to grid while in an under excited mode the motor the internal induced voltage is lower than the terminal voltage and takes reactive power from the grid.

- In a synchronous condenser operation, the synchronous machine in over excited mode provides reactive power to grid while in under excited mode the machine takes reactive power from the grid. In this case the machine obtains the required active power from the grid in order to cover in losses.

The mathematical model of the electrical excited synchronous generator with damping windings is depicted in the following equations. The following assumptions were considered [68],[85]:

- The phase symmetrical winding in the stator
- Sinusoidal flux in the air gap
- No zero current component
- Linear magnet path

The used generator in the experiment is electrical excited salient pole synchronous generator with damper winding. The equation of the stator and rotor is transformed to coordinates system, which rotates with the rotor. The real axis presents the d-axis while the imaginary presents the q-axis. The voltage relation for the stator can be written in stator coordinates as follows:

$$\underline{u}_S^s = R_S \underline{i}_S^s + \dot{\underline{\psi}}_S^s \qquad \textbf{(3-9)}$$

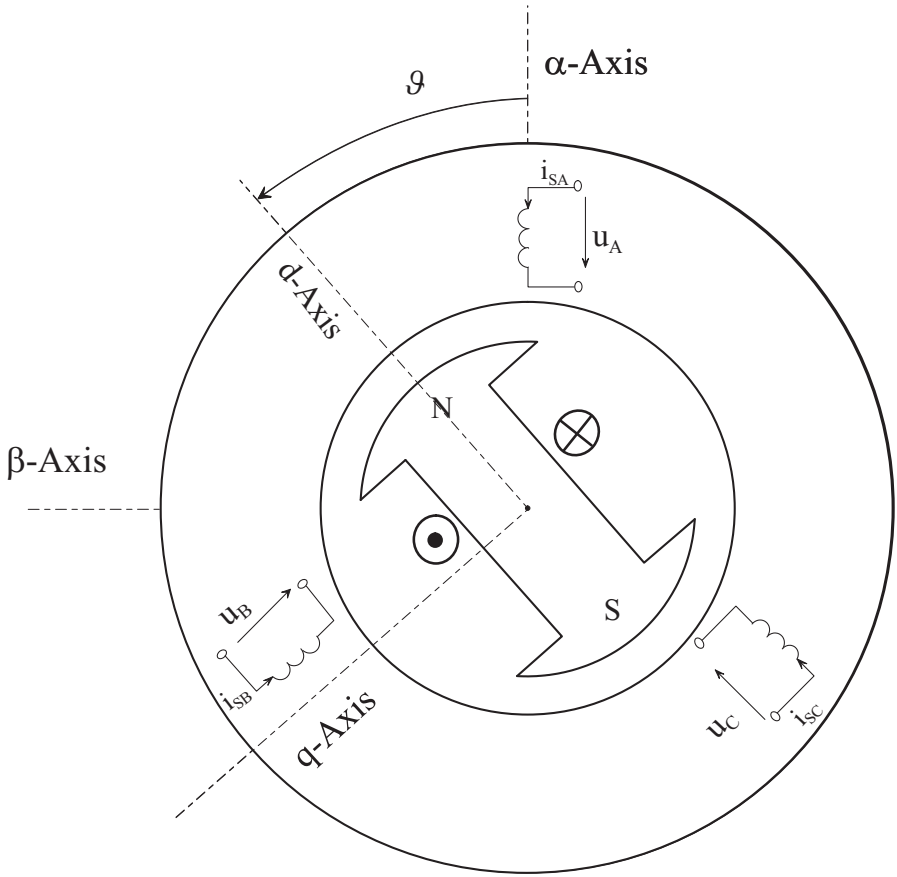

Fig. 3- 2 Schematic diagram of salient pole synchronous generator

Despite the stator windings note a time varying inductance due to the saliency of the rotor, the transformation of the stator winding to a frame rotating with rotor will let the stator see a constant magnetic path. This makes the transformation concept very useful.

In order to transform in the rotor coordinate we must multiply by $e^{j\vartheta}$ and differentiate it, the eq. 3-10 is obtained.

$$\underline{u}_S^s e^{j\vartheta} = R_S \underline{i}_S^s e^{j\vartheta} + \dot{\underline{\psi}}_S^s e^{j\vartheta} + \underline{\psi}_S^s j\omega e^{j\vartheta} \qquad \textbf{(3-10)}$$

Then we divide by $e^{j\vartheta}$ the stator equation is referring to the rotor coordinates

$$\underline{u}_S^r = R_S \underline{i}_S^r + \dot{\underline{\psi}}_S^r + \underline{\psi}_S^r j\omega \qquad \textbf{(3-11)}$$

The index will not be used from now on for simplicity. The equation will be resolved into the real and imaginary axis. The following equations are obtained.

$$u_{Sd} = R_S i_{Sd} + \dot{\psi}_{Sd} - \omega\psi_{Sq} \qquad \textbf{(3-12)}$$

$$u_{Sq} = R_S i_{Sq} + \dot{\psi}_{Sq} + \omega\psi_{Sd} \qquad \textbf{(3-13)}$$

The voltage equation of rotor field is presented in the below in eq. 3-14.

$$u_E = R_E i_E + \dot{\psi}_E \qquad \textbf{(3-14)}$$

The damper bars in the rotor of the synchronous generator are used to dampen the electromechanical oscillation and to stabilise the generator. The damper bars are short circuited together at the end of the rotor, forming a structure which appears much like the squirrel cage in the induction motor and whose function is similar. The damper bars are presented by two damper circuits one in the direct axis and the other in quadrature-axis, which are presented below:

$$0 = R_{Dd} i_{Dd} + \dot{\psi}_{Dd} \quad \textbf{(3-15)}$$

$$0 = R_{Dq} i_{Dq} + \dot{\psi}_{Dq} \quad \textbf{(3-16)}$$

The flux linkage equations in d-q coordinates for the stator and the rotor are presented by the following equation

$$\psi_{Sd} = L_{Sd} i_{Sd} + M_{SDd} i_{Dd} + M_{SE} i_E \quad \textbf{(3-17)}$$

$$\psi_{Sq} = L_{Sq} i_{Sq} + M_{SDq} i_{Dq} \quad \textbf{(3-18)}$$

$$\psi_E = L_E i_E + M_{DE} i_{Dd} + \frac{3}{2} M_{SE} i_{Sd} \quad \textbf{(3-19)}$$

$$\psi_{Dd} = L_{Dd} i_{Dd} + \frac{3}{2} M_{SDd} i_{Sd} + M_{DE} i_E \quad \textbf{(3-20)}$$

$$\psi_{Dq} = L_{Dq} i_{Dq} + \frac{3}{2} M_{SDq} i_{Sq} \quad \textbf{(3-21)}$$

where L_{Sd} is the direct axis synchronous inductance, M_{SDd} is the mutual inductance between the d-axis in stator and d axis damping winding in rotor, L_{Sq} is quadrature axis synchronous inductance, M_{SDq} is the mutual inductance between the q-axis stator and q-axis damping winding in rotor, L_E is the inductance of excitation winding, M_{DE} is the mutual inductance between the excitation winding and d-axis damping winding in rotor, M_{SE} is the mutual inductance between the d-axis stator winding and d axis damping winding in

rotor, L_{Dd} is the self inductance the d-axis damping winding, L_{Dq} is the self inductance the q-axis damping winding

Through substitution and simplification the flux equation can be presented in term of the time constants of the synchronous generator in the following equations. These time constants can be determined using experimental method which will be explained later.

We substitute eq. 3-21 in eq.3-16 and divide by R_{Dq}. Then we transform to Laplace, we obtain

$$0 = i_{Dq}(1 + sT_{Dq}) + i_{Sq} sT_{SDq} \qquad \textbf{(3-22)}$$

Where $T_{Dq}= L_{Dq}/R_{Dq}$, $T_{SDq}= M_{SDq}/R_{Dq}$

After solving the pervious equation and we get:

$$i_{Dq} = -i_{Sq} \frac{sT_{SDq}}{1 + sT_{Dq}} \qquad \textbf{(3-23)}$$

We substitute eq.3-23 in eq. 3-18 we get

$$\psi_{Sq} = L_{Sq} i_{Sq} \left(1 - \frac{M_{SDq}^{2}}{L_{Sq} L_{Dq}} \frac{sT_{Dq}}{1 + sT_{Dq}} \right) \qquad \textbf{(3-24)}$$

We substitute in eq. 3-24 by $\sigma_{SDq} = 1 - \frac{M_{SDq}^{2}}{L_{Sq} L_{Dq}}$, we get

$$\psi_{Sq} = L_{Sq} i_{Sq} \frac{1 + s\sigma_{SDq} T_{Dq}}{1 + sT_{Dq}} \qquad \textbf{(3-25)}$$

We substitute in eq. 3-25 by $T_{qo}^{``} = \sigma_{SDq} T_{Dq}$ and $T_{q}^{``} = T_{Dq}$ we get

$$\psi_{Sq} = i_{Sq} L_{Sq} \frac{1 + sT_{q}^{``}}{1 + sT_{qo}^{``}} = i_{Sq} L_{q}(s) \qquad \textbf{(3-26)}$$

Where $L_q(s) = L_{Sq} \dfrac{1 + sT_{q}^{``}}{1 + sT_{qo}^{``}}$

If we apply the same procedure, we can obtain the following equations:

$$\psi_{Sd} = L_d(s)\ i_{Sd} + G_E(s)\ u_E \qquad \textbf{(3-27)}$$

$$i_E = B(s) i_{Sd} + A(s) u_E \qquad \textbf{(3-28)}$$

Where $L_d(s) = \dfrac{s^2 T_d^{``} T_d^{`} + s(T_d^{`} + T_d^{``}) + 1}{s^2 T_{do}^{``} T_{do}^{`} + s(T_{do}^{`} + T_{do}^{``}) + 1} L_{Sd}$

Where $G_E = \dfrac{T_{do}^{`}}{(1 + sT_{do}^{`})} \dfrac{L_{Sd} - L_{Sd}^{`}}{L_E}$

$$A(s) = \frac{T_{do}^{`}}{1 + sT_{do}^{`}} \frac{1}{L_E},\ B(s) = \frac{L_{Sd}^{`} - L_{Sd}}{L_E} \frac{sT_{do}^{`}}{1 + sT_{do}^{`}}$$

The time constants are defined in table 3-1. The electrical induced torque of the synchronous generator is presented by the following equation

$$m_{el} = \frac{3}{2} z_p \, \mathrm{Im}\left\{ \underline{\psi}_S^{\bullet} \underline{i}_S \right\} \qquad \textbf{(3-29)}$$

Where $\underline{\psi}_S = \psi_{Sd} + j\psi_{Sq}$, $\underline{i}_S = i_{Sd} + j i_{Sq}$

Time Constant	Description
T_q''	Quadrature axis short circuit subtransient time constant
T_{qo}''	Quadrature axis open circuit subtransient time constant
T_d''	Direct axis short circuit subtransient time constant
T_{do}''	Direct axis open circuit subtransient time constant
T_d'	Direct axis short circuit transient time constant
T_{do}'	Direct axis open circuit transient time constant

Table 3-1 Definition of generator time constants

We substitute in eq. 3-29, we obtain eq. 3-30

$$m_{el} = \frac{3}{2} z_p \, \mathrm{Im}\{(\psi_{Sd} - j\psi_{Sq})(i_{Sd} + j i_{Sq})\} \qquad \textbf{(3-30)}$$

$$m_{el} = \frac{3}{2} z_p \, \mathrm{Im}\{\psi_{Sd} i_{Sd} + j\psi_{Sq} i_{Sq} - j\psi_{Sq} i_{Sd} + \psi_{Sq} i_{Sq}\} \qquad \textbf{(3-31)}$$

We obtain the torque of the synchronous by separating the imaginary part of eq. 3-31.

$$m_{el} = \frac{3}{2} z_p (\psi_{Sd} i_{Sq} - \psi_{Sq} i_{Sd}) \qquad \textbf{(3-32)}$$

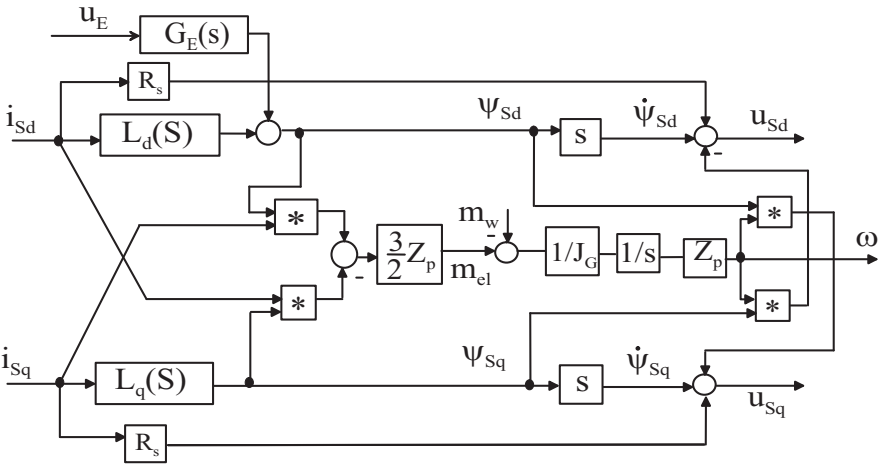

Fig. 3- 3 Equivalent circuit of the electrical excited synchronous generator

The electromechanical equation for synchronous machine is presented below

$$m_{el} - m_w = J_G \frac{d\omega_m}{dt} \qquad \textbf{(3-33)}$$

Where m_w the load torque, J_G the moment of inertia. Now we have completed the model of the electrical excited synchronous generator, which is available in the lab.

3.1.3 Permanent magnet synchronous generator

The model of the permanent magnet synchronous generator will be presented in this section. The equation of the stator and rotor are transformed to coordinates system, which rotates with the rotor as the electrical excited. The real axis presents the d-axis while the imaginary presents the q-axis. The voltage relation for the stator can be written in stator coordinates as follows:

$$\underline{u}_S^s = R_S \underline{i}_S^s + \dot{\underline{\psi}}_S^s \qquad \textbf{(3-34)}$$

The pervious equation is transformed to rotor coordinate and resolved into real and imaginary axis. We obtain the following equations:

$$u_{Sd} = R_S i_{Sd} + \dot{\psi}_{Sd} - \omega \psi_{Sq} \qquad \textbf{(3-35)}$$

$$u_{Sq} = R_S i_{Sq} + \dot{\psi}_{Sq} + \omega \psi_{Sd} \qquad \textbf{(3-36)}$$

The flux equation in d-q coordinates for the stator is presented in the following equation, where ψ_P is the flux of the permanent magnet

$$\psi_{Sd} = L_{Sd} i_{Sd} + \psi_P \qquad \textbf{(3-37)}$$

$$\psi_{Sq} = L_{Sq} i_{Sq} \qquad \textbf{(3-38)}$$

The electrical induced torque of the synchronous generator is presented by the following equation

$$m_{el} = \frac{3}{2} z_p \, \mathrm{Im}\left\{\underline{\psi}_S^* \underline{i}_S\right\} \qquad \textbf{(3-39)}$$

We obtain the electrical torque of the synchronous by separating the imaginary part of eq. 3-39.

$$m_{el} = \frac{3}{2} z_p (\psi_{Sd} i_{Sq} - \psi_{Sq} i_{Sd}) \qquad \textbf{(3-40)}$$

The electromechanical equation for synchronous machine is presented below

$$m_{el} - m_w = J_G \frac{d\omega_m}{dt} \qquad \textbf{(3-41)}$$

The model of the permanent magnet synchronous generator is driven and equivalent circuit is shown fig. 3-4.

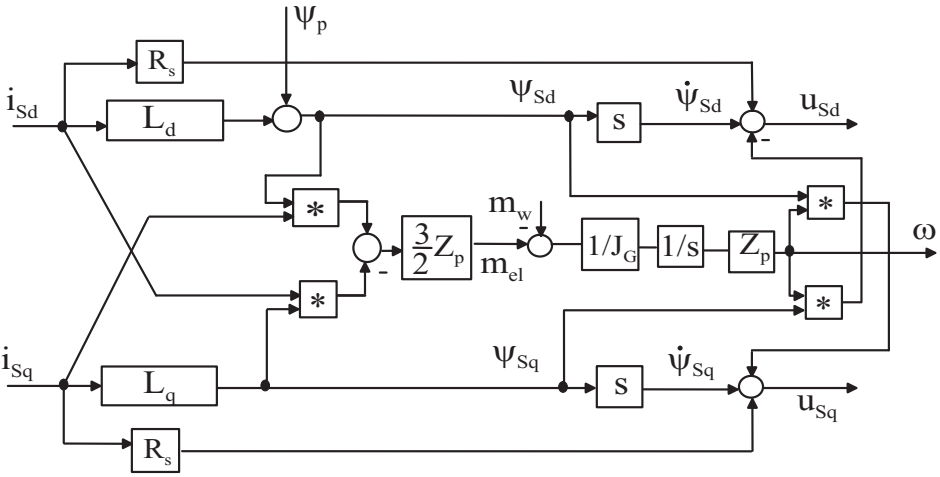

Fig. 3- 4 Equivalent circuit of permanent magnet synchronous generator

3.1.4 Coupling transformer model

The transformer consists of two windings interlinked by mutual magnetic flux. If one of these is connected alternating voltage source, an alternating voltage will be produced in the secondary, whose amplitude will depend on the primary voltage and number of turns. Transformer operation mainly depends on the mutual flux linking the two winding. This operation can be placed in air core but it will be much more effective in the iron core. The equivalent circuit diagram of the actual equivalent circuit is presented in fig 3-5.

In engineering analyses involving the transformer, it is customary to adopt several approximations, such as neglecting the shunt branch that represents the exciting current. This does not affect the accuracy of the model of the transformer. The series branch combined resistance and leakage reactance are referred to the same side as shown in fig 3-6.

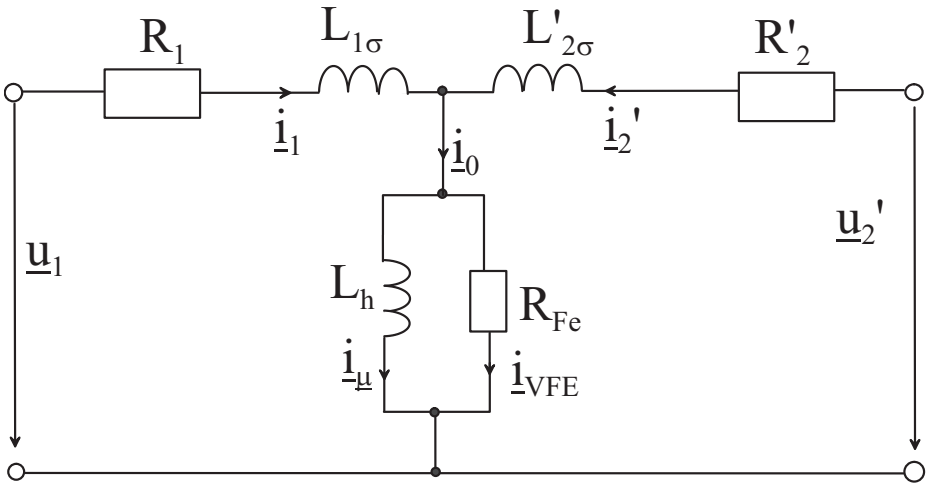

Fig. 3- 5 Equivalent circuit of the transformer

The equations of transformer are transformed to a reference frame fixed to the rotor of the synchronous generator.

$$\underline{u}_1 = \underline{u}_2^{'} + (R_1 + R_2^{'})\underline{i}_1 + j\omega(L_{1\sigma} + L_{2\sigma}^{'})\underline{i}_1 + (L_{1\sigma} + L_{2\sigma}^{'})\frac{d\underline{i}_1}{dt} \quad \textbf{(3-42)}$$

By resolving in a real and an imaginary axis, we will obtain the following equation

$$\begin{aligned} u_{1d} + ju_{1q} &= u_{2d}^{'} + ju_{2q}^{'} + (R_1 + R_2^{'})i_{1d} + j(R_1 + R_2^{'})i_{1q} \\ &+ j\omega(L_{1\sigma} + L_{2\sigma}^{'})i_{1d} - \omega(L_{1\sigma} + L_{2\sigma}^{'})i_{1q} + (L_{1\sigma} + L_{2\sigma}^{'})\dot{i}_{1d} \\ &+ j(L_{1\sigma} + L_{2\sigma}^{'})\dot{i}_{1q} \end{aligned} \quad \textbf{(3-43)}$$

We separate the real d axis from imaginary q axis in eq. 3-43 so we get the following equation

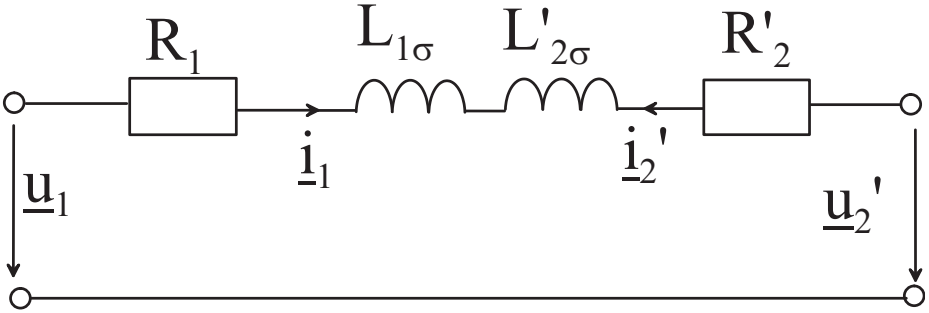

Fig. 3- 6 Simplified equivalent circuit of the transformer

$$u_{1d} = R_T i_{1d} + L_T \dot{i}_{1d} - \omega L_T i_{1q} + u_{2d}^{'} \quad \textbf{(3-44)}$$

$$u_{1q} = R_T i_{1q} + L_T \dot{i}_{1q} + \omega L_T i_{1d} + u'_{2q} \qquad \textbf{(3-45)}$$

Where $L_T = L_{1\sigma} + L'_{2\sigma}$, where $R_T = R_1 + R'_2$

Now the model of the coupling transformer is completed, where the secondary impedance is referred to the primary side of the transformer. The parameter of the model is obtained through the open circuit test and short circuit test of the three single-phase transformers found in the lab. In the short circuit the current should not exceed the rated current of the transformer. As a result we decrease the applied voltage to about 5% of the rated voltage. In the open circuit test the rated voltage is applied to the transformer, in this case the current is about 5%.

3.1.5 Rectifier bridge and dc network

In principle, both a diode and thyristor bridge could be used as a rectifier circuit, since the diode bridge does not have a firing circuit. As a result diode is more robust so it is used here. The equivalent circuit is shown in fig. 3-7. The load is via three-phase half wave connection, which is the upper diodes, the return current path via another half wave connection, which is the lower diodes, to the three-phase supply. In order to explain the principle of three-phase diode bridge rectifier, a real rectifier is idealised.

In order to drive the rectified output voltage waveform, we will consider that two diodes, which are conducting, are those connected to the lines with the highest voltage between at that instant. This means when U phase is the most positive phase diode D_1 conducts. During this period W phase is the most negative diode D_2 conducts. When V phase becomes the most negative so the diode D_6 conducts. The load voltage U_d follows in turn six sinusoidal voltages during one cycle. These voltages have the maximum value of the line voltage. The average value of the load voltage is given in the following equation:

$$U_d = \frac{2}{2\pi/6}\int_0^{2\pi/6}\sqrt{3}U\cos\theta\, d\theta = \frac{3\sqrt{3}}{\pi}U \qquad \textbf{(3-46)}$$

Each diode conducts the full load current for one third of a cycle. There dc grid is modeled as a dc voltage source with small resistance and small inductance.

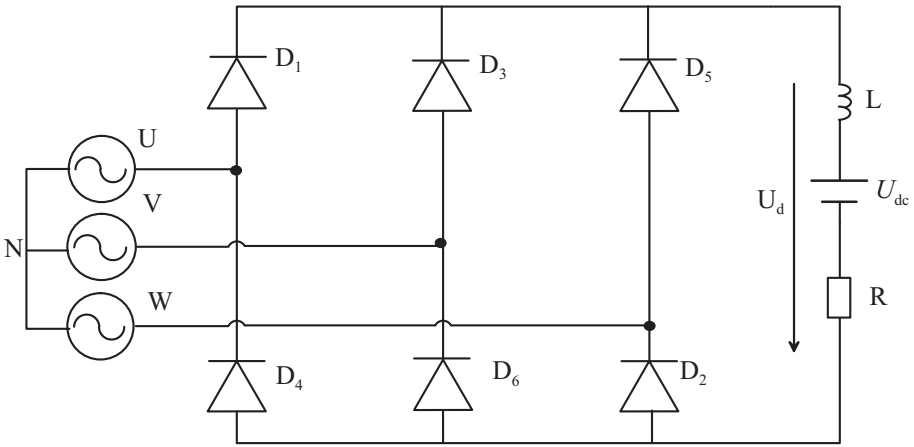

Fig. 3- 7 Schematic diagram of the rectifier

3.1.6 Space vector modulation voltage source

The VSC is the main component of the SSSC, since it is responsible for the generation of the compensation voltage. The common topology of the VSC has been used in shown in fig 3-8 as shown. This converter is known as the six pulses forced commutated converter. The converter consists of a six-semiconductor device for example the Insulated Gate Bipolar Transistor

(IGBT). Each leg consists of two valves. The restriction is that only three from the six values are conducting but only one of valve in each leg can be turned on at the same time in order to avoid short circuit. The output voltage referring to the middle point of dc link voltage is determined by the status of the conducting value. Each voltage is either $U_{dc}/2$ when the upper value is conducting or $-U_{dc}/2$ when the lower value is conducting.

The two- level converter is the simplest circuit configuration that can be used to build up a three phase forced commutated converter. Using multi-level converters with square wave modulation or using two or three level converters with a pulse width modulation scheme can reduce the harmonic content of the voltage. The reason why the three level bridge reduces the harmonic content, even with a square wave modulation because it enables three different voltage levels at the output voltages ($U_{dc}/2$, 0, $-U_{dc}/2$).

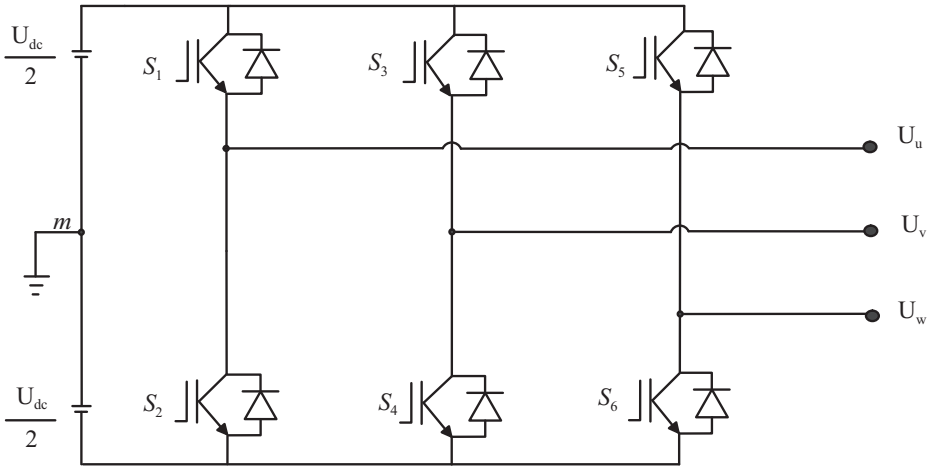

Fig. 3- 8 Schematic diagram of the inverter

As a result of the rapid development of power semiconductors and microprocessors, the implementation of sophisticated switching sequences employed in inverters can be applied, such as a space vector modulation

[24]. The modulation index of the space vector modulation is bigger than the modulation index of sinusoidal pulse width modulation by about 15%. Furthermore harmonic content of the inverter output voltages and currents is less for the space vector method than its counterpart. As result this will reduce the losses and torque pulsations in induction motors [74],[88]. There are eight different combinations, see table 3-2. Let the positive state be 1 when the upper IGBT is turned on and the negative state is 0 when the lower IGBT is turned on.

Vector	Phase u	Phase v	Phase w
u_0	0	0	0
u_1	1	0	0
u_2	1	1	0
u_3	0	1	0
u_4	0	1	1
u_5	0	0	1
u_6	1	0	1
u_7	1	1	1

Table 3-2 Standard voltage vector

In order to obtain the eight possible standard voltage vectors u_0, u_1.. u_7, the rotating vector voltage u_W must be produced. The voltage vector u_W can be analysed to the right component u_r and the left component u_l. The rotating voltage u_W has a maximum value of $2U_{dc}/3$. In order to implement u_{Wmax} the standard vector must have the following values

$$\left| \underline{u}_W \right|_{\max} = \left| \underline{u}_1 \right| = ... = \left| \underline{u}_6 \right| = \frac{2}{3} \cdot U_{dc} \qquad \textbf{(3-47)}$$

u_W equal to vector addition of the left component u_l and the right component u_r. In order to realise any required u_W we must change the switching time of the right component time T_r and the left component time T_l because we are

bounded with two vectors in each sector. For example, If u_W is very near u_l so the T_l will be greater than T_r, on the other hand if u_W is very near to u_r so T_r will be greater than T_l.

$$T_r = \frac{T_p}{2} \cdot \frac{\left| \underline{u}_r \right|}{\left| \underline{u}_W \right|_{\max}} \Rightarrow \text{Switching time for right vector} \qquad \textbf{(3-48)}$$

$$T_l = \frac{T_p}{2} \cdot \frac{\left| \underline{u}_l \right|}{\left| \underline{u}_W \right|_{\max}} \Rightarrow \text{Switching time for left vector} \qquad \textbf{(3-49)}$$

For the rest of the pulse period the zero vectors are switched according to eq. 3-50.

$$\underline{u}_W = \underline{u}_r + \underline{u}_l + \underline{u}_{0,7} \qquad \textbf{(3-50)}$$

$$\underline{u}_W = \frac{2 \cdot T_r}{T_p} \cdot \underline{u}_1 + \frac{2 \cdot T_l}{T_p} \cdot \underline{u}_2 + \frac{2 \cdot \left[T_p/2 - \left(T_r + T_l \right) \right]}{T_p} \cdot \underline{u}_{0,7} \qquad \textbf{(3-51)}$$

u_W can be analyzed into two components $u_{W\alpha}$ and $u_{W\beta}$ so that

$$\left| \underline{u}_W \right| = \sqrt{{u_{W\alpha}}^2 + {u_{W\beta}}^2} \qquad \textbf{(3-52)}$$

Using the two components $u_{W\alpha}$ and $u_{W\beta}$, we calculate the left component of the voltage u_l and the right component of the voltage vector u_r from table 3-3 in the different sectors.The space vector modulation has its limitation also. The previous discussion has shown that every reference u_W is realisable but in practice this is not the case. If we implement this maximum case voltage vector u_W and substitute in the previous equation, the scalar addition of the switching time T_r and T_l will be bigger than the half the pulse period T_p.

$$T_{\Sigma} = T_r + T_l = \frac{\sqrt{3}}{2} T_p \left| \frac{u_W}{U_{dc}} \right| \cos(30^\circ - \gamma) \qquad \textbf{(3-53)}$$

Sector	Quadrant	Right vector $\lvert \underline{u}_r \rvert$	Left vector $\lvert \underline{u}_l \rvert$
S1	Q1	$\lvert u_{W\alpha} \rvert - \frac{1}{\sqrt{3}} \cdot \lvert u_{W\beta} \rvert$	$\frac{2}{\sqrt{3}} \cdot \lvert u_{W\beta} \rvert$
S2	Q1	$\lvert u_{W\alpha} \rvert + \frac{1}{\sqrt{3}} \cdot \lvert u_{W\beta} \rvert$	$-\lvert u_{W\alpha} \rvert + \frac{1}{\sqrt{3}} \cdot \lvert u_{W\beta} \rvert$
S2	Q2	$-\lvert u_{W\alpha} \rvert + \frac{1}{\sqrt{3}} \cdot \lvert u_{W\beta} \rvert$	$\lvert u_{W\alpha} \rvert + \frac{1}{\sqrt{3}} \cdot \lvert u_{W\beta} \rvert$
S3	Q2	$\frac{2}{\sqrt{3}} \cdot \lvert u_{W\beta} \rvert$	$\lvert u_{W\alpha} \rvert - \frac{1}{\sqrt{3}} \cdot \lvert u_{W\beta} \rvert$
S4	Q3	$\lvert u_{W\alpha} \rvert - \frac{1}{\sqrt{3}} \cdot \lvert u_{W\beta} \rvert$	$\frac{2}{\sqrt{3}} \cdot \lvert u_{W\beta} \rvert$
S5	Q3	$\lvert u_{W\alpha} \rvert + \frac{1}{\sqrt{3}} \cdot \lvert u_{W\beta} \rvert$	$-\lvert u_{W\alpha} \rvert + \frac{1}{\sqrt{3}} \cdot \lvert u_{Ws\beta} \rvert$
S5	Q4	$-\lvert u_{W\alpha} \rvert + \frac{1}{\sqrt{3}} \cdot \lvert u_{W\beta} \rvert$	$\lvert u_{W\alpha} \rvert + \frac{1}{\sqrt{3}} \cdot \lvert u_{W\beta} \rvert$
S6	Q4	$\frac{2}{\sqrt{3}} \cdot \lvert u_{W\beta} \rvert$	$\lvert u_{W\alpha} \rvert - \frac{1}{\sqrt{3}} \cdot \lvert u_{W\beta} \rvert$

Table 3-3 Left and right voltage components

In order to get practical limitation with the following condition $0° \leq \gamma \leq 60°$ so we obtain eq .3-54.

$$T_{\Sigma \max} = T_p \frac{1}{\sqrt{3}} \cos(30^\circ - \gamma) \quad \textbf{(3-54)}$$

The maximum magnitude of voltage vector u_W is limited by the following equation

$$\left| \underline{u}_W \right|_{\max} = \frac{1}{\sqrt{3}} U_{dc} \quad \textbf{(3-55)}$$

The phase output voltage of the inverter is presented in fig 3-9 and the line output voltage is presented in fig 3-10. The output phase voltage and line voltage of the inverter contain harmonics. In order to get rid of these harmonic contents from the voltage and obtain a sinusoidal voltage, a LC filter is necessary [31],[32]. The resonance frequency of filter is discussed later. The equations of the LC filter are presented in the following unit.

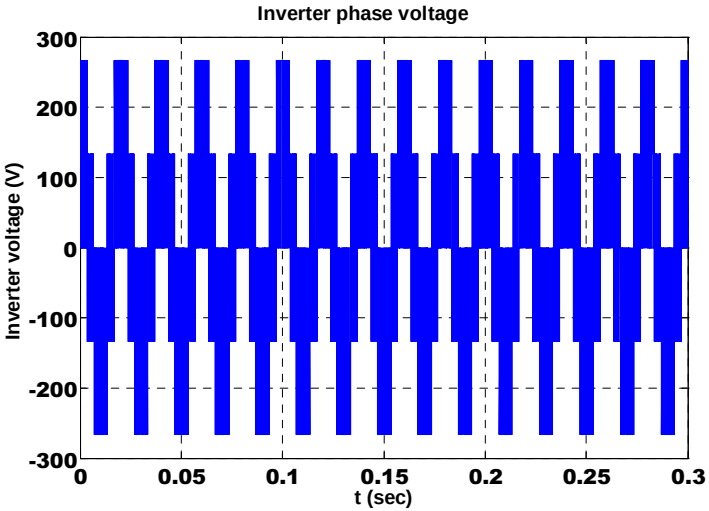

Fig. 3- 9 Inverter phase voltage

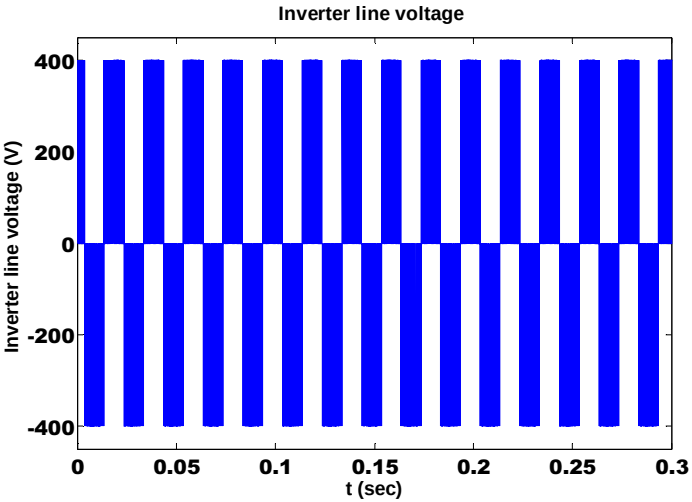

Fig. 3- 10 Inverter line voltage

3.1.6 Inverter output filter and SSSC compensation

The LC filter is used to suppress the harmonic generated by the inverter. The LC filter is shown in fig 3-11.Then output voltage of the filter is input primary voltage of the transformers. The equation of the filter is presented the following equation:

$$\underline{u}_W = R_F \underline{i}_F + L_F \dot{\underline{i}}_F + \underline{u}_1 \qquad \textbf{(3-56)}$$

Where L_F is the inductance of the filter, R_F is the resistance of the filter

The equation of the filter is transformed to the coordinates system, which rotate with the rotor. We obtain the following:

$$\underline{u}_W = R_F \underline{i}_F + L_F \dot{\underline{i}}_F + j\omega L_F \underline{i}_F + \underline{u}_1 \qquad \textbf{(3-57)}$$

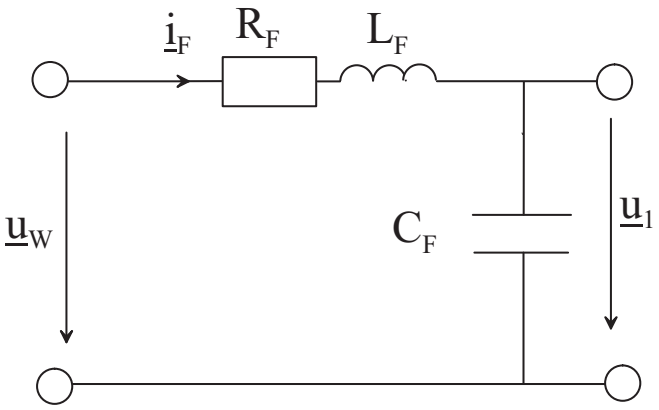

Fig. 3- 11 Equivalent circuit of the inverter and LC filter

Now we resolve equation into the real and imaginary axis

$$u_{Wd} + ju_{Wq} = R_F(i_{Fd} + ji_{Fq}) + L_F(\dot{i}_{Fd} + j\dot{i}_{Fq}) + j\omega L_F(i_{Fd} + ji_{Fq}) + u_{1d} + ju_{1q} \quad \textbf{(3-58)}$$

We separate the real axis and imaginary axis and we obtain the following equations

$$u_{Wd} = R_F i_{Fd} + L_F \dot{i}_{Fd} - \omega L_F i_{Fq} + u_{1d} \quad \textbf{(3-59)}$$

$$u_{Wq} = R_F i_{Fq} + L_F \dot{i}_{Fq} + \omega L_F i_{Fd} + u_{1q} \quad \textbf{(3-60)}$$

When we apply the SSSC to permanent synchronous generator, the output voltage of the secondary of the coupling transformers is the compensation voltage as shown in fig 3-12. The equation of the rectifier input voltage u_N, which is the summation of the compensation voltage u_C and the terminal voltage of the generator u_S, is presented the following equation.

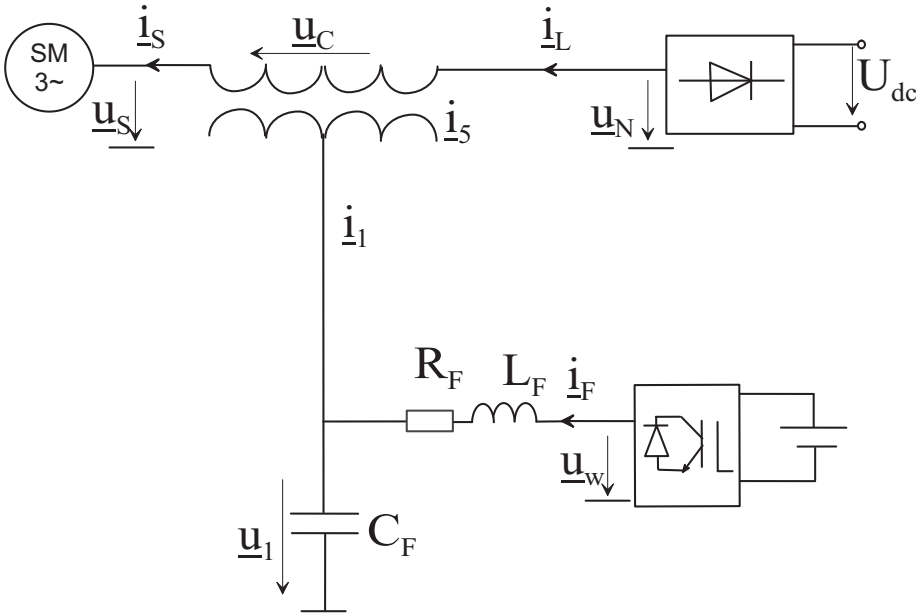

Fig. 3- 12 SSSC applied to synchronous generator

$$\underline{u}_N = \underline{u}_S + \underline{u}_C \quad \textbf{(3-61)}$$

Now we resolve the equation into the real and imaginary axis

$$u_{Nd} + ju_{Nq} = u_{Sd} + ju_{Sq} + u_{Cd} + ju_{Cq} \quad \textbf{(3-62)}$$

We separate the real axis from imaginary axis in eq. 3-62.

$$u_{Nd} = u_{Cd} + u_{Sd} \quad \textbf{(3-63)}$$

$$u_{Nq} = u_{Cq} + u_{Sq} \quad \textbf{(3-64)}$$

3.2 Control strategy

There are many control methods [33],[69], [70],[91] but we have used here the cascaded control. The basic idea for cascaded controlling is that inner control loops in a cascaded structure would have to be fast enough to make the inverter behaves as a current source for the outer control loop, which tracks the reference of the compensation voltage. The control variables are chosen so that the transformer voltage is the control variable of the outer loop and the filter current i_F is the control variable for the inner loop.

3.2.1 Current controller

In order to design the current controller, we must convert the filter eq. 3-59 and eq. 3-60 from the time domain to the s domain so we obtain the following equation

$$u_{Wd}(s) = R_F i_{Fd}(s) + sL_F i_{Fd}(s) - \omega L_F i_{Fq}(s) + u_{1d}(s) \qquad \textbf{(3-65)}$$

$$u_{Wq}(s) = R_F i_{Fq}(s) + sL_F i_{Fq}(s) + \omega L_F i_{Fd}(s) + u_{1q}(s) \qquad \textbf{(3-66)}$$

PI–controllers were chosen for the current control. Under the assumption of a small enough sample time the controllers were done in quasi-continuous approach. The sampling time is 100μsec. The current model was calculated in Laplace domain, which gave the following equations for d and q- axis.

$$i_{Fd} = \frac{1}{sL_F + R_F}(u_{Wd} + \omega L_F i_{Fq} - u_{1d}) \qquad \textbf{(3-67)}$$

$$i_{Fq} = \frac{1}{sL_F + R_F}(u_{Wq} - \omega L_F i_{Fd} - u_{1q}) \qquad \textbf{(3-68)}$$

After feed forward compensation of the cross-coupling terms, we can get rid of the following cross coupling terms $\omega L_{Fd,}$ ωL_{Fq}. Due to dq- transformation linear control analysis was carried out [90],[91]. We obtain the following transfer function

$$i_{Fd} = \frac{u_{Wd}}{sL_F + R_F} \qquad \textbf{(3-69)}$$

We divide by R_F so we obtain the following equation

$$\frac{i_{Fd}}{u_{Wd}} = \frac{1}{R_F} \cdot \frac{1}{s\frac{L_F}{R_F} + 1} = G_1 \qquad \textbf{(3-70)}$$

The value of the inductance and resistance of the filter are found in chapter five. The current controller acts on a plant contains of transfer function G_1, which contains gain $K_{S,}$ which has the value of $1/R_F$ and time constant T_1, which is L_F/R_F. G_1 is presented in eq. 3-71.

$$G_1 = \frac{K_S}{T_1 s + 1} \qquad \textbf{(3-71)}$$

A further transfer function with unity gain was added in order to take the system delay due to measuring, AD conversion, computing time and dead times. T_Σ is twice the sampling of the system. The transfer function of the delay G_D is presented in eq. 3-72. This control loop is shown in fig 3-13 below.

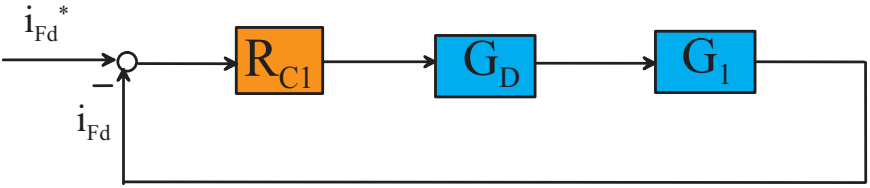

Fig. 3- 13 Block diagram of the filter current controller

$$G_D = \frac{1}{sT_\Sigma + 1} \tag{3-72}$$

The plant can be presented by second order system. The second order system has a big time constant T_1, K_s gain and a small time constant T_Σ as expressed in eq. 3-73.

$$G_i = \frac{K_s}{(T_1 s + 1)(sT_\Sigma + 1)} \tag{3-73}$$

Using the critical damping criteria the parameters of the controller R_{C1} are found as in the following expression below [69],[70]:

$$R_{C1} = \frac{10s + 50}{s} \tag{3-74}$$

This results to the proceeding closed loop transfer function

$$G_c = \frac{G_o}{1+G_0} = \frac{1.25.10^7}{s^2 + 5000\,s + 1.25.10^7} \qquad \textbf{(3-75)}$$

The bode plots of the open and closed loop are shown in fig 3-14. This indicates that the phase margin is 64°.

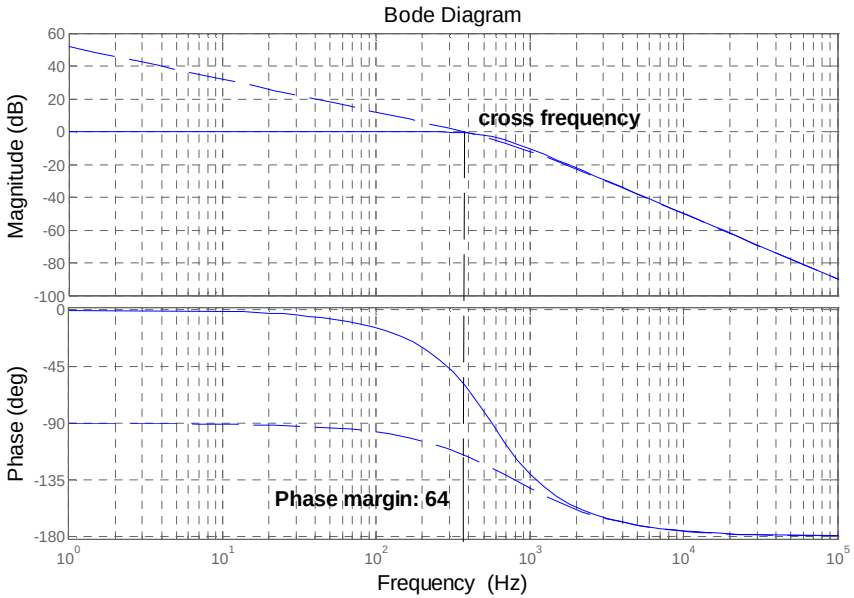

Fig. 3- 14 Bode diagram of the open (dotted line) and closed loop (continuous line) current controller

The step response of the current at d –axis current component is presented in fig. 3-15. The step response of the current controller has a low overshoot, which is about 5%. The rise time is $5T_{\Sigma}$.

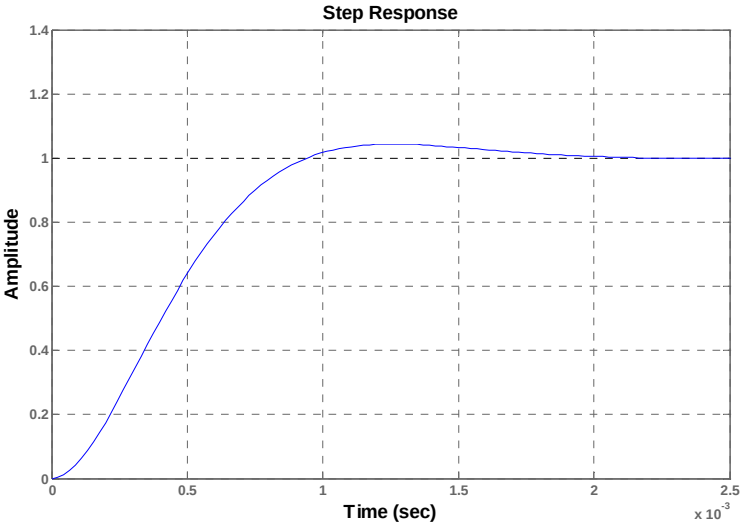

Fig. 3- 15 Step response of the current controller

3.2.2 Voltage Controller

The equation of output voltage of LC filter is needed in order to design the voltage controller. The output voltage of the LC filter is expressed in the following equation.

$$\underline{i}_F - \underline{i}_1 = C_F \dot{\underline{u}}_1 \qquad \textbf{(3-76)}$$

If we transform the pervious equation to the same coordinate rotating with the generator rotor, we obtain the following equation

$$\underline{i}_F - \underline{i}_1 = C_F \dot{\underline{u}}_1 + jC_F \omega \underline{u}_1 \qquad \textbf{(3-77)}$$

The pervious equation is resolved into the real and imaginary part.

$$i_{Fd} + ji_{Fq} - i_{1d} - ji_{1q} = C_F \dot{u}_{1d} + jC_F \dot{u}_{1q} + jC_F \omega u_{1d} - \omega C_F u_{1q} \quad \textbf{(3-78)}$$

We separate the real axis from the imaginary axis. We get the following two equations and transfer to s domain.

$$u_{1d} = \left(i_{Fd} - i_{1d} + \omega C_F u_{1q}\right)\frac{1}{C_F s} \quad \textbf{(3-79)}$$

$$u_{1q} = \left(i_{Fq} - i_{1q} - \omega C_f u_{1d}\right)\frac{1}{C_F s} \quad \textbf{(3-80)}$$

The transformer current is considered as disturbance. After feed forward compensation of the cross-coupling terms due to dq- transformation, linear control analysis was carried out.

$$u_{1d} = \frac{i_{Fd}}{C_F s} \quad \textbf{(3-81)}$$

$$u_{1q} = \frac{i_{Fq}}{C_F s} \quad \textbf{(3-82)}$$

For the voltage control loops the simplified current closed loop transfer function below was assumed the condition that T_Σ was small enough. As result the square of T_Σ can be neglected. This assumption simplifies the outer loops control of the current controller as follows.

$$G_c = \frac{1}{2T_\Sigma^2 s^2 + 2T_\Sigma s + 1} \approx \frac{1}{s2T_\Sigma + 1} \quad \textbf{(3-83)}$$

The block diagram is depicted in fig 3-16. G_c is the closed loop transfer function of the current controller. The transfer functions of the system in dq components are presented in eq. 3-83.

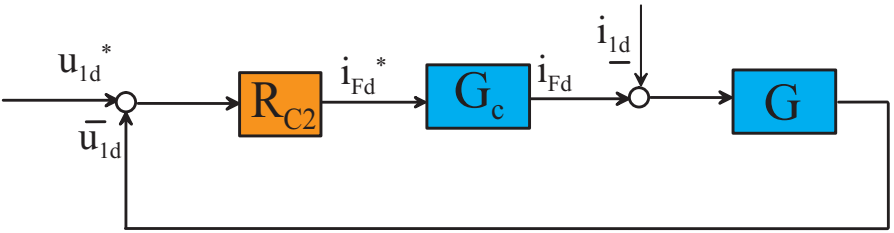

Fig. 3- 16 Block diagram of the filter voltage controller

The transfer function for the capacitor is pure integration part

$$G_{C_F} = \frac{1}{C_F s} \tag{3-84}$$

So the open loop transfer function

$$G_O = \frac{1}{C_F s(2T_\Sigma s + 1)} \tag{3-85}$$

The controller parameter is chosen according to the pole place methods and found giving the expression below

$$R_{C2} = \frac{0.0055s + 0.68}{s} \tag{3-86}$$

The bode plot of the open and closed voltage control loop are shown in fig 3-17. The phase margin is 65° degree as shown in the bode plot. The step response of the d-axis capacitor voltage component is presented in fig.3-18. The overshoot of the voltage controller is about 22%.

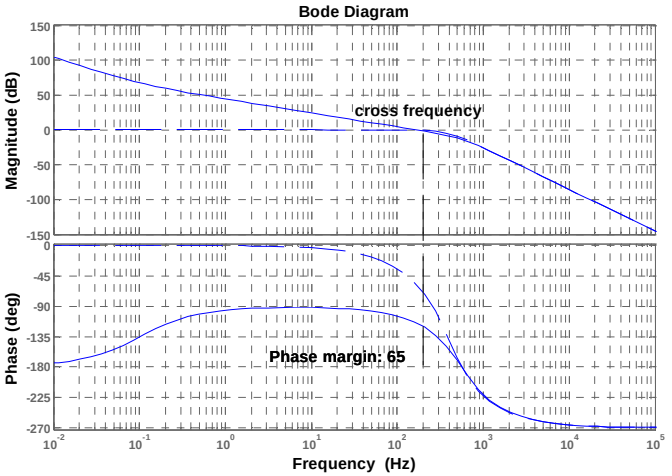

Fig. 3- 17 Bode diagram of the open (dotted line) and closed loop (continuous line) voltage controller

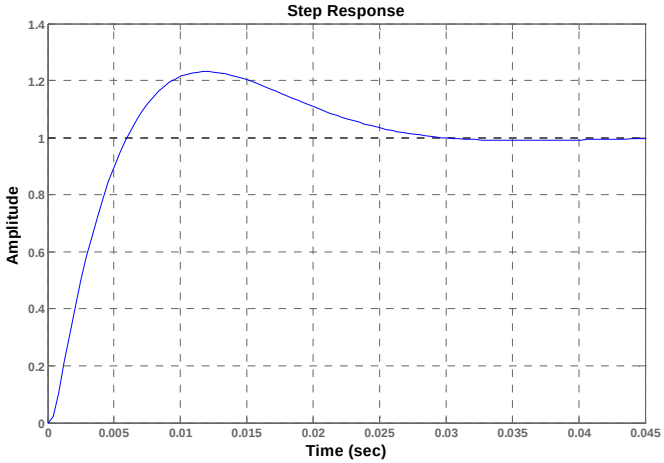

Fig. 3- 18 Step response of the voltage controller

3.3 Simulation of the system

3. 3.1 Simulation without SSSC

The mathematical model of different system components was presented previously. In this section simulation of whole system will be provided. At the beginning the system is without compensation, then SSSC compensation will be provided. Finally the system with SSSC compensation and passive filter will be presented. The following simulation results with Matlab program show the PSG connected to dc network at 50% of the rated power. The generator currents and the terminal voltage of the generator without SSSC are shown in fig 3-19, 3-20 respectively. The generator current contains harmonics as expected due the presence of the rectifier. The harmonic content is not constant. When the voltage level of dc network decreases, the harmonic content the generator current decreases also but the harmonic in the terminal voltage increases. This agrees with our experimental result.

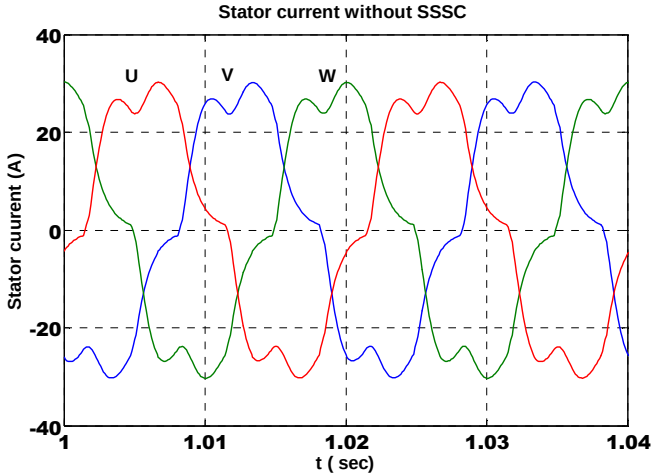

Fig. 3- 19 Simulation of stator current without SSSC at 50% loading

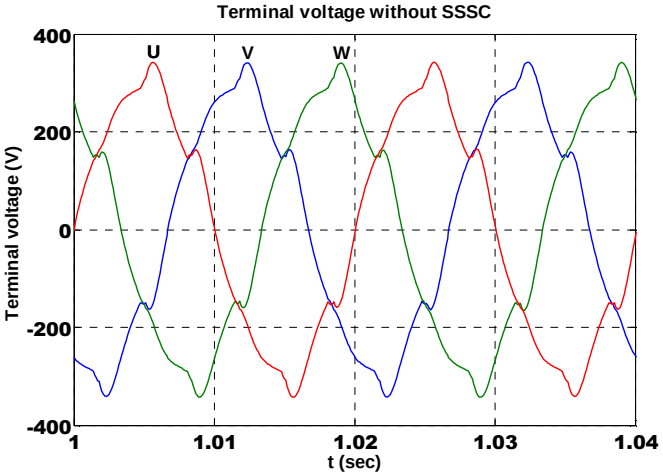

Fig. 3- 20 Simulation of the terminal voltage without SSSC at 50% loading

3. 3.2 Simulation with SSSC

The following simulation results show the effect of applying SSSC to PSG connected to dc network, which resulted in increasing the output power to 75% of the rated power. The generator currents and the terminal voltage with SSSC are shown in fig 3-21, 3-22 respectively.

The simulation results reveal that we have increased the output power from 50 % to 75 % of the rated load. The terminal voltage is constant although there is an increase of the generator current. The generator current with SSSC has a lower harmonic content in comparison to without compensation. The reason is that the magnetising impedance of the coupling transformer reduces the harmonic content in the current. On the hand the terminal voltage has more harmonic content with SSSC [53],[54].

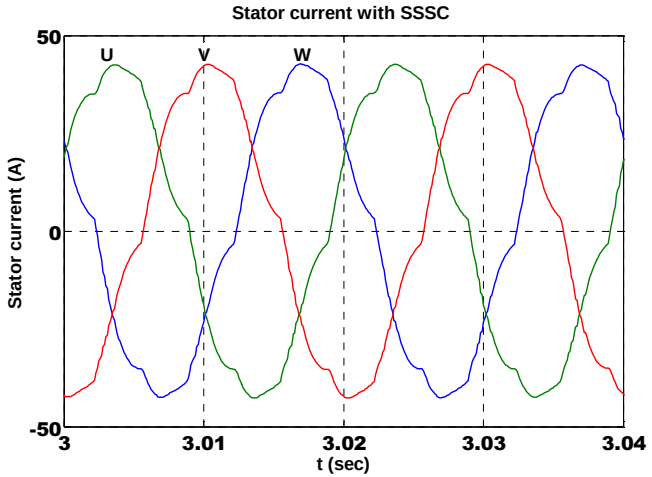

Fig. 3- 21 Simulation of stator current with SSSC at 75% loading

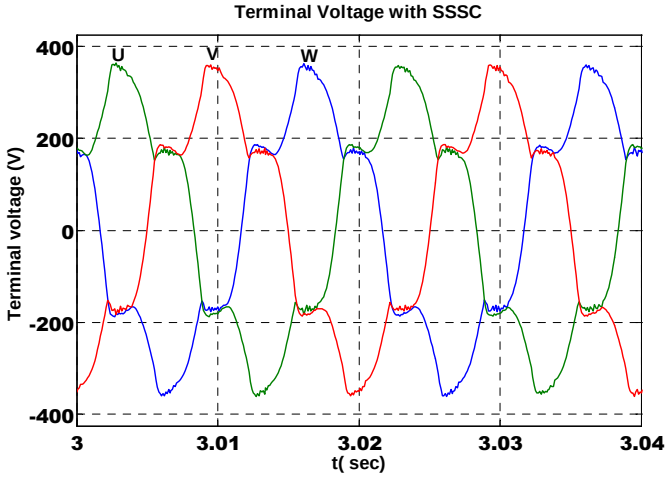

Fig. 3- 22 Simulation of the terminal voltage with SSSC at 75% loading

The reason is the harmonic component of generator current causes a harmonic voltage drop on the synchronous reactance. Although the generator current has lower harmonic content, there is an increment in the magnitude of this current. This increment of current causes the harmonics in the terminal voltage. The compensation voltage, which is applied to the generator, is shown in fig 3-23. The compensation voltage has also harmonic because the generator current passes the coupling transformers. This current also causes harmonics content in the compensation voltage and the harmonics are also generated by the inverter.

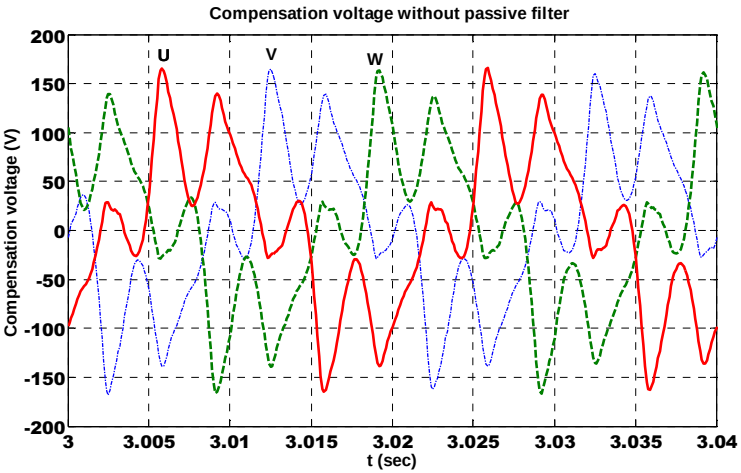

Fig. 3- 23 Simulation of the compensation voltage with SSSC at 75% loading

3. 3.3 Simulation with SSSC and passive filter

When applying the SSSC and passive filter for the fifth harmonic, the generator current increases. As a result the output power increases compared to the case with only SSSC when applying the same compensation voltage. The harmonics in the generator current will decrease. This is due to that fact the passive filters eliminate the harmonics generated by nonlinear load by

providing low impedance path. The amount of the harmonics in the current depends on the quality of the filter also. A filter with better quality can extract more harmonic current [55].The circuit diagram of the synchronous generator, SSSC and passive filter is shown in fig 3-24. The load current is the summation of the passive filter current and the generator current. The load current is expressed in eq. 3.-87.

$$\underline{i}_L = \underline{i}_S + \underline{i}_5 \qquad \textbf{(3-87)}$$

Now we resolve equation into the real and imaginary axis. Then we separate the real axis from imaginary axis in eq. 3-88 and eq. 3-89.

$$i_{Ld} = i_{5d} + i_{Sd} \qquad \textbf{(3-88)}$$

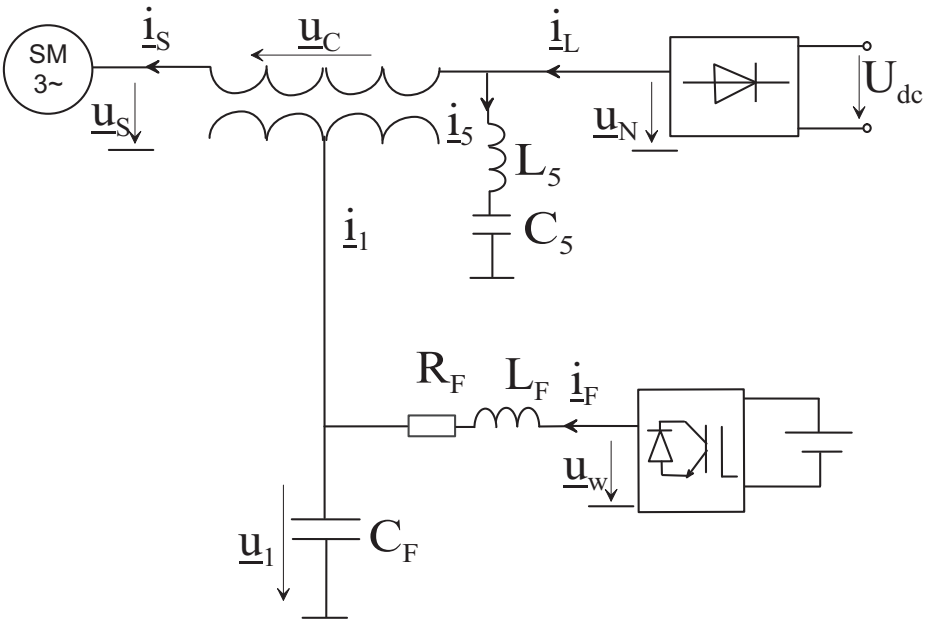

Fig. 3- 24 SSSC and passive filter applied to synchronous generator

$$i_{Lq} = i_{5q} + i_{Sq} \qquad \textbf{(3-89)}$$

The generator current, with the same compensation voltage as the condition without passive filter, is shown in fig. 3-25. The passive filter has increased current and output power from the generator. The terminal voltage has remained constant with loading. The terminal voltage of the generator is almost free from the fifth harmonic as shown in fig. 3-26. The simulation results have verified the proposed theory that the filter absorbs the harmonic of the terminal voltage. The passive filter has reduced the size of required SSSC compensation voltage. This will lead to reduction of the size of the coupling transformer and inverter also. Also the compensation voltage, which is shown in fig 3-27, contains less harmonic content as the generator current.

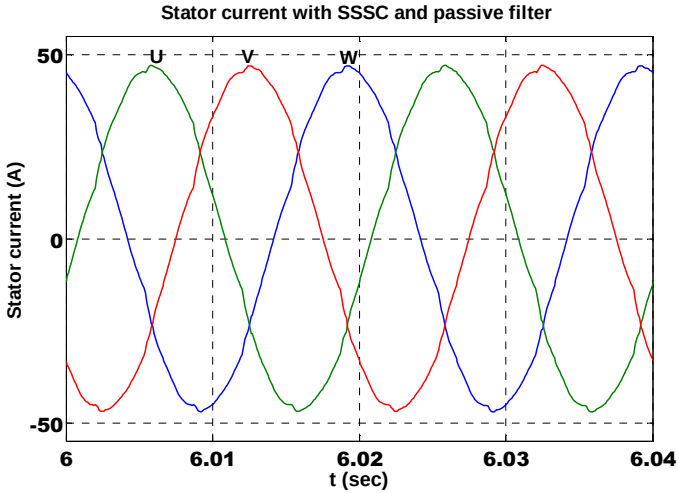

Fig. 3- 25 Simulation of stator current with SSSC and passive filter

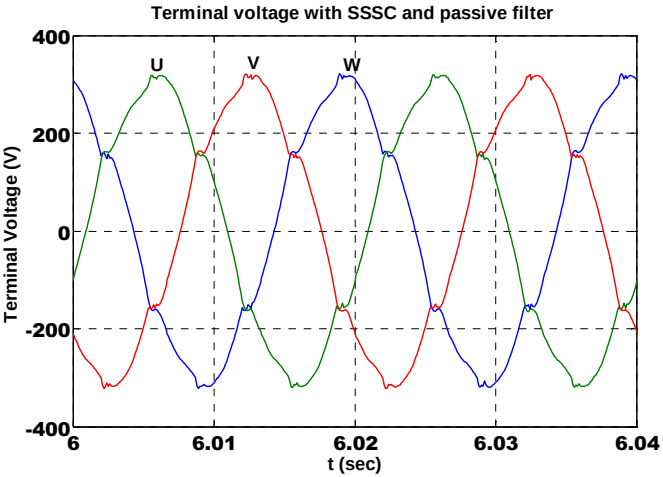

Fig. 3- 26 Simulation of terminal voltage with SSSC and passive filter

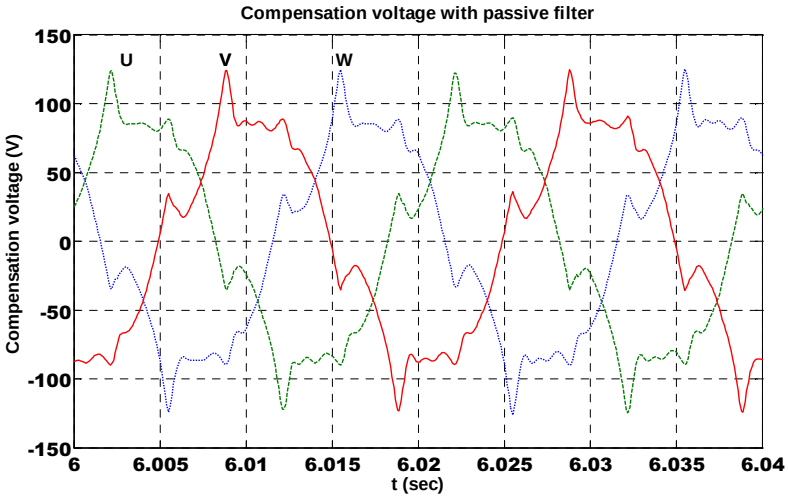

Fig. 3- 27 Simulation of compensation voltage with passive filter

4

Wind Turbine Modelling

The chapter focuses on the simulation of the wind turbine that can be used later to reproduce the realistic conditions that occur at the wind energy conversion system. Also two mass model of the coupling between the wind turbine and generator is developed. Finally emulation of the wind turbine with dc motor with real time measurement of wind speed is implemented.

4.1 Wind power model

In order to start building the model, we must understand the elements that will constitute it. First of all, we have to build a module that determines the magnitude of shaft mechanical power or torque that could be extracted from the wind. After that, we will have to know how the torque exerted on the rotor will drive the system composed of the rotor, generator and the coupling between them. These two modules will model the physical part of the wind turbine. Next, we shall start handling each of these modules in detail. We shall discuss the underlying physical concepts, as well as discuss the structure of the modules.

Suppose that we have a stream of wind of density ρ and velocity ν_w that flows perpendicularly through an area A. The amount of mechanical power held in the wind P_{wind} is given by the equation

$$P_{wind} = \frac{1}{2}\rho A \nu_w^3 \quad \textbf{(4-1)}$$

In the case of a wind turbine, the area A will be related to the radius R_r of the rotor blades by the equation:

$$A = \pi R_r^{\,2} \quad \textbf{(4-2)}$$

Unfortunately, a wind turbine can never extract this amount of power from the wind stream. This is because obtaining 100% of the wind stream power will require that all wind particles be decelerated to zero. This is, of course, impossible for many reasons, the simplest of which is that some air particles will pass without even colliding with the rotor blades. They will be only slightly affected by the presence of the wind turbine. Now, one may pose the following question. If we have the wind velocity, the rotor blade radius and the air density, then how can we compute the magnitude of toque of the wind turbine?

Scientists have been interested in answering this question ever since the advantages of wind power have started becoming obvious. Using practical experimentation, a group of curves called the wind curves have been obtained, that give C_m, which is the torque coefficient of wind turbine. C_m as a function of blade tip velocity and blade pitch angle [16]. A rotor blade rotating with angular velocity ω_r will have a tip speed ν_{tip} given by:

$$V_{tip} = \omega_r R_r \quad \textbf{(4-3)}$$

Now, let us define the tip speed ratio λ which is the relation between the angular velocity of the blade tip and the wind speed and is given by the expression:

$$\lambda = \frac{V_{tip}}{V_w} = \frac{\omega_r R_R}{V_w} \qquad \textbf{(4-4)}$$

Also, let us define the blade pitch angle θ is the angle between the plane of rotation of the rotor blade's tip and the plane of the rotor blade itself. Knowing θ and λ, we may use the wind curves shown below to obtain the value of C_m as shown fig. 4-1. This figure only presents some of the curves ranging from θ = 0° to 40°. The computer interpolates between the curves to obtain an approximation for the value of C_m at any value a of blade pitch angle. This was done all over the range covering blade pitch angles from 0 to 40 degrees. Having known the value of C_m, we may find T_{rotor} from the following equation:

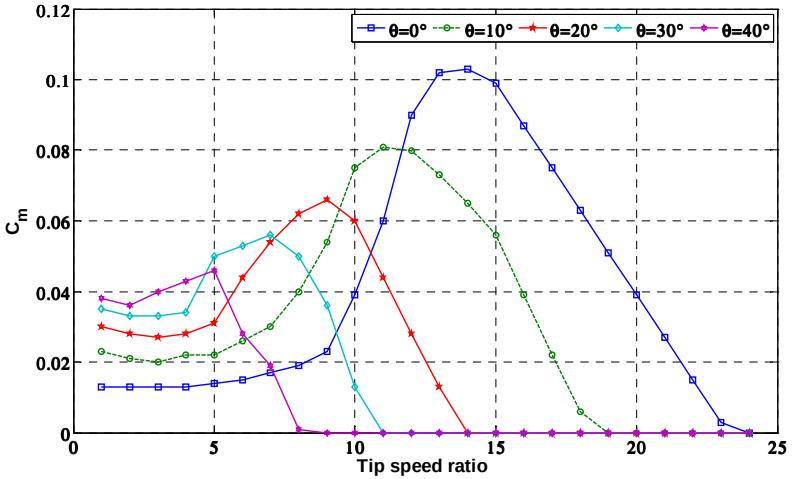

Fig. 4- 1 Torque coefficient curve

$$T_{rotor} = 0.5 A_r \rho R_r v_w^2 C_m \qquad \textbf{(4-5)}$$

One last thing to consider before moving on to building the model is that at every value of λ, there is a certain blade pitch angle that maximizes C_m, and hence the torque extracted from the stream.

4.2 Two mass system

In the ideal case, the rotor and generator would be ideally coupled. Ideal coupling means that the shaft is perfectly rigid against torsion, and there are no viscous moments that will oppose the rotation of the system. In such an ideal case, the rotor, the shaft and the generator will always run at the same speed. They would be considered a one mass system. Unfortunately, the rotor and the generator may never be ideally coupled. The real coupling between the rotor and the generator will always lead to some torsion occurring in the shaft and some damping moment that opposes the shaft rotation. As a result the rotor and generator won't in general move as a single body. Instead the motion of the generator will transiently follow the motion of the rotor. They are not one mass system any longer. There are two bodies with different motions, the rotor and the generator. Hence, there is two mass system [46],[92].

In developing a model in this situation to describe the motion under external torques, the rotational dynamics of the system was studied. The two mass system is presented in fig 4-2. It may be noticed that the system is running under the effect of two external moments. These moments are the mechanical torque exerted on the rotor by the wind stream, which is obtained in the wind power model, and the electrical load moment which opposes the rotation of the generator's rotor. As the rotor changes its angular velocity, the real coupling will make the generator unable to exhibit the same change simultaneously. Instead, a difference in rotor's and generator's angular velocities will start to appear. This differential velocity may be computed from the relation:

$$\omega_{diff} = \omega_{rotor} - \omega_{gen} \qquad \textbf{(4-6)}$$

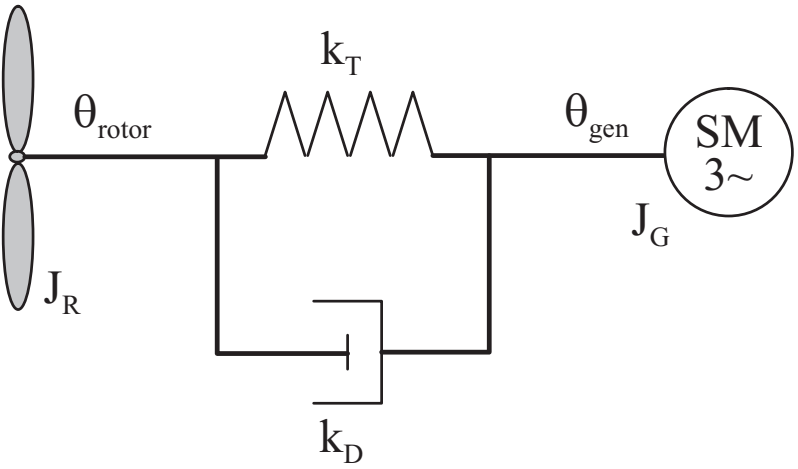

Fig. 4- 2 Block diagram of 2-mass system

Also, as result of having certain differential velocities at certain time intervals, a differential angle will also exist between the rotor and the generator. This differential angle is equal to the angle by which the coupling shaft is twisted. It is given by the following equation:

$$\theta_{diff} = \theta_{rotor} - \theta_{gen} \qquad \textbf{(4-7)}$$

The differential velocity will lead to a damping moment which opposes the motion of the rotor. This damping moment may be obtained from the relation:

$$M_D = k_D \omega_{diff} \qquad \textbf{(4-8)}$$

The differential angle will lead to a torsion moment which opposes the motion of the rotor. This torsion moment may be obtained from the relation:

$$M_T = k_T \theta_{diff} \quad \textbf{(4-9)}$$

Therefore, a total coupling moment due to real coupling M_C equal to the sum of both opposing moments will exist.

$$M_C = M_D + M_T = k_D \omega_{diff} + k_T \theta_{diff} \quad \textbf{(4-10)}$$

Understanding the dynamics is very important for building the mode of two mass. The model will describe the system dynamics.

First of all, there is a rotor driving moment M_{RD} which acts on the rotor as the result of the wind stream blazing against the rotors. This moment will actually be used to accelerate the rotor, and counter balance the coupling moment.

We may hence write:

$$M_{RD} = M_{RA} + M_C \quad \textbf{(4-11)}$$

Here, M_C is the total coupling moment, and M_{RA} is the rotor acceleration moment defined by Newton's second law for rotational dynamics:

$$M_{RA} = J_R \dot{\omega}_R \quad \textbf{(4-12)}$$

Where J_R is the rotor's moment of inertia and ω_R is the rotor's angular acceleration.

There are three moments in the generator's moment equation, which are the coupling moment, the electrical load moment and the generator's accelerating moment. These moments are expressed in eq. 4-13:

$$M_{GA} = M_C - M_L = J_G \dot{\omega}_R \quad \textbf{(4-13)}$$

Where M_L is the electrical load moment, J_G is the generator's moment of inertia and $\dot{\omega}_G$ is the generator's angular acceleration. The transfer function for generator angular velocity and rotor acceleration moment in case of zero electrical load moment is expressed in eq. 4-14 [92].

$$G(s) = \frac{1}{s(J_G + J_R)} \left[\frac{1 + s\frac{k_D}{k_T}}{1 + s\frac{k_D}{k_T} + s^2 \frac{J_G J_R}{(J_G + J_R)k_T}} \right] \quad \textbf{(4-14)}$$

The resonance frequency of the system is defined by the stiffness and damping coefficients of the shafts.

4.3 Dynamics of the blade pitching mechanism

It is very important to notice that no single blade pitch angle can always assure maximum power extraction for the whole range of tip speed ratios. Instead, the whole λ range may be divided into a group of intervals, each of which allows maximum power to be extracted using a certain single valued blade pitch angle. In our question for maximum power, we shall try to know the "optimum" blade pitch angle at our operating λ (the blade pitch angle which results in maximum power extraction from the stream), and try to make the actual blade pitch angle always equal to the optimum at the operating value of λ [36],[39],[61].

The blade pitching system consists of the rotor blades, motors, brakes, controllers and other auxiliary equipment. When we are operating at a certain λ and the actual blade pitch angle is not equal to the optimum blade pitch angle, the controller will issue a control signal, so that the motor rotates the blade about its own longitudinal axis in order to obtain the optimum blade angle. If needed, the brakes may also be initiated to stop the pitching process. While the blades are being pitched, they are subject to an inertial moment and many opposing moments. Since the blades consist of wings of metal distributed in some way about the blade's axis, each blade will have a certain moment of inertia. For this reason, we shall require a certain moment to act on the rotor blade in order to give it some angular acceleration. As the blades are pitched, some torsion occurs as a result of the blade's length, and the fact that it is pitched from one side and free on the other side. This causes the blade to twist slightly about its own axis during pitching. This produces a twisting moment that opposes the pitching of the blade. Both of the blade's inertial and aerodynamic disturbances, in addition to the some other effects such as wind shear, tower blockage, turbulence, yawed flow and turbine yawing, the Blades undergo an undesirable type of motion called teetering. A moment results from this effect and opposes the pitching process. Due to the accelerating and decelerating the blades, the air masses in contact with the blade must be as well accelerated and decelerated. This produces a torque which opposes the pitching process.

In the previous discussion, we have exposed ourselves to a physical interpretation of the moments opposing the process of blade pitching. If we wish to model the dynamics of the system fully, we shall indulge ourselves into deep physical analysis in order to obtain expressions for each of the opposing moments mentioned above. However, there is an easier way to achieve satisfactory results without going very deep into the aerodynamics of the pitching process [40].

Looking at the pitching process as a whole, we can regard the effect of all the individual opposing moments as if it consists of four components. The first component depends on the blades' angular acceleration, and corresponds to

the joint effect of all opposing moments resulting from the acceleration or deceleration of the blades, such as the air mass acceleration moment. The second component depends on the blades' angular velocity, and it corresponds to the joint effect of those moments resulting from the blades motion in air, such as the damping moment. The third component depends on the blades' angle, and this component corresponds to the joint effect of all the opposing moments depending on the torsion or twisting of the blades, such as the blade twisting moment. The fourth component is independent on the blades' motion, and it corresponds to the joint effect of all frictional moments. This method does not actually neglect the physically interpretable moments or introduce new ones. It only resembles a different way of handling these moments. We have classified them according to their mathematical nature, rather than their physical nature. By adopting this method of classification, we can write a general equation for the moments opposing the blade pitching mechanism on the form

$$M_{OPP} = C_A \ddot{\theta} + C_D \dot{\theta} + C_T \theta + M_F \quad \textbf{(4-15)}$$

Where:
C_A = Equivalent acceleration moment coefficient,
C_D = Equivalent damping coefficient,
C_T = Equivalent torsion coefficient, and
M_F = Equivalent frictional moment.

Instead of the detailed physical and aerodynamic analysis which would lead to complicated model. We are going to use the parameters, which are listed above, that we can determine by practical experiments. Practical experiments have shown the following:

- The coefficient C_A is almost 2% of the blades' moment of inertia, and the first component may hence be neglected.

- The coefficient C_D is almost equal to 32 Nms/rad. The coefficient C_T is almost equal to 0.6 Nm/rad.

- The moment M_F may be neglected compared to the sum of the second and third components.

For this reason, we may approximate the total resisting moment using the equation:

$$M_{OPP} = C_D \dot{\theta} + C_T \theta \quad \textbf{(4-16)}$$

Now, we are ready to start building the model for blade pitching. In building such a model, we shall start by implementing a part which corresponds to the blade moment of inertia and opposing forces. This part will accept as an input the positioning moment M_P, which is the moment exerted by the motor to actuate the pitching process, and must produce as an output the actual position of the blades at any time instant.

The first part of the model, which corresponds to the effect of the physical components of the system such as the blade moment of inertia, the damping and the torsion, may be modelled in regard of the equation:

$$M_P = M_{Inertia} + M_{OPP} = J_{RB} \ddot{\theta} + C_D \dot{\theta} + C_T \theta \quad \textbf{(4-17)}$$

Expressing this equation in the Laplace domain would give:

$$M_P(s) = \theta(s)(J_{RB} s^2 + C_D s + C_T) \quad \textbf{(4-18)}$$

This form might be useful because it can give us directly the transfer function of the system

$$\frac{\theta(s)}{M_P(s)} = \frac{1}{J_{RB} s^2 + C_D s + C_T} \quad \textbf{(4-19)}$$

The optimal pitch angle is required in order to obtain the maximum power from the wind turbine. The simulation of racking the optimal pitch angle is performed in Matlab/simulink program. The actual pitch angle and the reference optimal angle are shown in fig. 4-3.

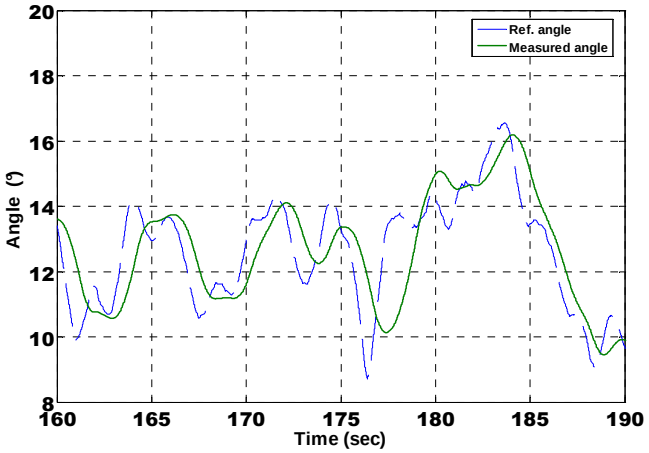

Fig. 4- 3 Simulated tracking of the reference optimal angle and actual pitch angle

4.4 Wind turbine emulator

A 58KW dc machine is used to emulate the wind turbine. A controlled 6-pulse thyristor converter drives the machine from the Control Techniques Company. The control of dc machine consists of a cascaded control scheme with an inner current and an outer speed control loops. The Control Techniques has only PI controller. The proposed scheme was implemented in the experiment. The wind turbine model was developed with Simulink program on PC. The PC has a DS1103-board, which contains a TMS320F240 DSP with master slave configuration. The wind turbine model is converted to C language by real time workshop and downloaded on the DS1103-board. The DS1103-board communicates with the dc converter through an RS-422 serial interface. The reference speed is calculated from the model on computer and transferred to

dc converter through DS1103 board. The recorded wind speed time, where the average wind speed is 9m/s, is shown in fig. 4-4. The reference speed and measured speed of the generator are presented in fig 4-5.

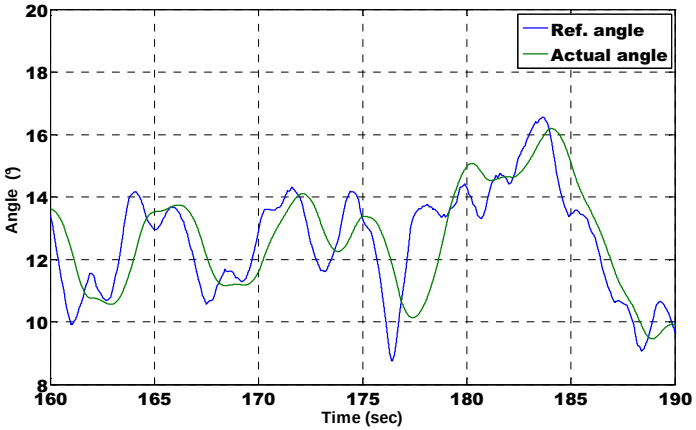

Fig. 4- 4 Wind profile

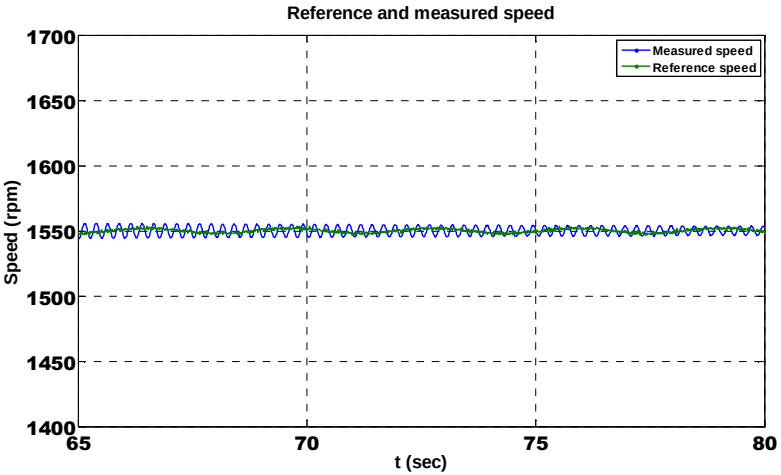

Fig. 4- 5 Reference and measured shaft speed of the generator

5

Experimental Results

In this chapter the dimensioning and the construction of the experiment are described. The experiment is found in the lab of the Electrical Machine and Drive department at Technical University Chemnitz. The aim is to apply static synchronous series compensation to permanent magnet synchronous generator. For the implementation of the control, dSPACE board DS1103 that contains two microprocessors from Texas Instruments Company was used. This chapter presents also the test performed in order to obtain the parameters of synchronous generator. A discussion of the practical results obtained when applying the SSSC with and without a passive filter. Finally the efficiency of the system is presented.

5.1 Experimental setup

Our small-scale experimental system of wind power generation consists of electrical excited synchronous generator, which is presented in fig. 5-1. A 58 KW dc machine fed by a three phase thyristor controlled bridge which is used to drive the generator shaft. The rotation speed of the dc motor is controlled by a thyristor bridge in order to simulate the fluctuation of wind speed.

Specification of synchronous generator used for the experiment is shown in table 5-1.

Fig. 5- 1 Experiment at the lab

Rated Power S_n	25 kVA
Rated voltage U_n	390V
Rated current I_n	37A
Rated power factor	0.8
Frequency f_n	50Hz
Direct axis reactance x_{Sd}	1.9 p.u
Quadrature axis reactance x_{Sq}	1.1 p.u

Table 5-1: Specification of synchronous generator

The compensation voltage is realised by an inverter output, whose output voltage is fed to LC filter. Then output voltage of the filter is connected in

series with the generator through three single-phase coupling transformers. The tapping changing of the three transformers has been set to the turn's ratio to 1:1.5. The coupling transformers are chosen to be single phase in order to avoid the magnetic coupling between the three phase transformers, which is found in the three limbs or five limbs. Specification of the transformers is presented in table 5-2. The specification of inverter, LC filter and passive filter is given in table 5-3.

Rated Power S_n	8 kVA
Rated primary voltage U_1	220V
Rated secondary voltage U_2	0-400V
Rated primary current I_1	37A
Rated secondary current I_2	20A
Resistance percentage	1%
Reactance percentage	3%

Table 5-2: Specification of transformers

Collector emitter voltage U_{CE}	1200V
Collector current I_c	25A
Filter inductance L_F	4mH
Filter capacitance C_F	22μF
Switching frequency	4KHz
Passive filter capacitance C_5	100μF
Passive filter inductance L_5	4mH
Q of passive filter Quality	5

Table 5-3: Specification of inverter and filter

The inverter consists of three legs IGBT from Semikron company type SkiiP 025HAB 1200V/25A. This module has short circuit, under voltage, earth leakage and over temperature protection. For over voltage protection a chopper is connected in parallel to the dc link voltage. The chopper conducts when the voltage exceeds 750V. The chopper consists of an IGBT with rated

current 90A so 10Ω are connected in series with IGBT in order to limit the current. The dc link has four capacitors. Each two are connected in parallel. Afterward the capacitors are connected in series. In order to equally divide the voltage 50KΩ is connected in parallel to the capacitor. A delay board was designed with a delay time of 3µsec in order to avoid that two IGBT in leg to conduct at the same time. Hall Effect sensors were used to measure the currents and the voltage. The voltage sensors have a ratio from 1000V/25mA, while the current transducers have a ratio 100A/25mA. As these sensors deliver a current signal, this latter must be converted to voltage by a resistance.

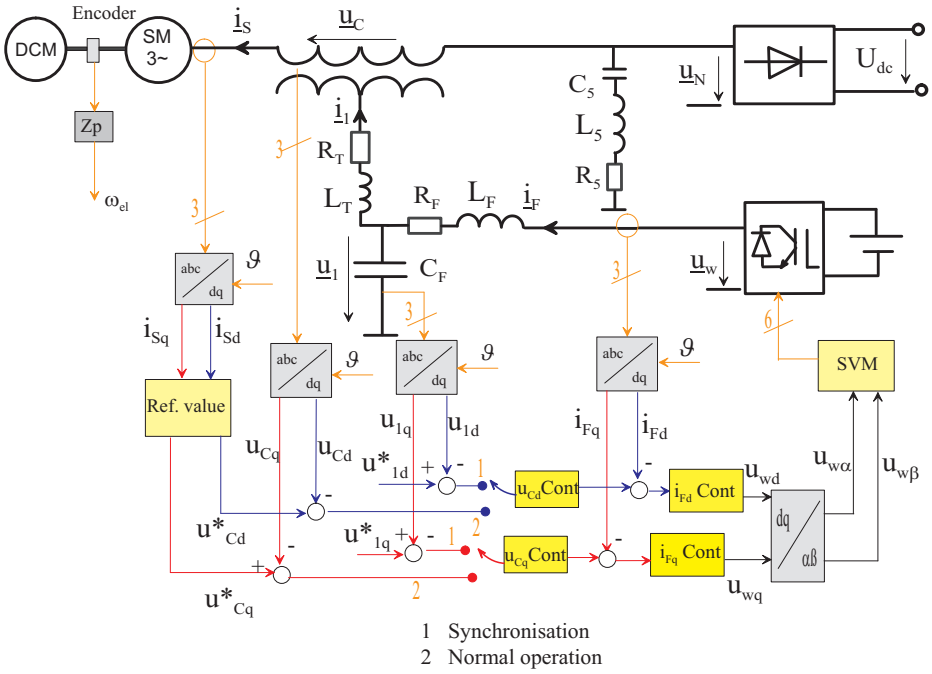

Fig. 5- 2 Schematic diagram of the experimental set-up

The DS1103-hardware board contains an AD converter unit and two incremental encoders. The AD converter unit has 4 converters with 4 multiplexed inputs each with 16 bits resolution and 4µs sampling time. This system enables one to work with models developed in Matlab /Simulink programs directly. The processor code is generated automatically. The inputs and outputs interfacing hardware and software are available as Simulink blocks in real time interface [66]. The schematic diagram shows in fig. 5-2 that the filter current is measured, which is used in the inner control loop. Also the generator current is measured in order to obtain the current angle. The compensation voltage lags this angle by 90°degrees. The compensation voltage is also measured, which is used in the outer control loop. Additionally the speed of the generator is measured via an incremental encoder.

At the beginning the dc motor is used to rotate the rotor of the synchronous machine and the required excitation voltage is provided. The voltage will appear on the terminal of the generator at no load. This terminal voltage in this case is equal to the internal induced voltage. This voltage is used by the phase locked loop in order to obtain the reference angle of the system. In this approach the d-axis voltage is compared to a reference value that should be zero and the error is corrected by PI controller which output is the net frequency. A further integrator gives the angular displacement that is fed back to voltage transformation in a rotating coordinate system. As result we can obtain the reference rotating at beginning of the experiment.

5.2 Synchronous generator at no load

Before starting the analysis of the practical results, we will analyse the output voltage of the generator at no load. This analysis will help to explain the existence of the third harmonic, which is present in the terminal voltage of the generator. The output voltage of the generator is presented below at the rated frequency. It is clear from fig 5-3 that the output voltage is not a sinusoidal waveform. If we analyse this wave we will find out that the third, fifth and the seventh harmonic exist. The third harmonic component is about 8% and the fifth harmonic is 2% as shown in fig 5-4. The third harmonic content exists

also at different frequencies. The third harmonic exists due to the saliency of the generator.

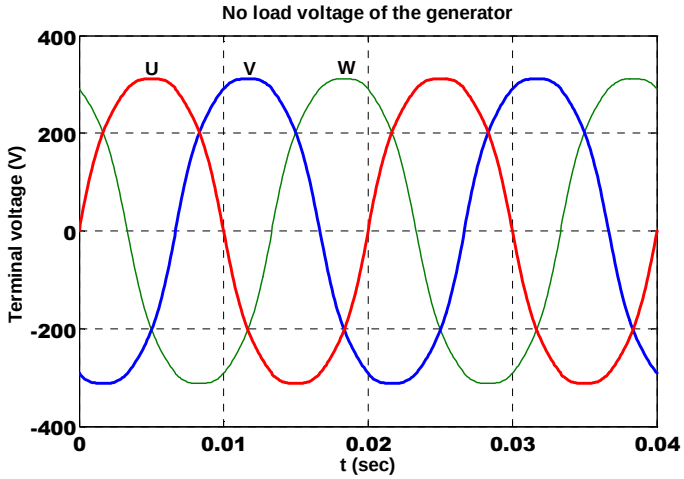

Fig. 5- 3 Output voltage of the generator at no load

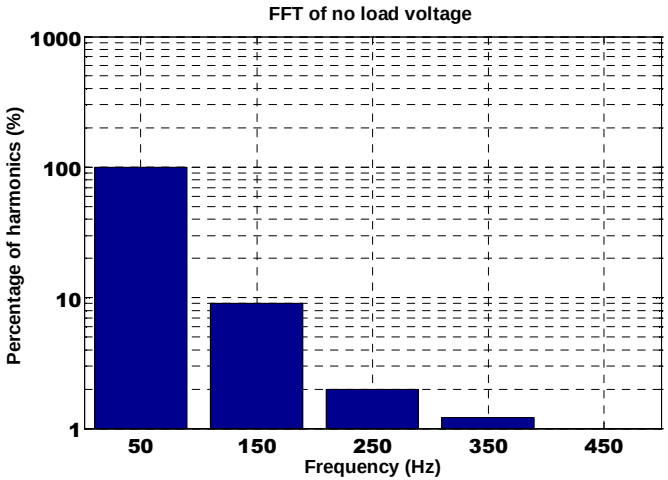

Fig. 5- 4 FFT of the terminal voltage of the generator at no load

5.3 Synchronous generator parameter

The reactances and the time constants of the synchronous generator, which are needed in the simulation, were unavailable due to the fact that the synchronous generator was built in 1973. As result we needed to carry out the tests in order to obtain these parameters.

5.3.1 Synchronous generator slip test

The slip test is used to determine the direct axis synchronous reactance and the quadrature axis synchronous reactance as shown in fig 5-5. The generator during the slip test is unexcited and a balanced three phase voltage is applied at the terminals. The field winding must be kept open in the slip test. The rotor is driven at a speed differing slightly from synchronous speed, which is easily calculated from the frequency of the supplied voltage and the number of poles of the machine. The stator currents are then modulated at the slip frequency by the machine, having maximum amplitude when the quadrature axis is in line m.m.f wave and minimum amplitude when the direct axis aligns with m.m.f. The terminal voltage is usually modulated at the slip frequency, the amplitude of the terminal voltage is greatest when the current is least and vice versa. The direct axis impedance can be measured, when the induced voltage the field winding has minimum value. The direct reactance is obtained according to eq 5-1.

$$X_{Sd} = \frac{U}{\sqrt{3}I_S} = \frac{80}{7.1} = 11.5\Omega \qquad \textbf{(5-1)}$$

The quadrature axis impedance can be measured, when the induced voltage the field winding has maximum value. The quadrature reactance is obtained according to eq. 5-2.

$$X_{Sq} = \frac{U}{\sqrt{3}I_S} = \frac{80}{11.9} = 6.7\Omega \qquad \textbf{(5-2)}$$

Where U is the line voltage and I_S is the stator current.

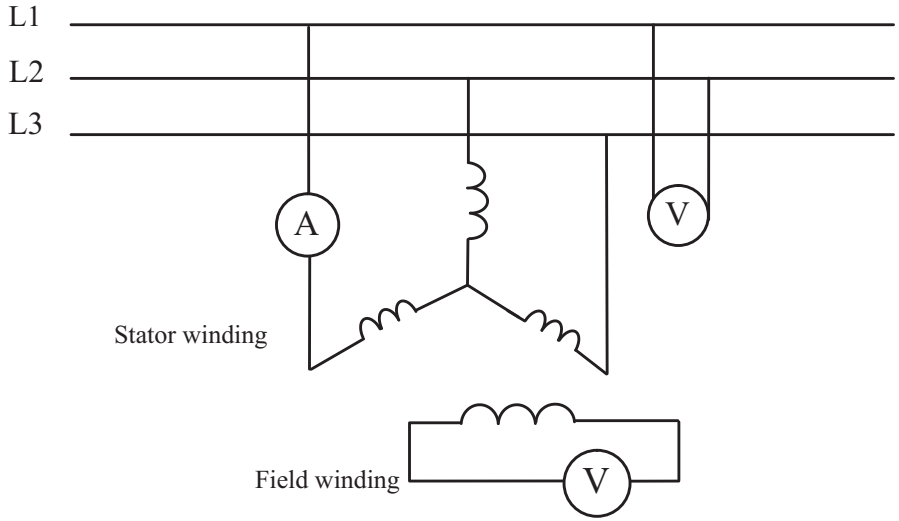

Fig. 5- 5 Slip test to determine the X_{Sd} and X_{Sq}

5.3.2 Synchronous generator short circuit test

Reactances and time constants of the synchronous generator are of great assistance for predicting the short circuit current. Conversely, a short circuit may be utilised to evaluate some of the reactance and time constants. Before we go into details of computing these constants from the test data, let us try to get a physical picture under short circuit conditions. Consider a synchronous generator rotates at a synchronous speed with constant excitation initially unloaded. If a three-phase short circuit is suddenly applied at the armature terminals, then the flux is produced by field circuit links the armature circuits. When the three phase short circuit fault occurs at t=0 as shown in fig 5-6, the trapped armature flux linkages are given by:

$$\psi_A = \psi_{\max} \cos \vartheta \qquad \textbf{(5-3)}$$

$$\psi_B = \psi_{\max} \cos(\vartheta - \frac{2\pi}{3}) \quad \textbf{(5-4)}$$

$$\psi_C = \psi_{\max} \cos(\vartheta + \frac{2\pi}{3}) \quad \textbf{(5-5)}$$

Where ϑ is the angle between phase u and d-axis. Thus it is seen that flux linking each phase is different. As the field moves away after t=0, since the flux cannot change immediately, the d.c current of appropriate magnitude appears in each phase to preserve the flux. Since the flux is different for all the phases depending on the angle ϑ , the d.c currents that appear will also be of different magnitude, depending on angle ϑ . If the magnitudes of all the d.c currents appearing in the armature phases were the same, there would not be any net resultant flux. But as they are unequal, there will be resultant flux, which produces a damped fundamental current in the field circuit. To an observer on rotor, the mentioned component produces a flux, which is a pulsating one. This flux can be resolved into rotating flux waves of same magnitude traveling in opposite directions at synchronous speed with respect to an observer on rotor. The one traveling with the direction rotation of the rotor travels at twice the synchronous speed with respect to the stator and the other one would be stationary with respect of the stator. So the latter cannot induce anything; but the former produces the double frequency component current in the armature phases, which are all of the same magnitude. These second harmonic currents give rise to net resultant flux. Sustained fundamental three phase armature circuits are induced from the constant flux of the field circuit. These currents produce an m.m.f rotating forward at the synchronous speed with respect to the stator, but stationary with respect to the rotor and centered on the direct on the direct axis of the field. This armature m.m.f opposes field m.m.f and tends to reduce the field current as well as damping currents are induced. Thus there exist the transient and subtransient d.c components in the rotor windings, damped by direct-axis transient short circuit time constant $T_d^{`}$ and the direct-axis sub transient short circuit time constant $T_d^{``}$ respectively. As result ac components in the armature windings will exist. The transient and subtransient fundamental components will decay by the time constants $T_d^{`}$ and $T_d^{``}$ respectively. The stator phase windings have

the following sustained fundamental a.c current, damped fundamental ac current with time constant $T_d^{`}$ and damped fundamental a.c with time constant $T_d^{``}$.

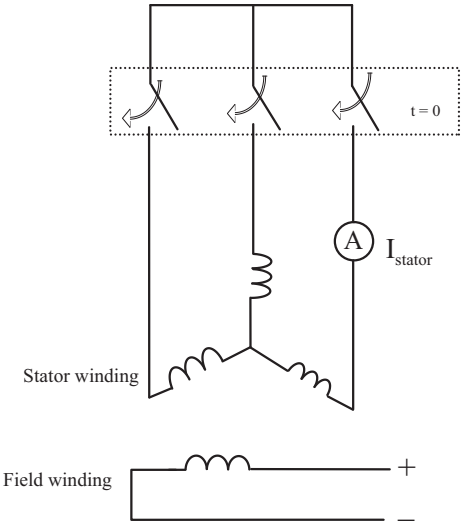

Fig. 5- 6 Short circuit test for synchronous generator

The subtransient period lasts only for the first few cycles, during which the decrement of the current is very rapid. The transient period covers a relatively longer time during which the decrement of the current is more moderate and finally the steady state is attained during which the current has a sustained value. The direct axis circuit time constants $T_d^{`}$ and $T_d^{``}$ can be evaluated from the transient and subtransient components. In a steady state the stator current reaches its final value. The magnitude of the stator current is given by U_p/X_d, where U_p is the open circuit voltage of the generator [76],[77]. This value should not exceed 20% of the rated voltage of the generator in order to that the stator current does not exceed the rated current of the machine. If we perform the short circuit taking into consideration the above mentioned precaution, we can obtain the subtransient and transient circuit time constants. The measured value of the short circuit is present in fig. 5-7. The difference

between the sub transient and the extended transient is plotted on semi log paper. The obtained sub transient direct short circuit is 24ms. The difference between the transient and the steady state is plotted on semi log paper also. The obtained transient direct short circuit is 190ms.

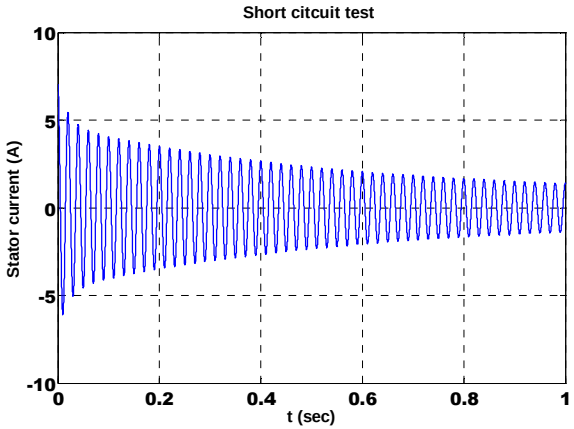

Fig. 5- 7 Stator current of synchronous generator at short circuit test

5.3.3 Synchronous generator standstill test

In order to obtain the subtransient direct reactance axis and subtransient quadrature reactance axis the standstill is performed. In the standstill only two-phase winding is energised with small voltage 20V as shown in fig 5-8. The field winding is short-circuited and the field current is measured. When the field current is at maximum, we obtain the subtransient direct reactance axis from the following equation [86].

$$X''_{Sd} = \frac{U}{2I} = 2.3\Omega \qquad \textbf{(5-6)}$$

We obtain the subtransient quadrature reactance axis from the following equation, when the field current is zero.

$$X''_{Sq} = \frac{U}{2I} = 1.9\Omega \qquad \textbf{(5-7)}$$

The stator current and the field current are shown in fig 5-9, 5-10 for the subtransient quadrature and direct axis respectively.

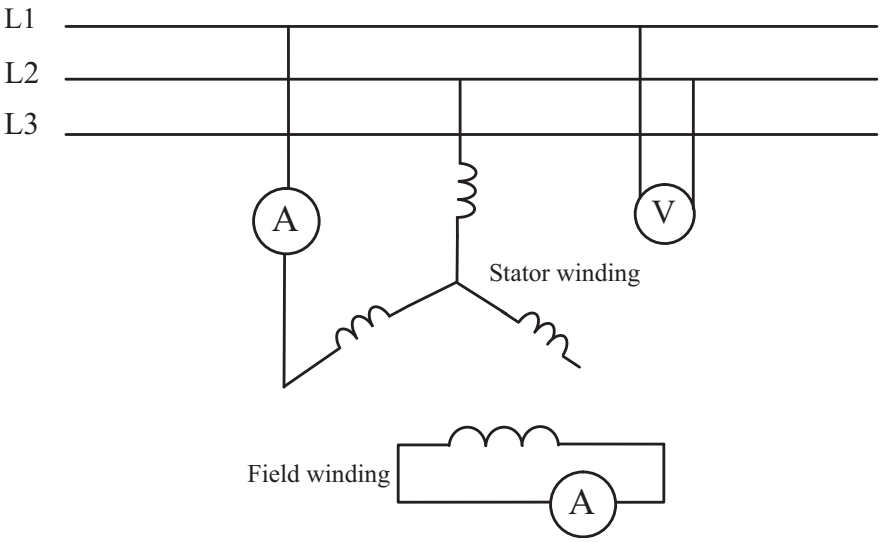

Fig. 5- 8 Standstill test circuit diagram

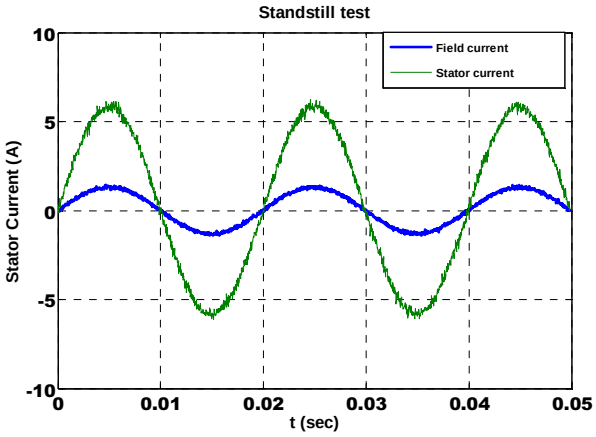

Fig. 5- 9 Standstill test for subtransient direct axis reactance

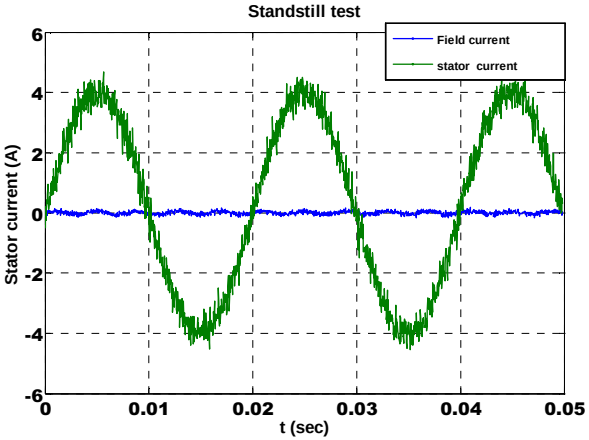

Fig. 5- 10 Standstill test for subtransient quadrature axis reactance

5.3.4 Synchronous generator switch slip test

In order to obtain the transient quadrature open circuit time constant the switch slip is performed. In the switch slip-phase winding is energised with small voltage, which is about 20V. The circuit diagram of the switch slip test is in shown in fig 5-11. The synchronous generator is rotated by an external drive with a very small slip of less than one percent. The slip can be calculated from the synchronous speed of the generator. The field winding is short-circuited and the field current is measured. The supply voltage is disconnected at the time zero field current as shown in fig 5-12. The maximum value of the voltage is drawn on semi log paper in order to obtain the transient quadrature open circuit time constant. The obtained transient quadrature open circuit time constant is 250 msec.

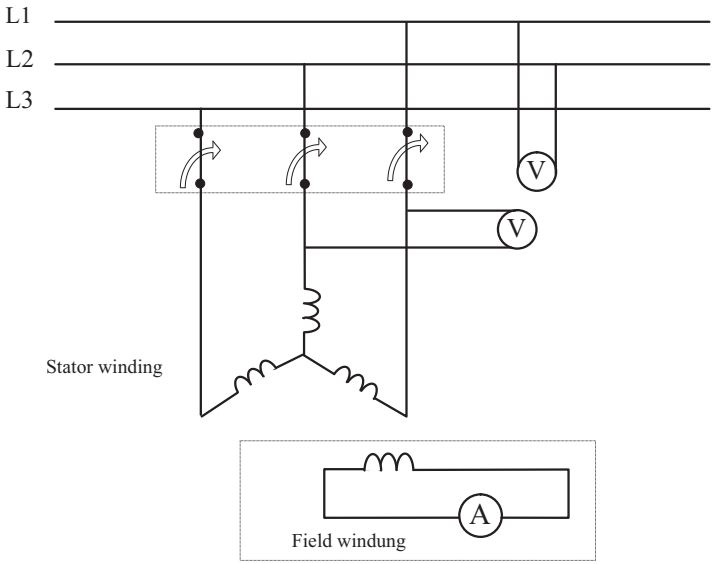

Fig. 5- 11 Switch slip test circuit diagram

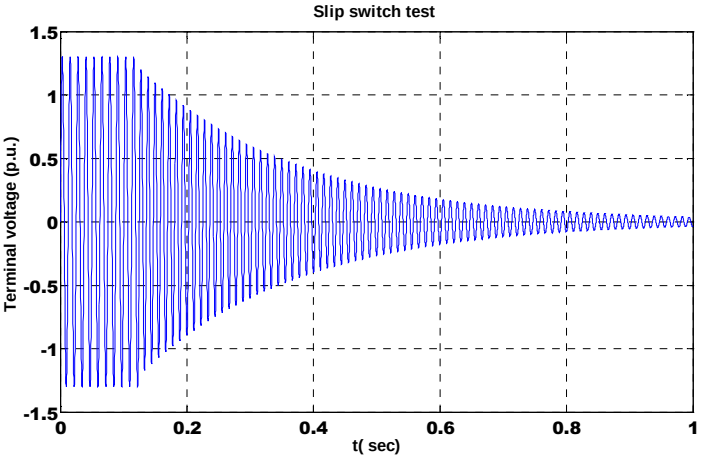

Fig. 5- 12 Terminal voltage of the generator at switch slip test

5.4 Output filter

All the available modulation methods generate harmonic pollution in the injected voltage [9],[26],[97]. These harmonics have harmful effects such as:

- The isolation of the winding of coupling transformer may not able to tolerate the dU/dt stress.
- The short time duration of the pulse
- High frequency interference may exist which may disturb the function of sensitive devices.

The output filter is used to attenuate the high frequency harmonics of the inverter to very small values. The output filter can be realised in different configurations such as band pass filter, low pass filter. The low pass filter consists of three types L filter, LC filter and LCL filter.

In practical application the LC filter is used due to simplicity and low cost. The LC filter consists of series inductor with inductance L_F and a shunt capacitance C_F .The LC filter together with inductance of the load will dampen the harmonic of the load voltage by 40 dB every decade after the resonance frequency. Also the harmonic in load current will be damped by 60dB every decade after the resonance frequency. The compensating voltage is defined by the following transfer function

$$U_1 = U_W \frac{1}{1 + sR_F C_F + s^2 L_F C_F} + I_F \frac{R_F + sL_F}{1 + sR_F C_F + s^2 L_F C_F} \qquad \textbf{(5-8)}$$

In designing the LC filter, the first step is to decide the resonance frequency. The resonance frequency of the filter is chosen to be much lower than the switching frequency thus eliminating the switching ripple of the output voltage [10]. In order to have a low ripple voltage in the output voltage the inverter, the resonance frequency of LC filter should be chosen at least ten times the fundamental frequency. The fundamental frequency in the experiment is 50 Hz. The resonance frequency is chosen to be 523Hz.The other important parameter of filter is the voltage drop of the inductance filter at rated current and maximum frequency. We can obtain the inductance from the voltage drop. In literature is stated that the nominal voltage drop 4% is good.

$$L_F = \frac{\Delta u_L U_{dc}}{I_F \, 2\pi f} = \frac{(0.04)(480V)}{(16A)(314 rad/\sec)} = 0.004\,\mathrm{H} \qquad \textbf{(5-9)}$$

Where U_{dc} is the inverter input voltage, Δu_L is the percentage of voltage drop. The capacitance is obtained from the resonance frequency.

$$C_F = \frac{1}{4\pi^2 f_{res}^2 L_F} = \frac{1}{4\pi^2 (523Hz)^2 (0.004H)} = 22\mu F \qquad \textbf{(5-10)}$$

5.5 Step response of the controllers

Before we present the practical results of the experiment, we must make sure that the current and voltage controller have a good response. A step function will be applied to the inner loop the current controller. Then a step function will be applied to the outer loop voltage controller. The measured step response of the filter current controller is presented in fig 5-13. From the figure it is obvious that there is good decoupling between the d-axis and q-

axis of the filter current. The three phase currents of the filter are shown in fig. 5-14.

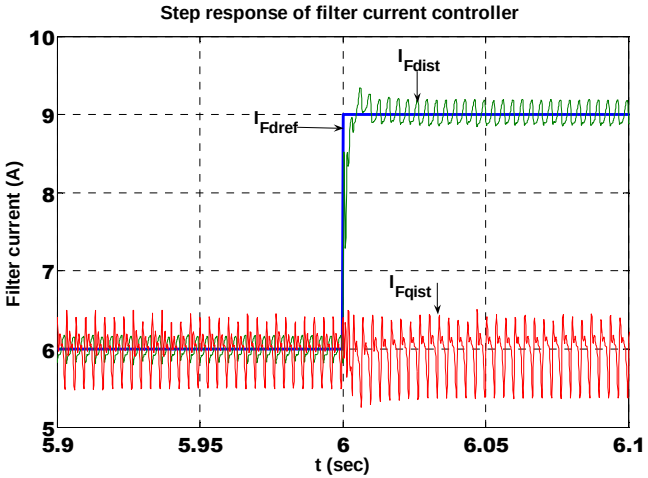

Fig. 5- 13 Measured step response filter of the current controller in d- axis

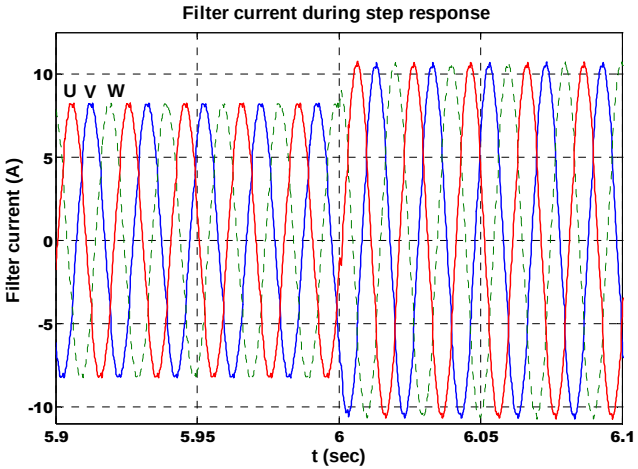

Fig. 5- 14 Filter current during step response

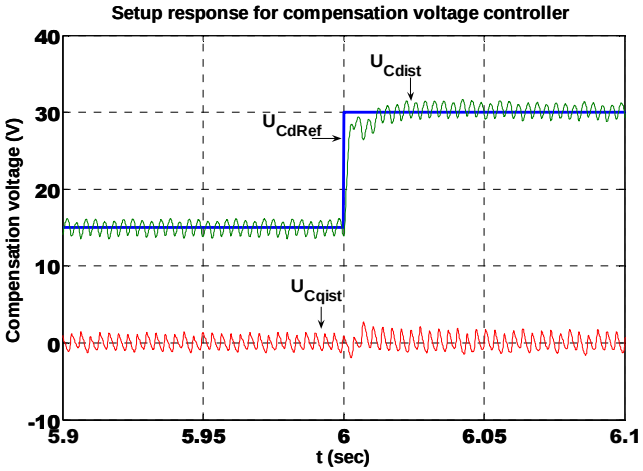

Fig. 5- 15 Measured step response of the voltage controller in d-axis

The measured step response of the voltage controller is presented in fig 5-15. The d-axis and q-axis of the voltage controller is well decoupled. The three phase compensation voltages are shown above in fig. 5-16.

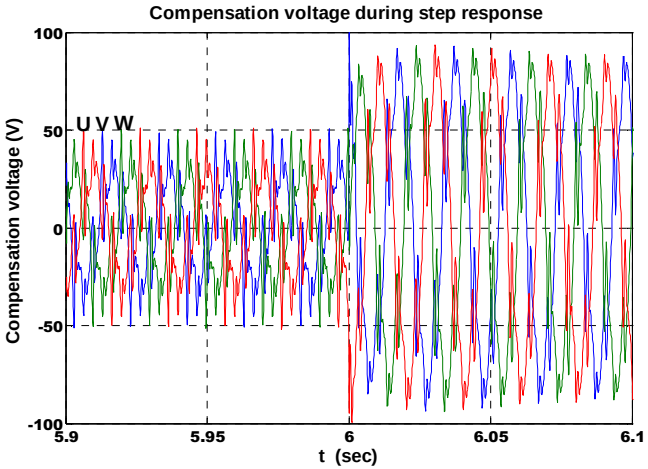

Fig. 5- 16 Compensation voltage during step response

5.6 Analysis of the results

In order to evaluate the effect of SSSC, the PGS is derived with the same velocity and fixed excitation for both cases with and without compensation. The practical results show that SSSC increases the output power of the generator compared to without compensation fig 5-17. The measurement shows that the terminal voltage will decrease with the increase of the current without compensation but SSSC stabilises the output voltage of PSG fig 5-18. At the beginning when the compensation voltage is zero, the output power with SSSC is less than without compensation, the reason being that the coupling transformers need reactive power and the voltage drop on the transformer impedance. SSSC should provide the reactive power at first needed by the coupling three transformers. Then SSSC begins to supply the reactive power, which enable the increase of the output power of the generator, mean time the terminal voltage can become constant. From the output power current curve, it is clear that output power increases with the increase of the current till the output power reach the maximum value. In this region the harmonic in the terminal voltage increase so there is no further increases in the output power.

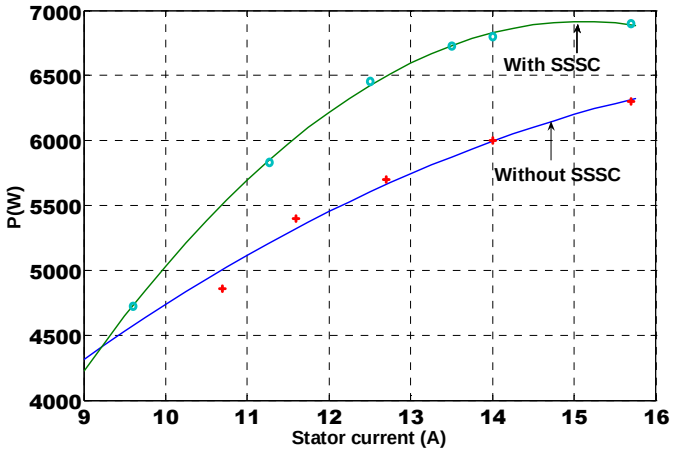

Fig. 5- 17 Output power versus stator current with and without SSSC

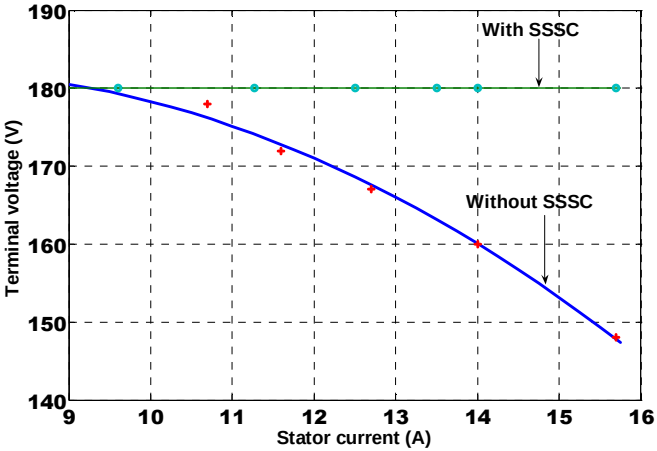

Fig. 5- 18 Terminal voltage versus stator current with and without SSSC

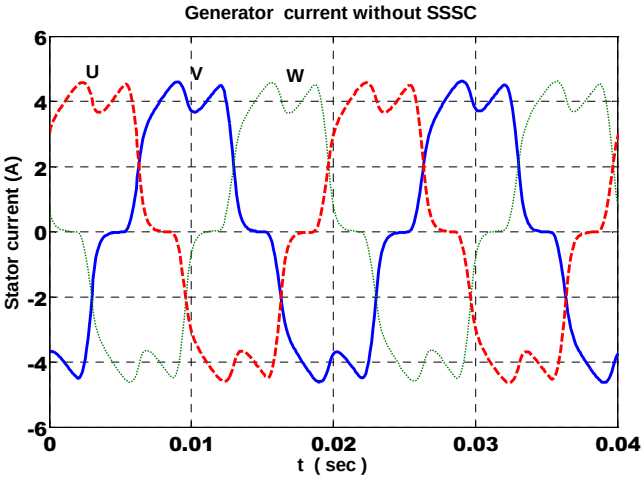

Fig. 5- 19 Measured stator current without SSSC

Our discussion here will focus on the three different cases, which are without SSSC, with SSSC and the last case with SSSC and a passive filter. The measured generator current without compensation is shown in fig. 5-19.The measured generator current contains the fifth and seventh harmonics. This is expected due to the presence of the rectifier bridge. The measured terminal voltage of the generator contains also the third, fifth and seventh harmonics. The fifth and seventh harmonics were generated from the rectifier's non-linear nature. The third harmonic was originally found in the generator at no load. The measured terminal voltage of the generator without SSSC is shown in fig.5-20.

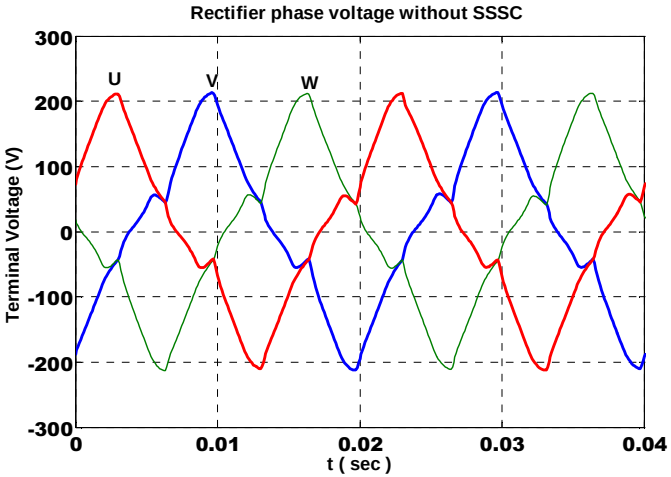

Fig. 5- 20 Measured terminal voltage without SSSC

When we apply the SSSC to the synchronous generator, the current and output power of the generator will increase. Also the terminal voltage of generator is almost constant with loading. Generator current is not completely sinusoidal but it contents harmonics. The harmonic content in generator current is less than without SSSC as shown in fig. 5-21.

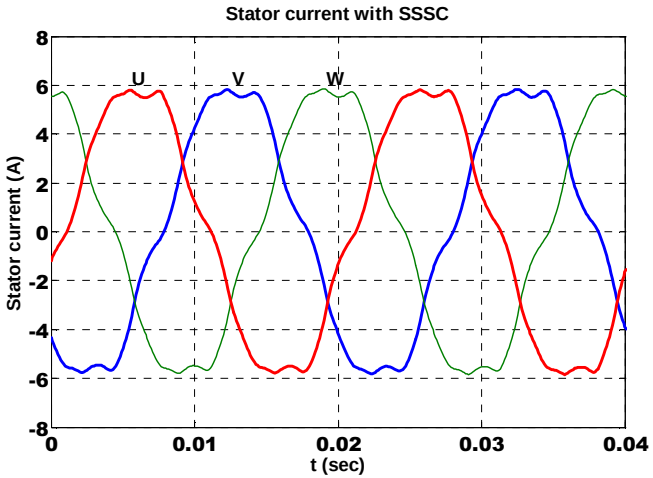

Fig. 5- 21 Measured stator current with SSSC

The terminal voltage of the generator is constant and contains the same spectrum of harmonic as shown in fig 5- 22. The only difference is that it has more harmonic content compared to the case without SSSC. Table 5-4 shows the THD of the both generator current and input voltage of the rectifier with and without compensation. The THD of the generator current decreases. On the other hand the THD of terminal voltage increases.

THD	Current	Rectifier voltage
Without SSSC	13.21%	17.11%
With SSSC	6.4%	20%

Table 5-4: THD of the current and input voltage of the rectifier

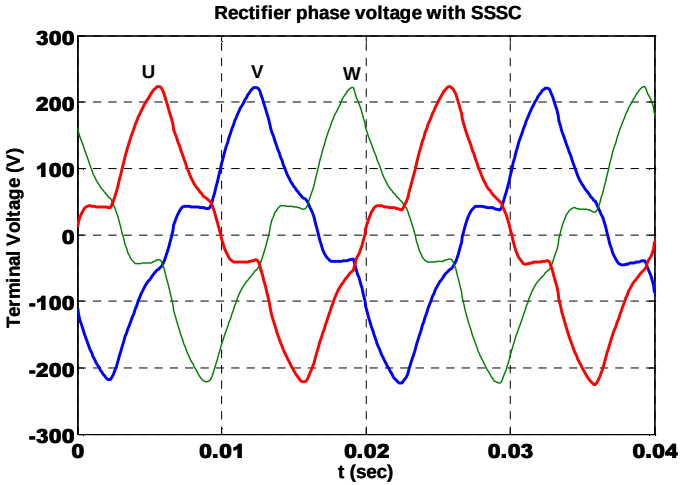

Fig. 5- 22 Measured terminal voltage with SSSC

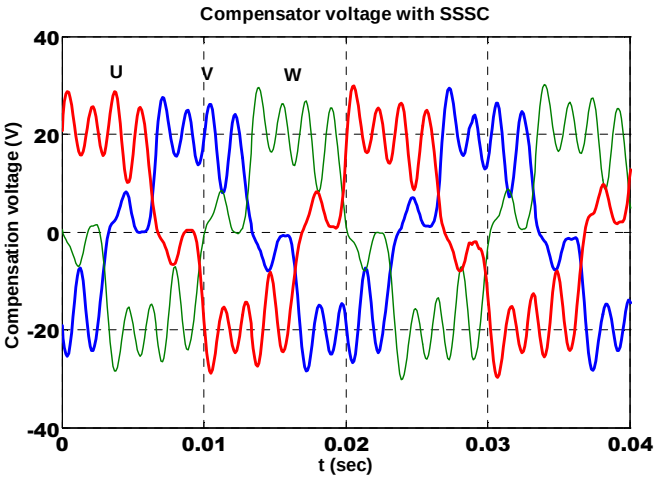

Fig. 5- 23 Compensation voltage in case SSSC only

The compensation voltage shown fig 5-23 is not free from harmonics. The reason for the harmonic is that the stator current of the generator that passes through the transformer contains harmonic. These harmonic currents produce voltages drop on the resistance and inductance of the transformer. Also these current cause losses in the transformer and increase the effective value the transformer currents. Passive filter was proposed in order to get rid of the harmonic in the compensation voltage and to decrease the compensation voltage amplitude. We connected a passive filter of fifth harmonic in parallel with the rectifier.

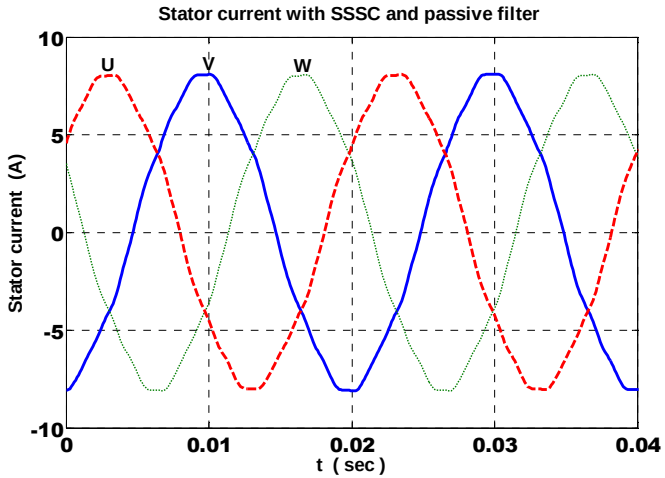

Fig. 5- 24 Measured stator current with SSSC and passive filter

This passive filter will provide a path to the fifth harmonic voltage. The stator current in the case of SSSC and passive is presented in fig 5-24. There is an increase in the current amplitude and a better quality of the current. The terminal voltage of the generator is constant and contains the same spectrum of harmonic as shown in fig 5-25. The harmonics content is less than with SSSC only. The fifth harmonic component is trapped due to the presence of the passive filter.

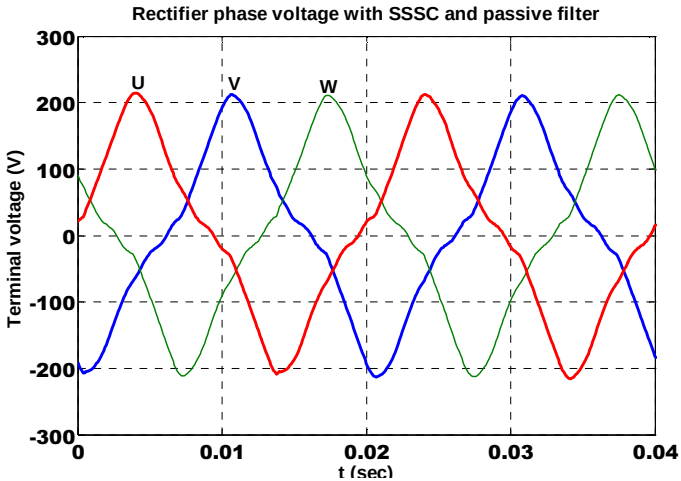

Fig. 5- 25 Measured terminal voltage with SSSC and passive filter

The FFT of the terminal voltage harmonic with and without passive filter are presented in fig 5-26. The terminal voltage contains the third harmonic in both cases with and without passive filter. This is due to its presence in the no load voltage of the terminal voltage. The fifth harmonic of the terminal voltage decreases from 12% to 2.5% and the seventh from 7% to 1.1%. The THD of the terminal voltage decreases from 33.42% to 23.6%. The decrease of the harmonics in the terminal voltage of the generator enables the increase of the output power of the generator.

The FFT of the generator current harmonic with and without a passive filter are presented in fig 5-27. The fifth harmonic of the generator current decreases from 10.3% to 2.7% as well as the seventh harmonic from 7% to 4 %. The THD of the generator current decreases from 12.5% to 5.16%.

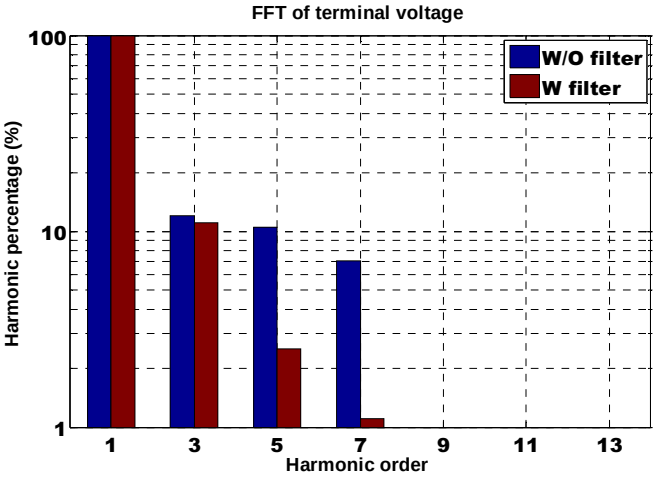

Fig. 5- 26 FFT of terminal voltage with SSSC and without passive filter

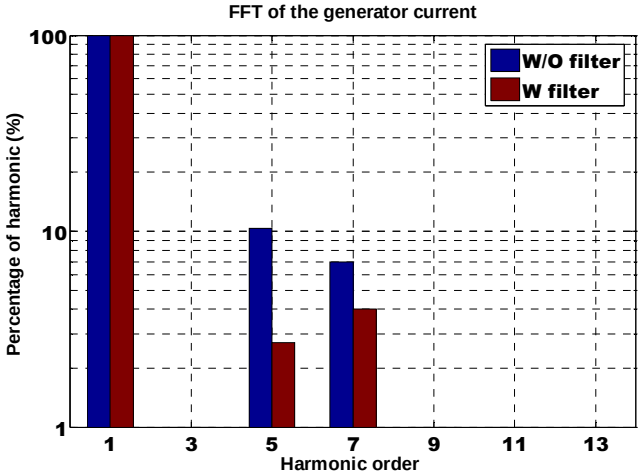

Fig. 5- 27 FFT of stator current with and without passive filter

The compensation voltage, which is shown in fig 5-28, has fewer harmonic in the case of the SSSC with passive filter compared to without passive filter. This is due to less harmonic content of the generator current. When connecting the fifth harmonic passive filter, the fifth harmonic is trapped in this filter.

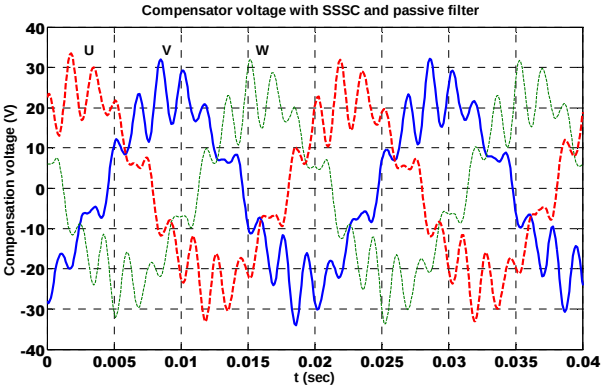

Fig. 5- 28 Measured compensation voltage in case of SSSC and passive filter

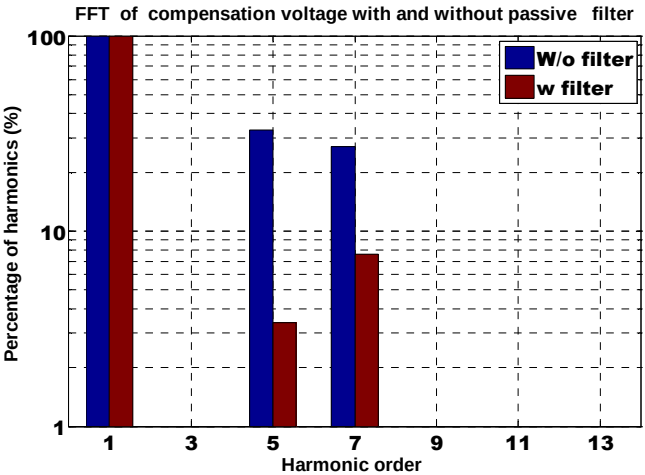

Fig. 5- 29 FFT of compensation voltage with and without passive filter

The FFT of the compensation voltage harmonic with and without passive filter are presented in fig 5-29. The fifth harmonic of the terminal voltage decreases from 12% to 2.5% and the seventh from 11.8% to 8%.

The proposed equivalent circuit which is explained in chapter two, is modified by adding by third harmonic component to the internal induced voltage which is exists in the generator at Technical University Chemnitz lab. The actual parameters of the generator and the same dc bus level were used. In order to compare the measurement and the calculated result, we were forced due to the limitation of the available components to small portion of the output power of the generator. The measured output power and the calculation of the output power in both cases without and with passive filter agree to a far extend together when we apply certain compensation voltage as shown in fig. 5-30. Although calculated output power of the generator for both cases is more than the measured amount. The assumption of considering the output voltage of the inverter is ideal as sinusoidal source, led to the deviation between measured and calculated efficiency. The other reason is that the parameters of the system are not accurate enough.

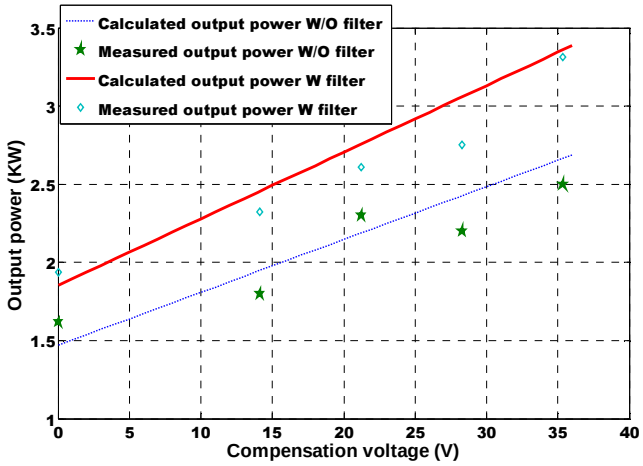

Fig. 5- 30 Measured and calculated output power versus compensation voltage for both with and without passive filter

Figure 5-30 shows that the combination of the passive filter and SSSC reduces the compensation voltage needed. The reduction of the compensation voltage depends on the capacitance of the filter. An economical solution must be found, in order to dimension the magnitude of the permanent magnet, the needed compensation voltage and capacitance of the passive filter.

5.7 System losses and efficiency

The application SSSC introduces additional losses in systems, which are losses in coupling three transformers, in the inverter, passive filter and LC filter losses. The generator losses consist of friction losses, iron losses and copper losses P_{LCo} which are presented in eq.5-11. The transformer losses consist of copper losses P_{LT}, which are presented in eq. 5-12. The LC filter losses P_{LC} are the copper losses of the filter, which are presented in eq. 5-13. Dielectric losses of the filter capacitance are presented in eq. 5-14.

$$P_{LCo} = 3I_S^2 R_S \quad \textbf{(5-11)}$$

$$P_{LT} = 3I_1^2 R_T \quad \textbf{(5-12)}$$

$$P_{LC} = 3I_F^2 R_F \quad \textbf{(5-13)}$$

$$P_{LDi} = 3U_C^2 \omega C_F \tan\delta \quad \textbf{(5-14)}$$

Where R_S is the stator resistance, R_T is the transformer resistance, C_F capacitance of the filter, tan δ is the loss angle of the capacitor. The equation for the inverter is presented chapter two in equation 2-30 till equation 2-34. The losses of different components are presented in fig. 5-31.

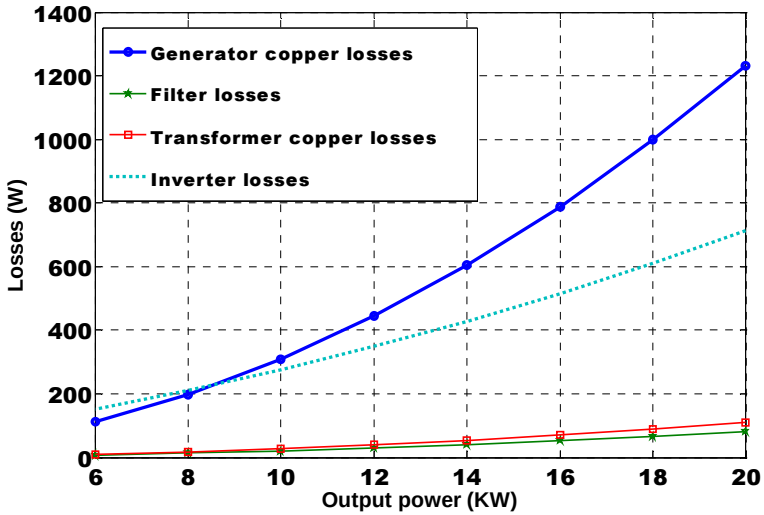

Fig. 5- 31 Losses of different components

The measured efficiency of the system without SSSC and with SSSC at different tapping of the transformer is presented in fig 5-32. The SSSC decreases the efficiency of the system compared to without SSSC. Also with SSSC the efficiency increases by increasing the tapping of the transformer. This is due to the decrease in the inverter current.

If we compare the calculated efficiency with the measured efficiency, we will find out that the measured efficiency is less by 1.5% as shown in fig. 5- 33. The voltage and current are assumed to be sinusoidal in efficiency calculation. This assumption caused a difference between the measured and calculated efficiency. The measurement of the parameters of the generator and the transformer also contains error.

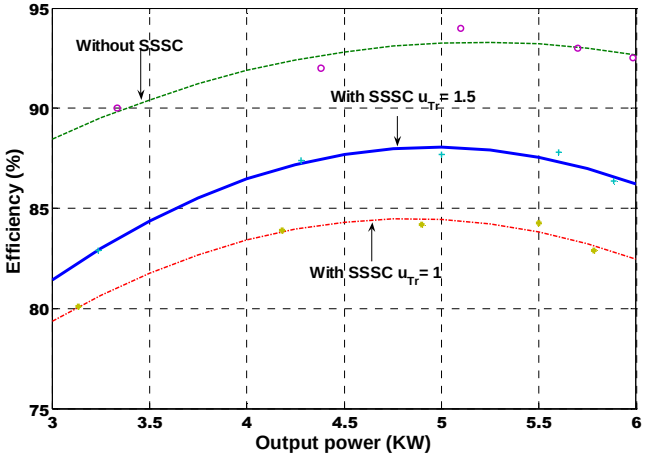

Fig. 5- 32 Measured efficiency without and with SSSC at different tapping of transformer

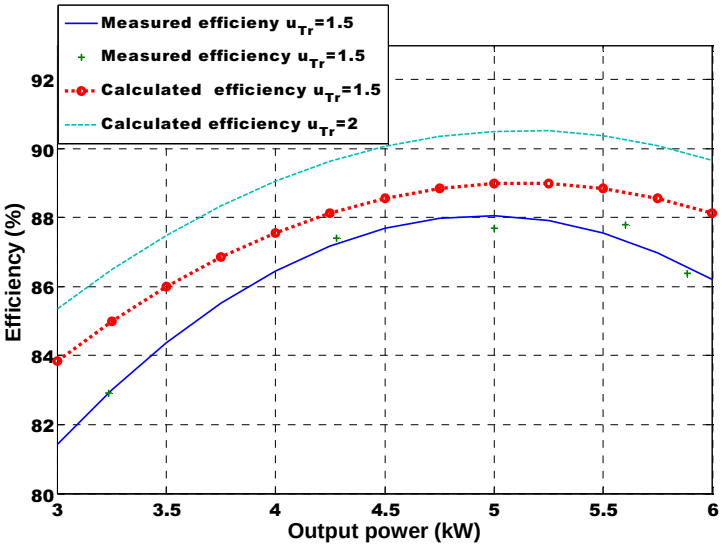

Fig. 5- 33 Measured and calculated efficiency of SSSC only

The efficiency of the system is slightly higher, when the passive filter is connected parallel to the rectifier as shown in fig 5-33. The efficiency increased because the currents and the terminal voltages of the generator are almost sinusoidal. On the hand there are additional losses in the resistance of the passive filter R_5. These losses are expressed in eq. 5-15.

$$P_{PF} = 3I_5^2 R_5 \qquad \textbf{(5-15)}$$

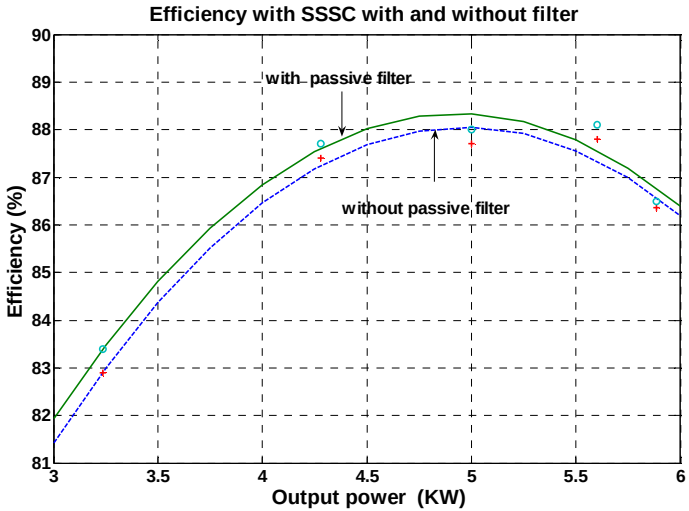

Fig. 5- 34 Measured efficiency of the system with and without passive filter

6

Conclusion

Worldwide, the total of installed wind power capacity as well as the average rated power per windmill is constantly increasing. In many European countries, particularly in Denmark, Germany and Spain, wind power has experienced a rapid growth during the past years and contributes nowadays considerably to the overall electricity production. Presently, for units above 1MW, variable speed concepts are usually applied that is either based on doubly fed induction machines or synchronous machines. Some of the largest units are currently available and therefore especially suited for offshore. Permanent magnet salient pole synchronous generators have usually a higher efficiency and are more compact than electrical excited generator. This is due to the absence of the excitation winding. However, they are more expensive. The main disadvantage of permanent synchronous generators is that the terminal voltage of generator is not controlled. The measurements of an electrical excited synchronous generator connected to dc network showed that electrical power is directly proportional to rotation velocity and to the excitation voltage. The measurements revealed that the PSG delivers less than its rated power at rated excitation. The measured terminal voltage decreases with an increase of stator current. Terminal voltage increases with the increase of excitation level. The measurements have shown that in order to obtain the rated power of the PSG connected to dc grid, we must exceed the rated excitation.

External reactive power compensation provides an attractive to overcome this problem of constant magnet in the permanent magnet synchronous generator. As a result we can control the terminal voltage of the generator and increase the output power of generator.

Different compensation methods were examined. Static synchronous series compensator (SSSC) changes the generator impedance. Voltage regulator changes the terminal voltage and phase regulator changes the power angle. Static synchronous compensator (STATCOM) generates reactive power.

In this thesis the mathematical derivation for the required compensation voltage for the fundamental frequency has been considered at the beginning. We can conclude that STATCOM does not increase electrical output power. Voltage regulation increases the active power but must be accompanied by increasing the excitation voltage because it does not deliver reactive. SSSC increases output power and stabilises the terminal voltage at both normally and over excited mode. The phase regulator delivers reactive power and it can operate only in the over excited mode. It has better efficiency than SSSC by 0.6%. On the other hand the phase regulation requires more compensation voltage than SSSC about 40% for our generator. It is worth mentioning that this value depends on the reactance of the generator. As result the rating of the inverter and the coupling transformers can be smaller with SSSC than with phase regulator. SSSC method has been used this research for above mentioned reasons.

The other important point after the decision of using SSSC is dimension the required SSSC voltage U_C. The required SSSC compensation voltage depends on the ratio between the internal induced voltage U_P and the terminal voltage U_S. As ratio U_P / U_S increases the required compensation voltage will decrease. The ratio of U_P/U_S will determine the amount of the required permanent magnet for the generator. The required permanent magnet increases with increase of the U_P/U_S ratio. On the other hand the cost of the generator will increase due to the cost of permanent magnet material. Calculation of the permanent magnet mass was presented. Cost comparison of the three different alternatives was presented. SSSC increases the cost of the system due to the cost of the coupling transformers and the inverter.

Simulation of the complete system was done using Simulink program. The system consists of the permanent magnet synchronous generator, SSSC and dc grid. The simulation result verified the theatrical theory proposed. In order to validate the simulation and the proposed theory, the SSSC compensation was applied to 25KVA electrical excited salient pole synchronous generator connected to dc network in the lab at the Technical University Chemnitz. The measurement showed the terminal voltage will decrease with the increase of the current without compensation but SSSC stabilises the output voltage of synchronous generator. At the beginning when the compensation voltage is zero, the output power with SSSC is less than without compensation. This is due the reactive power required by the coupling transformers and the voltage drop on the transformer impedance. SSSC should provide the reactive power at first needed by the coupling three transformers then the output power can increase and the terminal voltage can become constant. On the other hand the efficiency of the system will decrease due to the additional component losses. It is worth mentioning that the THD of the generator current decreases with SSSC while the THD of terminal voltage increases with SSSC.

The compensation voltage is not free from harmonics in case of SSSC. The stator current which passes through the coupling transformer contains harmonics. These harmonic currents produce voltages drop on the resistance and inductance of the transformer. This is the source of the harmonic in the compensation voltage. Also these harmonic currents cause losses in the transformer and increase the effective value the transformer currents.

Addition of a passive filter was proposed in order to get grid of the harmonic. This passive filter will provide a path to the harmonic voltage. Numerical analysis is presented to take the harmonics into consideration. Finally comparison between the active filter and hybrid is presented. The needed SSSC compensation voltage was decreased with the installation of a passive filter. This is due to the improvement in the power factor and the absence of the harmonic in the generator current and terminal voltage. The reason is that the passive filter is capacitive at the fundamental frequency. The passive filters with bigger capacitance are able to provide more reactive power. As result less compensation voltage is required. The reduction of the rating of

SSSC depends on the capacitance of the filter and the quality of the filter. Based on the fundamental frequency calculation the required compensation voltage will reduced be by 17% by the installation of the passive filter with 0.2 p.u capacitance.

Simulation of complete system, which includes synchronous generator, compensation voltage and passive filter and dc network, was done using Simulink program. The simulation results validated the proposed theory. The passive filter was built in the experiment. The measured terminal voltage and generator current with the passive filter had fewer harmonics compared with SSSC alone. The output power of the generator increased with the installation of the passive filter compared to the SSSC alone. The efficiency of the complete system slightly increased due the passive filter.

Future Work

Cost function including different component of the system have to be optimised. There must be a compromise between the cost of the permanent magnet generator, the coupling transformer and the needed inverter.

The new trends are usage of the SSSC without coupling transformer. The coupling transformers are bulky component of the system. It would very positive to grid rid of this bulky component in order to reduce the cost of the supports in offshore plants and the cost of the transformers. On the other hand the transformers help to reduce the harmonic content in the generator current. In transformer less configuration, the inverter will consist of a three single phase converter instead of three phase inverter compared to the case with coupling transformer. In order to reach an optimal solution, the size of permanent magnet and compensation voltage in both cases with and without coupling transformer has to be optimised.

7

Theses

1. There is boom worldwide in the number of the installed wind power plant in order to reduce carbon dioxide emission. Offshore wind power plant provides a huge potential.

2. The major obstacles to offshore power plant are the maintenance, the connection to grid and the weight of the plant.

3. The permanent magnet synchronous generator provides an attractive solution due to its own advantages i.e. High power to weight ratio, high efficiency. The main disadvantage is the terminal voltage is not controllable.

4. The measurement indicated of the electrical excited synchronous generator that the terminal voltage decrease with increase of the stator current.

5. Over excitation is required by synchronous generator, when feeding dc network through a diode rectifier, in order to obtain the rated power of the generator.

6. External reactive power compensation provides a means to control the terminal voltage of the generator.

7. Different compensation methods were examined. Static synchronous series compensator (SSSC) changes the generator impedance. Voltage regulator changes the terminal voltage and phase regulator changes the power angle. STATCOM generates reactive power.

8. STATCOM does not increase the output power of the generator.

9. Voltage regulator increases the output power of the generator but must be accompanied by increasing the excitation voltage because it does not deliver reactive power.

10. SSSC increases the output power of the generator. It can operate in a normally excited and over excited mode.

11. Phase regulator delivers reactive power and it can operate only in the over excited mode.

12. Phase regulator requires more compensation voltage than SSSC by about 40% in over excited mode at rated load. This value depends on the reactance of the generator. On the other hand a phase regulator has better efficiency than SSSC by 0.6 % at the rated load.

13. The practical result showed that the SSSC stabilises the terminal voltage increases the output power. On the other hand the efficiency of the system is less than without compensation.

14. Compensation voltage in case of SSSC is not free from harmonics. The reason of harmonic is that the stator current that passes through the transformer contains harmonic. These harmonic currents produce voltages drop on the resistance and inductance of the transformer.

15. In order to get rid of the harmonic content, the passive filter is proposed. The passive filter absorbs these harmonics.

16. The passive filter reduces the compensation voltage because it provides reactive power. The passive filter is capacitive at the fundamental frequency. The reduction of the compensation voltage

with passive filter depends on the value of the capacitance of the filter.

17. The compensation voltage will be reduced by 17% by the installation of the passive filter with 0.2 p.u capacitance based on the fundamental frequency calculation.

Reference

Papers

[1] Akagi H.; Fujita H.

A Shunt Active Filter Based on Voltage Detection for Harmonic Termination of a Radial Power Distribution Line, IEEE Trans. on Industry Application Vol. 35 No. 3 May/June 1999, pp. 638-645.

[2] Akagi H.

New Trends in Active Filter for Power conditioning, IEEE Trans. on Industry Applications, Vol. 32 No. 6 November / December 1996, pp. 1312- 1322

[3] Ametani A.

Harmonic Reduction in Thyristor by Harmonic Current Injection , IEEE Trans on power app. Vol PAS –95, No. 2, March/April 1976, pp. 441-449

[4] Awad H.; Blaabjerg F.

Mitigation of Voltage Swells by Static Series Compensator, IEEE Power Electronics Specialists, Aachen 2004, pp. 3505- 3511 Specialist Conference

[5] Bhattacharya S.; Divan D.; Banerjee B.

Synchronous Frame Harmonic Isolator Using Active Series Filter, EPE 91 Firenze, pp. 30-35

[6] Bhowmik S. ; Spee R. ; Enslin J.

Performance Optimization for Doubly Fed Wind Power Generation Systems, IEEE Trans. on Industry Application Vol. 37 No. 1 July /August 1999, pp. 949-958.

[7] Binder A. ; Schneider T.

Permanent Magnet Synchronous Generator for Regenerative Energy conversion- a Survey, EPE 2005 Dresden Germany, CD ROM

[8] Borrup M. ; Karsson P.; Alaküla M.; Gertmar L.

Multi Rotating Integrator Controller for Active Filters, EPE 88 Laussanne

[9] Van Der Broeck H. ; Christoph H.

Analysis and Realisation of a Pulse width Modular Based on Voltage Space Vector, IEEE Trans. on Industry Application Vol. 24 No.1 January /February 1998, pp. 1639- 1644.

[10] Van der Broeck H. ; Loef Chr.

Use of LC Filters in Hard Switching PWM Inverter Drives, EPE95 Sevilla, pp.1536 - 1541

[11] Carlson O. ; Grauers A.; Svensson J.; Larsson A.

A Comparison of Electrical Systems for Variable Speed Operation of Wind Turbines, EWEC 94, Greece 1994

[12] Dixon J.; Venegas G. ; Moran L.

A Series Active Power Filter Based on Sinusoidal Current Controlled Voltage Source Inverter, IEEE Trans. on Industrial Electronics Vol. 44 No. 5 October 1997 , pp. 639-644.

[13] Edris A.; Mehraban A. ; Rahman M.; Gyugyi L., Arabi S.

Controlling the flow of Real and Reactive Power, IEEE Journal of Computer Applications in Power Vol. 11 Issue 1 August 2002, pp.20-25

[14] Erinmetz Ed.

Stator Var Compensator, CIGRE Working Group 38-01 Task Force No. 2, 1986

[15] Fitzer C.; Arulampalam A.; Barnes M.

Mitigation of Saturation in Dynamic Voltage Restorer Connection Transformer, IEEE Trans. on Power Electronics Vol.17 No. 6 November 2002, pp.1058-1066

[16] Fleckenstein K.

Windenergie in der Raumordnung. Theorie und Praxis Energiewirtschaft Jg.101 (2002) H.3 S. 76-81

[17] Fritz W.

WKA-Generatoren richtig ausgelegt. ETZ 1998 H.18, S.52-53

[18] Fujita H .;Akagi H.

The Unified Power Quality Conditioner: The Integration of Series and Shunt Active Filters, IEEE Trans. on Power Electronics, Vol. 13 No. 2 March 1998, pp. 315-322.

[19] Fujita H. ; Akagi H.

A Practical Approach to Harmonic Compensation in Power Systems Series Connection of Passive and Active Filters, IEEE Trans. on Industry Application Vol. 27 No.26 November / December 1991, pp.1020-1025.

[20] Gyugyi L.

Converter-Based FACTS Technology: Electric Power Transmission in the 21st Century. IPEC 2000 Tokyo Proceedings, p p.15-26

[21] Hansen LH. ; Blaabjerg, F.

Generators and Power Electronics Technology for Wind Turbines, 27 Annual Conf. of the IEEE IES IECON'01 Proceedings pp. 2000-2005

[22] Hartkopf T.; Hofmann M. ; Jöckel S.

Direct-Drive Generators for Megawatt Wind Turbines, EWEC97 Proceedings pp.668-671

[23] Häusler M.

Netzanbindung von Offshore Windparks mit Gleichstrom.
Elektrizitätswirtschaft 2000 H.24 S.83-85

[24] Holtz J.

Pulsewidth Modulation for Electronic Power Conversion,Proceeding of the IEEE Vol. 82 No. 8 August 1994, pp. 1194-1212.

[25] Kolhatkar Y.; Das S.

An Optimum UPQC with Minimum VA Requirement and Mitigation of unbalanced Voltage Sag, International Journal of Emerging Electric Power Systems Vol. 2, Issue 2, 2005, www.bepress.com/ijeeps/vol2/iss3/art1

[26] Kreienberg M.

50 Jahre Hochspannungs- Gleich- Stromübertragung(HGÜ),
Energiewirtschaft Heft10 /2004, S.58-59

[27] Kubo K.; Sakai K.

Feed forward Voltage Compensation for Digital Active Filter Using Frequency Domain Decomposition, EPE 97 Trondheim, pp.4786-4791

[28] Myoung G.; Lee D.; Seok J.

Control of Series Active Power Filters Compensating for Source Voltage Unbalance and Current Harmonics, IEEE Trans. on Industrial Electronics Vol. 51 No. 1 February 2004, pp. 132-139.

[29] Liccardo F. ; Marino P.; Triggianese M.

An efficient connection between grid and Wind Farm by Synchronous Active Front End, SPEEDAM 2006 Italy. CD- ROM

[30] Lindgren M. ; Svensson J.

Connecting Fast Voltage Source Converter to the Converters to the Grid Harmonic Distortion and its Reduction, IEEE Power Tech. Conference Sweden 1995, pp. 191-195

[31] Loh P.; Holmes D.

Analysis of Multi loop Control Strategies for LC/CL/LCL –Filtered Voltage Source and Current Source Inverters, IEEE Trans. on Industry Application Vol. 41 No. 2 March /April 2005, pp. 644-654.

[32] Magueed F.; Svensson J.

Control of VSC the Grid through LCL Filter to Active Balanced Currents, IEEE Industry Application Society 4oth Annual Meeting Hong Kong 2005, pp. 572-578

[33] Mattavelli P. ; Buso S.

Robust Dead beat Current Control for PWM Rectifiers and Active Filters, IEEE Trans. on Industry Application Vol. 35 No. 3 May /June 1999, pp.613-620.

[34] Meyl C.; de Haan S.; Bauer P.

Inventory of Electrical Configurations for Offshore Wind Farms, PEMC 2000, pp. 4-184 – 4-189

[35] Meyer W.

Stationäre Ortkurven der hpn und hsz Komponenten, Archiv für Elektrotechnik 69, 1986, S. 41-48

[36] Moor G.; Beukes H.

Maximum Power Point Trackers for Wind Turbines, IEEE Power Electronics Specialist, Aachen 2004, pp. 2044-2049 Specialist Conference.

[37] Monteiro L. ; Aredes M.

A control Strategy for Unified Power Quality Conditioner, ISIE'2003, Rio de Janeiro, Brazil, June 2003, CD ROM

[38] Monteiro L.; Aredes M.

A control Strategy for Shunt Active filter, IEEE/PES 10th Int. Conf. on Harmonics and Quality of Power, Rio de Janeiro, Brazil, October 2002, pp. 472-477

[39] Miller A.; Muljadi E. ; Zinger D.

A Variable Speed Turbine Power Control, IEEE Trans. on Energy Conversion Vol. 12 No. 2, June 1997, pp. 181-186.

[40] Muljadi E.; Butterfield C.

Pitch Controlled Variable Speed Turbine Generation; IEEE Trans. on Industry Application Vol. 37 No. 1 January /February, pp. 240-246.

[41] Newman M.; Holmes D.; Blaabjerg F.

A Dynamic Voltage Restorer (DVR) with Selective Harmonic Compensation at Medium Voltage Level, IEEE Trans. on Industry Application Vol. 41 No.6 November /December 2005, pp.1744-1753.

[42] Nielsen J. ; Newman M. ; Blaabjerg F.

Control and Testing of a Dynamic Voltage Restorer (DVR) at Medium Voltage Level, IEEE Trans. on Power Electronics Vol. 19 No.3, May 2004, pp. 806-813.

[43] Nielsen J. ; Blaabjerg F.

Control Strategies for Dynamic Voltage Restorer Compensation Voltage Sags with Phase Jump, APEC 2001, California, pp. 1267-1273.

[44] Peng F.; Akagi H.

A New Approach to Harmonic Compensation in Power Systems, A Combined of Shunt Passive and Series Active Filters, IEEE Trans. on Industry Applications Vol. 26 No. 6 November /December 1990, pp.983-990

[45] Prinz S.; Pietzsch H.

Optimal Control of Static VAR Compensators in Power Supply Systems with Electrical Arc Furnaces, EPE 2005, Dresden, CD ROM

[46] Rabelo B.; Hofmann W.; Glück M.

Emulation of the Static and Dynamic Behaviour of Wind Turbine with a DC Machine, IEEE Power Electronics Specialist, Aachen 2004, pp. 2107-2112. Specialist Conference

[47] Raju A.; Fernandes B.; Chatterjee K.

A UPF Power Conditioner with a Simple Maximum Power Point Tracker fir Grid Connected Variable Speed Wind Energy Conversion System, EPE 2003, CD ROM

[48] Rollik D.; Schleede B.

Nd-Fe-B Magnets are Going Offshore in Wind Mill Generators, Bodo Power System November 2007, pp. 30-31

[49] Sakui M. ; Shioya M.

A Method for Calculating Harmonic Currents of a Three Phase Bridge Uncontrolled Rectifier with DC Filter, IEEE Trans. on Industrial Electronics Vol. 36 No.3 August 1989, pp. 434-440.

[50] Simon K.

Netzrückwirkungen bei Frequenzumrichtern, Energiewirtschaft Heft 10 /2003, S.32-33

[51] Singer A.;Hofmann W.

Local Compensation of Wind Energy Conversion System, EPE 2005, Dresden CD ROM

[52] Singer A.; Hofmann W.

Static Synchronous Series Compensation applied to Small Wind Energy Conversion System, EPE 2007, Aalborg, CD ROM

[53] Singer A.; Hofmann W.

Comparison between different Compensation Methods Applied to Permanent Synchronous Generator, PCIM 2005 Nürnberg, CD ROM

[54] Singer A.; Hofmann W.

Static Synchronous Series Compensation applied to Permanent Synchronous Generator, PCIM 2007 Nürnberg, CD ROM

[55] Singer A.; Hofmann W.

Combined System of Static Synchronous Series Compensation and Passive Filter applied to Wind Energy Conversion System, PEDS 2007 Bangkok, CD ROM

[56] Singh B.; Al Haddad K.

A New Control Approach to Three Phase Active Filter for Harmonics and Reactive Power Compensation, IEEE Trans. Power Systems, Vol. 13 February 1998, pp.133-140.

[57] E. Spooner E.; Williamson A.

Direct Coupled, permanent magnet generators for wind turbine applications. IEE Proc. Electrical Power Applications Vol.143, No.1, 1996, pp.1-8

[58] Strzelecki R.; Rusinski J.; Jarnut M.

Properties, Simulation and Experimental Investigation of the Series Parallel Active Power Filters, EPE2005 Dresden, CD ROM

[59] Sun Z.;Sakui M.

Calculation of Harmonic Currents in Series Connected Converter with AC Filters under unbalanced Power Supply , PEDS 99 July 1999, Hong Kong, pp.1044-1048.

[60] Svensson J. ; Sannino A.

Active Filtering of Supply Voltage with Series Connected Voltage Source Converter, EPE 2001, Graz, CD ROM

[61] Thiringer T. ; Linders J.

Control by Variable Rotor Speed of a Fixed Pitch Wind Turbine Operating in Wide Speed Range, IEEE Trans. on Energy Conversion Vol. 8, No.3 September 1993, pp.520-526.

[62] Vilsboll N.; Pinegin A.; Bugge J.

Weiterentwicklung des Konzeptes von vielpoligen direktgetriebenen Permanent-Magnet-Generatoren für Windkraftanlagen mit variabler Drehzahl, Wind Kraft Journal 1996, H.6, S. 14-19

[63] Vizireanu D. ; Kestelyn X. ; Brisset S. ; Brochet P.; Milet Y

Polyphased Modular Direct Drive Wind Turbine Generator, EPE2005 Dresden, CD ROM

[64] Wu C.; Y. Lee Y.

Damping of synchronous Generator by Static reactive power Compensator with digital Controller, IEE proceeding C Vol. 138 No.5 September 1991, pp.427-433

[65] Yano M.; Kuramochi S.; Nanaumi N.

New Control Method of Harmonic Current Compensation Using Individual Rotating P-Q Frame of Corresponding Frequency, EPE 97 Trondheim , pp. 4842-4847

Books

[66] dSPACE

Control Desk for Experiment Guide

[67] Fischer R.

Elektrische Maschinen, Hanser Verlag 1992

[68] Fitzgerald A. ; Kingsley C. ; Umans S.

Electric Machinery, McGraw Hill 1992

[69] Föllinger O.

Regelungstechnik Einführung in Methoden und ihre Anwendung, Hüthig Verlag 1994

[70] Gerd S.

Regelungstechnik, Mehrgrößenregelung, digitale Regelungstechnik, Fuzzy-Regelung, München 2002

[71] El Hawary M.

Electrical Power Systems Design and Analysis, Prentice Hall 1995

[72] Heier S.

Grid Integration of Wind Energy Conversion Systems, John Wiley & Sons 1998

[73] Hingorani N. ; Gyugyi L.

Understanding FACTS, Concepts and Technology of Flexible AC Transmission Systems, IEEE press 1990

[74] Jenni F.; Wüest D.

Steuerverfahren für selbstgeführte Stromrichter, Hochschulverlag AG der ETH Zürich 1995

[75] Just W.

Blindstrom Kompensation in der Betriebspraxis, Ausführung, Regelung, Wirtschaftlichkeit, Umweltschutz, Oberschwingungen, VDE Verlag 2003

[76] Kloeppel F.;Fiedler H.

Kurzschluß in elektrischen Anlagen und Netzen, VEB Verlag Technik 1960

[77] Kovacs K.P; Racz I.

Transiente Vorgänge in Wechselstrommaschinen, Verlag der Ungarischen Akademie der Wissenschaften 1957

[78] Kundur P.

Power System Stability and Control, McGraw Hill,1994

[79] Lander C.

Power Electronics, McGraw Hill 1993

[80] Leonhard W.

Regelung in der elektrischen Energieversorgung. Teubner Verlag 1980

[81] Mathur R.

Thyristor Based FACTS Controller for Electrical Power Transmission Systems, IEEE Press, New York 2002

[82] Miller T.

Reactive Power Control in Electric Systems, John Willey, New York 1982

[83] Mohan N.; Underland T.

Power Electronics, Converter, Applications and Design, John Wiley 2003

[84] Müller G.

Elektrische Maschinen, Grundlagen, Aufbau und Wirkungsweise, VEB Verlag 1989

[85] Müller G.

Elektrische Maschinen Betriebsverhalten rotierender elektrischer Maschinen, VEB Verlag 1985

[86] Nürnberg W.; Hanitsch R.

Die Prüfung elektrischer Maschinen, Springer Verlag 1955

[87] Paice D.

Power Electronic Converter Harmonics Multipulse Methods for Clean Power IEEE Press 1999

[88] Quang N.; Dittrich J.

Praxis der Feldorientierten Drehstromantriebesregelung, Expert Verlag 1993

[89] Schlabbach J. ; Blume D. ; Stepbanblome T.

Voltage Quality in Electrical Power Systems, Power and Energy Series 36, Institution of Electrical Engineers 2001

[90] Schönfeld R.; Hofmann W.

Elektrische Antriebe und Bewegungssteuerungen: Von der Aufgabenstellung zur praktischen Realisierung, VDE Verlag 2005

[91] Schönfeld R.

Regelungen und Steuerung in der Elektrotechnik, Verlag Technik Berlin 1993

[92] Schröder D.

Elektrische Antriebe 2 , Springer Verlag 1985

[93] Semikron

Semikron application manual, Nürnberg 2003

[94] Song Y.

Flexible ac Transmission Systems (FACTS), IEE Power and Energy Series 30, 2000

[95] Staudt V.

Ein Beitrag zu Leistungsbegriffen und Kompensationsverfahren für Mehrleitersysteme. VDI-Fortschrittsberichte Reihe 21 Nr. 291 VDI-Verlag Düsseldorf 2000

[96] Stevenson W. ; Grainger J.

Power System Analysis, Mcgraw- Hill 1994

Doctor Thesis

[97] Awad H.

Control of Static Series Compensation for Mitigation of Power Quality Problems, Thesis for Doctor degree, Chalmers University Sweden 2007

[98] El-Barbari S.

Steuerung und Regelung eines Vierphasenwechselrichters an Photovoltaik Inselnetzanlagen, Shaker Verlag 2004

[99] Grauers A.

Design of Direct driven Permanent magnet Generators for Wind Turbines Thesis for Doctor degree, Chalmers University Sweden 1996

[100] Heller M.

Die doppeltgespeiste Drehstrommaschine für Drehzahlvariable Pump Speicherkraftwerke. Diss. 1998 TU Braunschweig Germany

[101] Jöckel S.

Calculation of Different Generator Systems for Wind Turbines with Particular Reference to Low- Speed Permanent – Magnet Machines. Thesis for Doctor degree 2002, TU Dortmund Germany

[102] Lampala P.

Directly Driven Low Speed Permanent Magnet Generator for Wind Power, Thesis for Doctor degree 2000, Helsinki University of Technology Finland

[103] Mauricio A.

Active Power Line Conditioners, Thesis for Doctor degree 1996, TU Berlin Germany

Figures

Chapter 1

Chapter 2

Chapter 3

Chapter 4

Chapter 5

Versicherung

Hiermit versichere ich, dass ich die vorliegende Arbeit ohne unzulässige Hilfe Dritter und ohne Benutzung anderer als der angegebenen Hilfsmittel angefertigt habe; die aus fremden Quellen direkt oder indirekt übernommenen Gedanken sind als solche kenntlich gemacht.Bei der Auswahl und Auswertung des Materials sowie bei der Herstellung des Manuskripts habe ich Unterstützungsleistungen von folgenden Personen erhalten:

.....

.....

.....

Weitere Personen waren an der Abfassung der vorliegenden Arbeit nicht beteiligt. Die Hilfe eines Promotionsberaters habe ich nicht in Anspruch genommen. Weitere Personen haben von mir keine geldwerten Leistungen für Arbeiten erhalten, die im Zusammenhang mit dem Inhalt der vorgelegten Dissertation stehen.Die Arbeit wurde bisher weder im Inland noch im Ausland in gleicher oder ähnlicher Form einer anderen Prüfungsbehörde vorgelegt.

....

Ort, Datum Unterschrift